Juliana Gomes Freitas

Estudos Populacionais e Delimitação Específica do Complexo de Espécies *Tibouchina pereirae* Brade & Markgraf

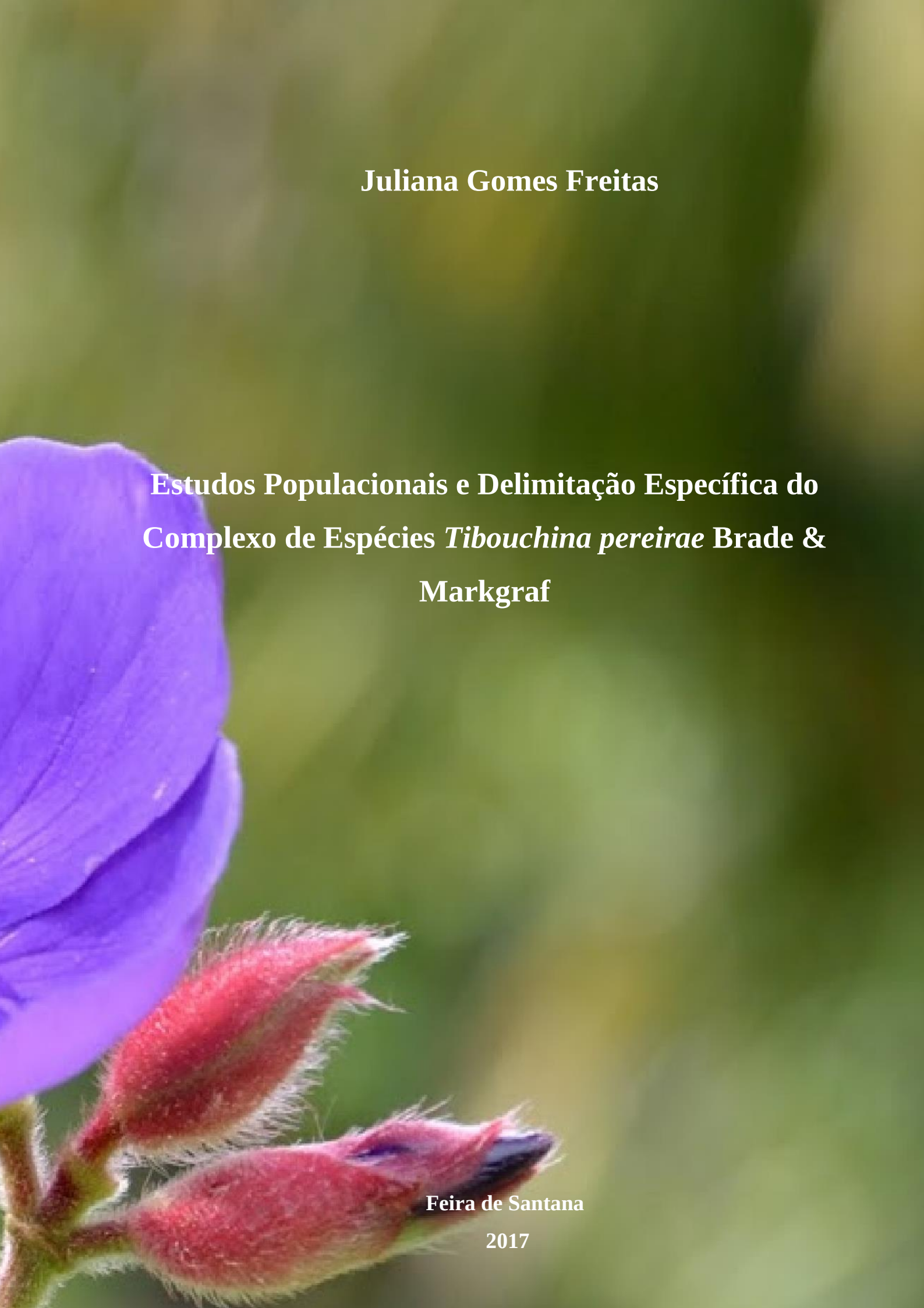

Feira de Santana

2017

UNIVERSIDADE ESTADUAL DE FEIRA DE SANTANA
DEPARTAMENTO DE CIÊNCIAS BIOLÓGICAS
PROGRAMA DE PÓS-GRADUAÇÃO EM BOTÂNICA

Estudos Populacionais e Delimitação Específica do Complexo de Espécies *Tibouchina pereirae* Brade & Markgraf

Juliana Gomes Freitas

Tese apresentada ao Programa de Pós-Graduação em Botânica da Universidade Estadual de Feira de Santana como parte dos requisitos necessários para a obtenção do Título de Doutora em Botânica.

Orientador: Dr. Cássio van den Berg

Feira de Santana
2017

Ficha Catalográfica – Biblioteca Central Julieta Carteado

Freitas, Juliana Gomes
F936e Estudos populacionais e delimitação específica do complexo de espécies *Tibouchina pereirae* Brade & Markgraf./Juliana Gomes Freitas. Feira de Santana, 2017.
140f.: il.

Orientador: Cássio van der Berg
Tese (doutorado) – Universidade Estadual de Feira de Santana, Departamento de Ciências Biológicas, Programa de Pós-Graduação em Botânica, 2017.

1.*Tibouchina pereirae*. 2Diversidade biológica. 3. Campos rupestres – Chapada Diamantina. 4.Melastomataceae. I.Berg, Cássio van der, orient. II.Universidade Estadual de Feira de Santana. III. Titulo.

CDU : 582.884

Dedico aos meus irmãos José Marcos G. Freitas *in memoriam* e Patricio G. Freitas *in memoriam*, meus companheiros em busca do tão esperado "conhecimento"! O primeiro, por me ensinar a sair escondido para a escola, sedento por conhecimento, exímio guarda-costas, sempre pronto para garantir a segurança no caminho. O segundo, por assumir precocemente a mesma função, perfeitamente exercida, apesar da pouca experiência e baixo condicionamento físico (aos três anos de idade), porém, com entusiasmo de atleta nas caminhadas diárias de doze quilômetros a caminho da escola.

AGRADECIMENTOS

Existe grande semelhança entre o começo e o fim de cada ciclo na vida acadêmica. É sempre o momento de buscar algo ou alguém que complemente uma ideia ou simplesmente encoraje para que possamos prosseguir. Nesse ciclo que está findando, tenho muito e a muitos que agradecer por diversos motivos!

Deixo aqui a minha imensa e sincera gratidão por todo incentivo e apoio recebido durante esse período, independente da forma como tenha vindo, certamente contribuiu muito para a efetivação deste resultado que está sendo entregue.

Sou imensamente grata a minha família, pelo imensurável apoio, compreensão e admiração, mesmo daqueles que não tem ideia do real significado da profissão que eu escolhi. Mas certamente, e apenas eles, são capazes de reconhecer o que esse título representa para mim, para eles e para as minhas origens. Apenas a minha família conhece todas as minhas dores, os caminhos que trilhei e os "espinhos" que perfuraram o meu ser!

Ao meu amado Lizandro Peraza, minha imensa gratidão por cuidar de mim, pelo companheirismo, compreensão, grande contribuição no meu trabalho, e muita paciência com meus "ataques" de ansiedade. Admiro muito a sua humildade ante sua inteligência!

À Universidade Estadual de Feira de Santana, Departamento de Ciências Biológicas e todos que compõem o Programa de Pós-graduação em Botânica, pelo apoio destinado a esse trabalho.

Ao meu orientador Dr. Cássio van den Berg, especialmente por ter acreditado em mim. Além disso, por ter abraçado a minha ideia de projeto, cujo grupo botânico de pesquisa, difere muito das orquídeas. Grata pela valiosa orientação sem cobranças!

À Coordenação de Aperfeiçoamento Pessoal de Nível Superior (CAPES) pela concessão da bolsa de estudo e PRONEX pelo financiamento de parte das despesas com viagens de coleta e toda a parte de laboratório.

À professora Valdira J. Santos, minha mestra! Por ter me levado ao mundo da botânica clássica, uma diversão que chamam de trabalho. Me apresentou, junto a Marcos Fábio (funguinho) um dos lugares mais incríveis que já tive a oportunidade de coletar (Parque Estadual das Sete Passagens), que é um lugar que guardo no coração!

À Andrea Karla por ser a primeira pessoa a me apresentar, pacientemente, os encantos e nuances das Melastomataceae, grupo ao qual eu tenho adoração, além de me receber em sua casa com a atenção de um amigo, quando não nos conhecíamos.

À Uiara Catharina por me “alfabetizar” tecnicamente no LAMOL e antes de qualquer coisa, por ser uma grande amiga. Sempre junto a mim, especialmente nos momentos difíceis! Obrigada pelo apoio quando eu perdi o meu "Norte" e o chão sumiu dos meus pés! Muitíssimo obrigada!

À Michella Del’Rei pela amizade, preocupação com minha sanidade mental e renal, bem como, pelas orações e muito incentivo. Obrigada pelo apoio quando estive frágil e precisei de um ombro amigo! Valeu pelas longas conversas e aventuras em campo! Nunca foi tão emocionante pisar em cascavéis! rsrs

À Zelma Soares, pela amizade, apoio moral e psicológico, pela preocupação e bons ouvidos quando os desabafos se faziam necessários! Nada como ter uma amiga psicóloga!!!

Ao Anderson Machado, pelas boas conversas (quase sempre acompanhadas de café com cuscuz), incentivo, preocupação e também pelo envio de todas as publicações que encontrou sobre *Tibouchina*. Obrigada!!!

À Mariana Telles da Universidade Federal de Goiás, pelo envio do material de DNA do seu acervo pessoal, para que eu realizasse alguns testes.

Ao Rafael Martins, pela amizade, apoio na minha qualificação e por levar meu material à Europa e adquirir amostras de *Tibouchina* do sudeste do Brasil.

Ao Mario Hibert por algumas fotografias das populações coletadas e companhia em uma das viagens de coleta.

Ao meu vizinho mais barulhento, Lamarck Rocha, por todo apoio e incentivo. Obrigada pelas conversas sempre entusiasmadas e acompanhadas de um bom cafezinho!!!

Ao Tiago Arruda Pontes, por me apresentar os primeiros passos da morfometria geométrica, com muita paciência e disponibilidade para ajudar.

Ao pessoal do HUEFS, especialmente a Teo Nunes, pela disponibilidade em ajudar a agilizar os processos referentes ao herbário.

Aos funcionários do LAMOL, Evandro, Daniela, Adriana, pelo grande auxílio técnico e moral, para que desse tudo certo, especialmente ao Ricardo Vilas-Boas, pelas muitas contribuições no trabalho do laboratório, às vezes fazendo milagres. Obrigada pelo auxílio na configuração e programas do computador.

À turma do “barulho” no LAMOL, Juliana-PE, Catharina, Michella, João, Iasmin, Tiago Arruda, Anderson Silva, Mario Hibert, Rafael Martins, Aluisio, Augusto (*Carrara*), Evandro, Tiago Andrade, Lamarck, Wallace e os demais que não mencionei, porém sou grata. Agradeço pelo convívio familiar e trocas de experiências com reagentes e equipamentos. Foram muito bons aqueles minutos de tardes e noites de cafezinho para resistir até o fim do "expediente"! Obrigada pelas conversas e piadas que me faziam esquecer as frustrações de passar o dia dedicado a poucos ou nenhum resultado positivo! Lembranças que guardarei com carinho!

Aos amigos extra-LAMOL, Catharina, Michella, Zelma, Juliana-PE, Lizandro, Rafael, Aluisio, Augusto, Fernando “gordinho”, Lamarck e Hibert, pelas refeições e aniversários improvisados com as mais diversas desculpas, apenas pela intenção de estar juntos e compartilhar alegria em momentos extratrabalho! Foi muito bom!!!

Muito obrigada!!!

SUMÁRIO

RESUMO GERAL

É apresentado um estudo da variação morfológica e genética do complexo de espécies *Tibouchina pereirae*, composto por cinco espécies endêmicas da Chapada Diamantina, ocorrentes em áreas de campos rupestres. As espécies são morfologicamente caracterizadas por arbustos com folhas agrupadas no ápice dos ramos, flores lilás a púrpura, com heteranteria, especializadas para a polinização por abelhas de grande porte, além das sementes diminutas, agrupadas em cápsulas loculicidas que promovem a dispersão por gravidade. Essas espécies apresentam morfotipos com sobreposição de caracteres morfológicos que dificultam a delimitação específica por meios tradicionais. Foram amostrados 540 indivíduos em 27 localidades de coleta, por toda a área de distribuição das espécies, os quais foram analisados através de métodos da morfometria geométrica, estudos da diversidade genética e filogeografia, buscando-se conhecer um pouco sobre a história evolutiva do complexo, com informações sobre a diversidade morfológica e genética, padrões de fluxo gênico e história demográfica do complexo. Dessa forma, estamos contribuindo com o entendimento dos processos que afetaram a distribuição das espécies, a diversificação, o histórico evolutivo dos táxons e a delimitação específica dentro do complexo. Os resultados preliminares revelaram a distinção de uma das linhagens do complexo sob a categoria de espécie, a qual foi descrita (*Pleroma rubrum*) e está incluída nas investigações deste trabalho. Resultados obtidos nas análises de morfometria geométrica mostram que existe forte relação entre a variação da forma e o tamanho das folhas nas espécies do complexo *T. pereirae*. Além disso, análises de assimetria foliar revelaram padrões morfológicos, não explorados em variação morfológica de plantas. Os dados genéticos obtidos através do ITS e *rpl32-trnL*, revelaram elevada diversidade genética no complexo de espécies e distinção interespecífica, apesar de notórias diferenças entre a delimitação morfológica tradicional e os dados genéticos em populações de todas as espécies. Isto sugere que hibridização e introgressão tem exercido um papel importante na dinâmica evolutiva do complexo. O tempo de diversificação estimado para o complexo *T. pereirae* é coincidente com a diversificação de linhagens de plantas adaptadas ao fogo, bem como com a expansão dos ecossistemas de savana que são dominados por ervas C4. Além disso, os resultados revelaram que as localidades mais ao norte da Chapada Diamantina, possivelmente funcionaram como refúgios para as espécies durante as variações climáticas do passado.

Palavras chave: Campos rupestres, Chapada Diamantina, Diversidade genética, Filogeografia de *Tibouchina*, Melastomataceae, Morfometria geométrica, *Pleroma*.

ABSTRACT

A study of morphological and genetic variation within the *Tibouchina pereirae* species complex, a group of five species endemic to the "campos rupestres" of Chapada Diamantina, is here presented. These species are generally shrubs with leaves grouped at the apex of branches, lilac to purple flowers with dimorphic in size anthers pollinated by large solitary bees, and loculicidal capsules with small seeds dispersed by gravity. These species have different morphotypes with overlapping morphological characters that difficult species delimitation by traditional methodologies. A total of 540 specimens from 27 sampling localities were collected along all the distribution range of the complex. These specimens were analyzed with several methodologies to assess patterns of morphologic and genetic variation in order to infer the evolutionary history of the group, patterns of morphologic and genetic diversity, gene flow, and demographic history. Thus, this is a contribution for the understanding of processes affecting lineage distribution, diversification, evolutionary history, and species delimitation within the species complex. Preliminary results indicated one of those lineages within the complex should be better treated as a different species (*Pleroma rubrum*) and its formal description is included here. Results from the morphometric analyses showed a relationship between leaf shapes and size among species in the complex. Furthermore, leaf asymmetry analyses revealed patterns not generally included in plant morphologic variation studies. The DNA data indicated high genetic diversity within species and genetic separation between them, despite differences between traditional morphologic delimitation and genetic data for all species. This suggest hybridization and introgression has played and important role in the evolutionary dynamic of the complex. The estimated diversification time of the complex corresponded with the lineage diversification of fire-adapted plants and the expansion of tropical savanna ecosystems dominated by C4 grasses. In addition, results showed that northernmost localities from Chapada Diamantina provably served as refugia for these species during past climatic oscillations.

Keywords: "*campos rupestres*", Chapada Diamantina, Genetic diversity, Geometric morphometrics, Melastomataceae, Phylogeography of *Tibouchina*, *Pleroma*.

INTRODUÇÃO GERAL

A Cadeia do Espinhaço é remanescente de um território antigo, produto de uma evolução descontínua, policíclica e poliistórica ao longo de 1.7 Ga (Danderfer & Dardenne 2002). Suas montanhas se estendem descontinuamente ao longo de 1.200 km desde o Nordeste até o Sudeste do Brasil nos Estados da Bahia e Minas Gerais. Os solos são usualmente pobres em nutrientes, altamente drenáveis, e dominados por quartzitos e areias. A extensão da Cadeia e as diferentes características geomorfológicas das montanhas criam um mosaico de solos e microclimas ao longo de toda a sua extensão, o que contribui com a alta diversidade vegetal (Rapini et al. 2002, Fernandes 2016, Silveira et al. 2016).

A Chapada Diamantina é um sistema de montanhas complexo que ocupa a porção norte da Cadeia do Espinhaço na região central da Bahia com extensão de 50.610 km². Esse sistema está constituído, geralmente, por grandes maciços residuais de topos rochosos e encostas íngremes ao longo de serras altas, estreitas e alongadas no sentido N-S. A elevação dessas montanhas varia entre os 200 m a 1.800 m com picos isolados de até 2.033 m (ex: Pico do Barbado). Os diversos tipos de vegetação na área, estão associados às características fisiográficas locais e incluem mosaicos vegetacionais de cerrado, campos rupestres, florestas e/ou caatingas. Os cerrados de altitude geralmente prevalecem nas áreas entre 900 e 1.200 m e se entremeiam com o campo rupestre nas maiores elevações, onde os afloramentos rochosos aparecem com maior frequência. As florestas secas e/ou caatinga ocupam uma grande extensão nas partes mais baixas da ecorregião em solos do tipo Latossolo. Nas regiões intermediárias ocorrem diversos tipos de florestas (semidecíduas e perenifólias) fragmentadas, acompanhando as calhas dos rios e/ou distribuídas nas encostas das serras. Porém, diversas zonas de transição ocorrem entre os diferentes tipos de vegetação nessas montanhas, especialmente entre caatinga e cerrado (Misi & Silva 1994, Stannard 1995, Velloso et al. 2002, Juncá et al. 2005, Funch 2008).

Os campos rupestres são ecossistemas antigos considerados como savanas tropicais associadas ao bioma Cerrado e reconhecidas pela alta taxa de endemismos e diversidade biológica. Esses ecossistemas se estendem descontinuamente ao longo da Cadeia do Espinhaço em altitudes geralmente acima dos 900 m. (Conceição & Giulietti 2002, Conceição & Pirani 2005, Rapini et al. 2008, Carvalho et al. 2014, Negreiros et al. 2014, BFG 2015, Fernandes 2016, Silveira et al. 2016). A maior parte dos campos rupestres se

estendem em solos quartzíticos, arenosos ou ferruginosos, pobres em nutrientes e com alta drenagem ou lixiviação. Além disso, eles são caracterizados pela alta variação em latitude, altitude, declividade, isolamento e antiguidade do substrato. Essas características criam um mosaico de tipos de solo e microclimas com grande variação de temperatura, luminosidade e umidade. Nestas áreas, estão registradas quase cinco mil espécies de plantas com 39% de endemismo, porém em algumas famílias este número pode chegar até 90%. Essas plantas desenvolvem várias adaptações (ex: morfológicas, fisiológicas, anatômicas, tróficas e simbióticas) para sobreviver nesses ambientes que são frequentemente afetados por incêndios naturais ou induzidos pelo homem (Giulietti & Pirani 1988, Ratter et al. 1997, Silva et al. 2006, Belo et al. 2013, Fernandes 2016, Silveira et al. 2016). Portanto, os campos rupestres constituem fragmentos de vegetação limitados por barreiras geográficas e micro ambientais que restringem a distribuição das espécies e favorecem suas altas taxas de diversidade e endemismo. Esses ecossistemas abertos, tem sofrido diversos ciclos de expansão e contração durante as oscilações climáticas do passado, as quais transformaram a composição e diversidade biológica de cada área.

Os mais recentes ciclos de variações climáticas do Holoceno influenciaram grandemente na composição e distribuição das espécies vegetais do Nordeste brasileiro (Oliveira et al. 1999, Harrison et al. 2003, Pessenda et al. 2010, Schellekens et al. 2014, Horák-Terra et al. 2015). Em geral, esses ciclos forçaram as populações a contrair sua distribuição nos períodos quentes e úmidos, e expandir nas temporadas frias e secas (Hewitt 2011, Werneck 2011, Werneck et al. 2011, Bueno et al. 2017).

O isolamento geográfico representa uma das principais causas de diferenciação morfológica e genética como resultado da especialização de habitats e adaptação local (Schaal et al. 1998, Avise 2000, Schaal & Olsen 2000, Hodel et al. 2016, Cramer & Verboom 2017). A geografia, portanto, exerce forte influência na estruturação das populações e diversificação das linhagens (Avise 2000, Caetano et al. 2008, Pfennig et al. 2010, Silva 2015). No entanto, as diferenças morfológicas e genéticas entre populações separadas geograficamente, podem ser fixadas por meio de vários processos ao longo do tempo e do espaço e assim, promover a divergência entre elas (Knowles & Carstens 2007, Knowles et al. 2007). Porém, a taxa de mudanças nessas variações, pode não seguir o mesmo ritmo e alterações morfológicas rápidas com pouca divergência genética entre

espécies, além disso, podem se apresentar em grupos sob irradiação adaptativa (Ando et al. 2005, Bradburd et al. 2013, Hoban et al. 2016).

O fato dos campos rupestres serem representados por mosaicos ambientais e biológicos complexos, distribuídos num marco temporal e espacial, faz com que as espécies respondam à essa heterogeneidade biótica e abiótica através de adaptações locais e/ou plasticidade fenotípica (Kawecki & Ebert 2004, Pfennig et al. 2010, Palacio-López et al. 2015, Volis et al. 2015). Ambos os processos produzem padrões de variação entre as populações e espécies, contribuindo para a geração de novas espécies ou irradiação adaptativa. Porém, a adaptação local e a plasticidade fenotípica podem apresentar limites difusos, levar a resultados similares, e não ser mutuamente exclusivas (Kawecki & Ebert 2004, Pfennig et al. 2010, Volis et al. 2015). Por isso, diferenças regionais entre populações podem representar tanto adaptação local e/ou plasticidade fenotípica que promovem divergência entre elas, constituindo uma estruturação da variação afetada pelos diversos fatores contemporâneos e históricos que modificam as taxas de mutação, migração e extinção nas linhagens (Willis & Whittaker 2002, Kawecki & Ebert 2004, Fuchs et al. 2015, Volis et al. 2015, Chavez-Pesqueira & Nunez-Farfan 2016).

Melastomataceae está representada por cerca de 5.000 espécies (incluídas em 170 gêneros) distribuídas em sua maioria, nas regiões tropicais e subtropicais do globo terrestre (Renner 1993, Renner et al. 2016). No Brasil, é a quinta maior família entre as angiospermas e está entre os grupos mais abundantes e diversificados de plantas nos campos rupestres, com ca. de 335 espécies endêmicas dessas áreas, dentre as 1.393 que ocorrem no país (BFG 2015, Silveira et al. 2016). Como a maioria das plantas que habitam esses ecossistemas, suas espécies também possuem sementes com baixa capacidade de dispersão à longas distâncias, e grande parte delas são geralmente dispersas nas proximidades da planta mãe, favorecendo o endemismo e elevada diferenciação entre populações (Hopper 2009, Clausing & Renner 2001, Silveira et al. 2016). Poucos estudos filogenéticos e/ou biogeográficos foram realizados com a família (Clausing & Renner 2001, Morley & Dick 2003), os quais demonstraram que Melastomataceae constitui um grupo monofilético, mas ainda perduram várias indagações sobre os limites e relações entre tribos e gêneros. Muitas das questões ainda não elucidadas devem-se a ausência de estudos evolutivos, aliada à alta variabilidade morfológica dentro da família (Kribel 2012, Rocha et al. 2016).

Os estudos filogenéticos em Melastomataceae sustentam o reconhecimento de oito grandes clados. Dois deles, Melastomeae e Microlicieae, compartilham com exclusividade, a presença do pedoconnectivo (prolongamento na base da antera, especializado para a polinização) e fruto capsular (Clausing & Renner 2001). Este clado provavelmente sofreu irradiação e especiação em ambientes abertos, por meio da dispersão anemocórica de suas sementes, reafirmando a importância dos frutos capsulares neste papel (Clausing & Renner 2001, Michelangeli et al. 2013). Essa hipótese pode ser reforçada pelo histórico evolutivo de Microlicieae, uma tribo com radiação e diversificação recente (~10 Ma) nos campos rupestres, sugerindo que houve uma mudança adaptativa para habitats sazonalmente secos durante a evolução inicial deste grupo (Simon et al. 2009, Silveira et al. 2016). Além disso, a competição por polinizadores e heteranteria, podem ter atuado como propulsores da evolução e diversificação morfológica dos estames nestes grupos (Renner et al. 2001, Michelangeli et al. 2013). Segundo Michelangeli et al. (2013), essas hipóteses corroboram com as previsões de conservação de nicho e hipótese de colonização de ambientes semelhantes ou adjacentes.

Melastomeae corresponde a uma das maiores tribos de Melastomataceae em composição genérica (47) e diversidade morfológica. As 870 espécies que a compõe, são de distribuição pantropical, porém, a maioria delas (ca. de 570 spp. e 30 gêneros) ocorre na América do Sul, principalmente no Cerrado brasileiro (Renner 1993, Michelangeli et al. 2013, Rocha et al. 2016). Suas relações internas ainda continuam pouco claras, carecendo de estudos que esclareçam a sua história evolutiva (Kribel 2012, Rocha et al. 2016). Subordinado à tribo Melastomeae, *Tibouchina* Aubl. é um gênero cujas designações taxonômicas são ainda complexas, dado ao número variado de espécies 250 a 350, que ocorrem desde o México e Antilhas até o Norte da Argentina e Paraguai (Guimarães & Martins 1997, Peralta 2002, Almeda 2009). No Brasil, inclui ca. de 167 espécies (146 endêmicas), habitando quase todos os tipos vegetacionais, embora sejam pouco frequentes em vegetação de Caatinga (Freitas et al. 2013, BFG 2015).

Análises filogenéticas das Melastomeae neotropicais mostram que *Tibouchina* não constitui um grupo monofilético, porque há inclusão de outros gêneros no clado que constitui o gênero como está atualmente circunscrito (Michelangeli et al. 2013). Portanto, as espécies brasileiras de *Tibouchina*, serão redistribuídas entre três ou quatro gêneros distintos: *Tibouchina* Aubl., *Pleroma* Don, *Chaetogastra* Candolle e, provavelmente,

Brachyotum Triana (Michelangeli et al. 2013, Meyer 2016). No entanto, os rearranjos genéricos dentro do clado PLEROMA, ao qual pertencerão a maioria das espécies do leste do Brasil, ainda não estão publicados. Por tal motivo, este trabalho trata *Tibouchina* segundo a circunscrição ainda aceita, porém, incluindo a espécie recém descrita, já em *Pleroma* (*P. rubrum* J.G.Freitas).

Tibouchina é um gênero que representa bem a baixa dispersabilidade inerente às plantas que ocupam os campo rupestre, dado as características morfológicas dos frutos (cápsulas secas com numerosas sementes diminutas), especificidade dos polinizadores (abelhas solitárias de grande porte), bem como o número de espécies endêmicas e restritas a estas áreas (44 spp.) (ver Renner 1989, BFG 2015). Existem espécies povoando hábitats de microclimas adversos como os inselbergs na Bahia (ex: *T. noblickii* Wurdack e *T. lithophilla* Wurdack), bem como, espécies restritas a áreas pequenas em grandes ecossistemas como cerrado ou restinga (ex: *T. bracteolata* J.G.Freitas, A.K.A.Santos & R.P.Oliveira, *T. salviifolia* (Cham.) Cogn., *T. subglabra* Wurdack, *T. johnwurdakiana* Todzia, *T. melobarretoi* Brade, *T. angustifolia* Cogn., *T. arenaria* Cogn., *T. bergiana* Cogn. e *T. cardinalis* (Humb. & Bonpl.) Cogn ver BFG (2015). Dentre as espécies de *Tibouchina* que são consideradas restritas ao cerrado *s.l.*, 25 ocorrem na Bahia, que é um Estado reconhecido pela grande diversidade biológica e alto grau de endemismos, especialmente a Chapada Diamantina (Giulietti & Pirani 1988, Freitas 2011, Freitas et al. 2016, Silveira et al. 2016). Contudo, o gênero apresenta alta complexidade na delimitação taxonômica, devido à grande variabilidade morfológica interespecífica nesta localidade.

O complexo de espécies *T. pereirae* foi observado por Freitas (2011) e confirmado em Freitas et al. (2016), pela presença de morfotipos que compartilham características macromorfológicas com outras espécies do gênero, sendo, portanto reconhecido como um complexo de espécies com carência de estudos morfológicos e genéticos detalhados, visando o reconhecimento das relações e identidades específicas. A partir de viagens em campo e comparações morfológicas dos espécimes de herbário, concluiu-se que o complexo estava inicialmente composto por quatro espécies (*T. blanchetiana, T. carvalhoi, T. velutina* e *T. pereirae*) e alguns morfotipos intermediários entre estas. Contudo, com base nos resultados preliminares obtidos neste trabalho, confirmou-se o status taxonômico de um destes morfotipos, o qual foi formalmente descrito como *Pleroma rubrum*, conforme citado acima.

Todas as cinco espécies do complexo *T. pereirae*, são endêmicas da Chapada Diamantina, às vezes ocorrendo de forma simpátrica nas diferentes montanhas da cordilheira. Apresentam alto grau de dificuldade na delimitação específica através de métodos taxonômicos tradicionais, especialmente pela observação de um gradiente interespecífico nos caracteres morfológicos (forma, indumento e tamanho das folhas e inflorescências), apresentando morfotipos indistinguíveis entre elas (ver Freitas 2011, Freitas et al. 2016). Tais aspectos nos chamaram a atenção, especialmente por tratarem-se de espécies restritas aos campos rupestres da Chapada Diamantina e apresentarem um complexo padrão morfológico num habitat cuja história biogeográfica é intrigante (ver Giulietti & Pirani 1998, Rapini et al. 2008, Collevatti et al. 2009, Telles et al. 2010, Ribeiro 2011, Barbosa et al. 2012, Carvalho et al. 2014, Silveira et al. 2016). Os hábitats que ocupam, as variações geológicas e climáticas locais, junto às propriedades intrínsecas das espécies (tais como a capacidade de dispersão ou dependência de habitats exclusivos), ditam a conectividade física e fluxo gênico entre as populações trazendo desafios para designações taxonômicas e decisões de conservação (ver Souza et al. 2017). Apesar de serem realizados muitos trabalhos florísticos e filogenéticos nos campos rupestres, ainda são poucos aqueles que utilizam uma abordagem populacional para compreender os eventos históricos, buscando assim esclarecer seu efeito nos padrões de distribuição da diversidade genética contemporânea (ver Telles et al. 2010, Ribeiro 2011, Barbosa et al. 2012, Colevatti et al. 2012a, Colevatti et al. 2012b, Silva 2015, Souza et al. 2017).

Baseado nos dados até aqui citados, o objetivo principal desse trabalho é identificar padrões de variação morfológica e genética dentro do complexo *T. pereirae*, condizentes com a distribuição das espécies nas diferentes montanhas da porção do Espinhaço correspondente à Chapada Diamantina. Portanto, as metodologias morfométricas e filogeográficas aplicadas neste trabalho, buscará compreender os padrões morfológicos, diversidade genética, padrões de fluxo gênico e inferir a história evolutiva do complexo. O estudo também contribuirá secundariamente para a delimitação específica do complexo *T. pereirae*. Dessa forma, pretende-se contribuir para o entendimento dos processos inerentes a divergências entre essas linhagens e o padrão de distribuição tão peculiar.

REFERÊNCIAS

Almeda F. 2009. Melastomataceae. In: Davidse G., Sousa-Sánchez M., Knapp S. & Chiang F. (eds.). Flora mesoamericana. Vol. 4. Universidad Nacional Autónoma de México, México City. Pp. 164–338.

Ando T., Ishikawa N., Watanabe H., Kokubun H., Yanagisawa Y., Hashimoto G., Marchesi E. & Suarez E. 2005. A morphological study of the *Petunia integrifolia* complex (Solanaceae). *Annals of Botany* 96: 887–900.

Avise J.C. 2000. Phylogeography: The History and Formation of Species. Cambridge, Harvard University Press.

Barbosa A.R., Fiorini C.F., Silva-Pereira V., Borba M.E.L. 2012. Geographical genetic structuring and phenotypic variation in the *Vellozia hirsuta* (Velloziaceae) ochlospecies complex. *American Journal of Botany* 99: 1477–1488.

Belo R.M., Negreiros D., Fernandes G.W., Silveira F.A.O., Ranieri B.D. & Morellato P.C. 2013. Fenologia reprodutiva e vegetativa de arbustos endêmicos de campo rupestre na Serra do Cipó, sudeste do Brasil. *Rodriguésia* 64: 817–828.

BFG. 2015. Growing knowledge: an overview of Seed Plant diversity in Brazil. *Rodriguésia* 66: 1085–1113.

Bradburd G.S., Ralph P.L. & Coop G.M. 2013. Disentangling the effects of geographic and ecological isolation on genetic differentiation. *Evolution* 67: 3258–3273.

Bueno M.L., Pennington R.T., Dexter K.G., Kamino L.H.Y., Pontara V., Neves D.M., Ratter J.A. & Oliveira-Filho A.T. 2017. Effects of Quaternary climatic fluctuations on the distribution of neotropical savanna tree species. *Ecography* 40: 403–414.

Caetano S., Prado D., Pennington R.T., Beck S., Oliveira-Filho A., Spichiger R. & Naciri Y. 2008. The history of Seasonally Dry Tropical Forests in eastern South America: inferences from the genetic structure of the tree *Astronium urundeuva* (Anacardiaceae). *Molecular Ecology* 17: 3147–3159.

Carvalho F., Godoy E.L., Lisboa F.J.G, Moreira F.M.S., SOUZA F.A., Berbara R.L.L. & Fernandes G.W. 2014. Relationship between Physical and Chemical Soil Attributes and Plant Species Diversity in Tropical Mountain Ecosystems from Brazil. *Journal Mt. Science* 11(4): 875–883.

Chavez-Pesqueira M. & Nunez-Farfan J. 2016. Genetic diversity and structure of wild populations of *Carica papaya* in northern mesoamerica inferred by nuclear microsatellites and chloroplast markers. *Annals of Botany* 118: 1293–1306.

Clausing G., Renner S.S. 2001. Molecular phylogenetics of Melastomataceae and Memecylaceae: implications for character evolution. *American Journal of Botany* 88: 486–498.

Collevatti R.G., Rabelo S.G. & Vieira R.F. 2009. Phylogeography and disjunct distribution in *Lychnophora ericoides* (Asteraceae) and endangered cerrado shrub species. *Annals of Botany* 104: 655–664.

Collevatti R.G., Castro T.G., Lima J.S. & Telles M.P.C. 2012a. Phylogeography of *Tibouchina papyrus* (Pohl) Toledo (Melastomataceae), an endangered tree species from rocky savannas, suggests bidirectional expansion due to climate cooling in the Pleistocene. *Ecology and Evolution* 2: 1024–1035.

Collevatti R.G., Lima-Ribeiro M.S., Souza-Neto A.C., Franco A.A., Terribile L.C. 2012b. Recovering the demographical history of a Brazilian Cerrado tree species Caryocar brasiliense: coupling ecological niche modeling and coalescent analyses. *Natureza e Conservação* 10: 169–176.

Conceição A.A. & Giulietti A.M. 2002. Composição floristica e aspectos estruturais de campo rupestre em dois platôs do Morro do Pai Inácio, Chapada Diamantina, Bahia, Brasil. *Hoehnea* 29: 34–48.

Conceição A.A & Pirani J.R. 2005. Delimitação de habitats em campos rupestres na Chapada Diamantina, Bahia: substratos, composição florística e aspectos estruturais. *Bol Bot Univ São Paulo* 23: 85–111.

Cramer M.D. & Verboom G.A. 2017. Measures of biologically relevant environmental heterogeneity improve prediction of regional plant species richness. *Journal of Biogeography* 44: 579–591.

Danderfer A. & Dardenne M.A. 2002. Tectonoestratigrafia da bacia Espinhaço na porção centro–norte do cráton do São Francisco: registro de uma evolução poliistórica descontínua. *Revista Brasileira de Geociências* 32: 449–460.

Fernandes G.W. 2016. Ecology and conservation of mountaintop grasslands in Brazil. New York: Springer.

Freitas J. G. 2011. Estudos floristicos e taxonoˆmicos em Tibouchina Aubl. (Melastomataceae; Melastomeae) no Estado da Bahia, Brasil. Dissertação de mestrado. Feira de Santana, Bahia: Universidade Estadual de Feira de Santana.

Freitas J.G., Santos A.K.A. & Oliveira R.P. 2013. A new and unusual species of *Tibouchina* (Melastomataceae) occurring in Caatinga vegetation in Bahia, Brazil. *Systematic Botany* 38: 418–423.

Freitas J.G., Santos A.K.A., Guimarães P.J.F. & Oliveira R.P. 2016. Flora da Bahia: Melastomataceae – *Tibouchina* s.l. *Sitientibus série Ciências Biológicas* 16: 1–46.

Fuchs J., Ericson P.G., Bonillo C., Couloux A. & Pasquet E. 2015. The complex phylogeography of the indo-malayan *Bulbuls alophoixus* with the description of a putative new ring species complex. *Molecular Ecology* 24: 5460–5474.

Funch L.S. 2008. Florestas da região norte do Parque Nacional da Chapada Diamantina e seu entorno. In: Funch L.S., Funch R.R. & Queiroz L.P. Serra do Sincorá – Parque Nacional da Chapada Diamantina. Ed. Radam, Feira de Santana. Pp. 63-77.

Giulietti A.M. & Pirani J.R. 1988. Patterns of geographic distribution of some plant species from the Espinhaço Range, Minas Gerais and Bahia, Brazil. In: Vanzolini, P. E. & Heyer, W. R. (eds.), Proceedings of a Workshop on Neotropical Distribution Patterns. Academia Brasileira de Ciências, Rio de Janeiro. Pp.39–69.

Guimarães P.J.F. & Martins A.B. 1997. *Tibouchina* sect. *Pleroma* (D. Don) Cogn. (Melastomataceae) no estado de São Paulo. *Revista Brasileira de Botânica* 20: 11–33.

Harrison S.P., Kutzbach J.E., Liu Z., Bartlein P.J., Otto-Bliesner B., Muhs D., Prentice I.C. & Thompson R.S. 2003. Mid-Holocene climates of the Americas: A dynamical response to changed seasonality. *Climate Dynamics* 20: 663–688.

Hewitt G.M. 2011. Quaternary phylogeography: the roots of hybrid zones. *Genetica* 139: 617–638.

Hoban S., Kelley J.L., Lotterhos K.E., Antolin M.F., Bradburd G., Lowry D.B., Poss M.L., Reed L.K., Storfer A. & Whitlock M.C. 2016. Finding the genomic basis of local adaptation: Pitfalls, practical solutions, and future directions. *The American Naturalist* 188: 379–397.

Hodel R.G.J., Cortez M.B.S., Soltis P.S. & Soltis D.E. 2016. Comparative phylogeography of black mangroves (*Avicennia germinans*) and red mangroves (*Rhizophora mangle*) in Florida: Testing the maritime discontinuity in coastal plants. *American journal of Botany* 3: 730–739.

Hopper S.D. 2009. OCBIL theory: towards an integrated understanding of the evolution, ecology and conservation of biodiversity on old, climatically buffered, infertile landscapes. *Plant Soil*, 322: 49–86.

Horák-Terra I., Martínez Cortizas A., Da Luz C.F.P., Rivas López P., Silva A.C. & Vidal-Torrado P. 2015. Holocene climate change in central–eastern Brazil reconstructed using pollen and geochemical records of Pau de Fruta mire (Serra do Espinhaço

Meridional, Minas Gerais). *Palaeogeography, Palaeoclimatology, Palaeoecology* 437: 117–131.

Juncá F.A., L. Funch & Rocha W. 2005. Biodiversidade e Conservação da Chapada Diamantina. Brasilia: Ministério do Meio Ambiente. 411 p

Kawecki T.J. & Ebert D. 2004. Conceptual issues in local adaptation. *Ecology Letters* **7**: 1225–1241.

Knowles L.L. & Carstens B.C. 2007. Delimiting species without monophyletic gene trees. *Systematic Biology* 56: 887–895.

Knowles L.L., Carstens B.C. & Keat M.L. 2007. Coupling genetic and ecological-niche models to examine how past population distributions contribute to divergence. *Current Biology* 17: 940–946.

Kribel R. 2012. A synopsis of the genus *Poteranthera* (Melastomeae: Melastomataceae) with the description of a new, apparently pollinator deceiving species. *Brittonia* 64(1): 6–14.

Meyer F.S. 2016. *Estudos sitemáticos no clado de* Chaetogastra *DC. e gêneros aliados (Melastomataceae: Melastomeae)*. Universidade Estadual de Campinas, Campinas, 295 pp.

Michelangeli F.A., Guimarães P.J.F., Penneys D.S., Almeda F. & Kriebel R. 2013. Phylogenetic relationships and distribution of New World Melastomeae (Melastomataceae). *Botanical Journal of the Linnean Society* 171: 38–60.

Misi A. & Silva M.G. 1994. Chapada Diamantina Oriental Bahia: geologia e depósitos. Salvador. Secretaria da Indústria, Comércio e Recursos Minerais. Série Roteiros Geológicos, Salvador, SBG Nucleo BA-SE, 194 p.

Morley R.J. & Dick C.W. 2003. Missing fossils, molecular clocks, and the origin of the Melastomataceae. *American Journal of Botany* 90: 1638–1644.

Negreiros D., Le Stradic S., Fernandes G.W. & Rennó H.C. 2014. CSR analysis of plant functional types in highly diverse tropical grasslands of harsh environments. *Plant Ecology* 215: 379–388.

Oliveira P.E., Barreto A.M.F. & Suguio K. 1999. Late Pleistocene/Holocene climatic and vegetational history of the Brazilian caatinga: The fossil dunes of the middle São Francisco River. *Palaeogeography Palaeoclimatology Palaeoecology* 152: 319–337.

Palacio-López K., Beckage B., Scheiner S. & Molofsky J. 2015. The ubiquity of phenotypic plasticity in plants: a synthesis. *Ecology and Evolution* 5: 3389–3400.

Peralta P. 2002. Las espécies del género *Tibouchina* (Melastomataceae) en Argentina. *Darwiniana* 40: 107–120.

Pessenda L.C.R., Gouveia S.E.M., Ribeiro A.d.S., Oliveira P.E. & Aravena R. 2010. Late Pleistocene and Holocene vegetation changes in northeastern Brazil determined from carbon isotopes and charcoal records in soils. *Palaeogeography, Palaeoclimatology, Palaeoecology* 297: 597–608.

Pfennig D.W., Wund M.A., Snell-Rood E.C., Cruickshank T., Schlichting C.D. & Moczek A.P. 2010. Phenotypic plasticity's impacts on diversification and speciation. *Trends in Ecology & Evolution* 25: 459–467.

Rapini A., Ribeiro P.L., Lambert S. & Pirani J.R. 2008. A flora dos campos rupestres da Cadeia do Espinhaço. *Megadiversidade* 4: 16–24.

Rapini A., Mello-Silva R. & Kawasaki M.L. 2002. Richness and endemism in Asclepiadoideae (Apocynaceae) from the Espinhaço Range of Minas Gerais, Brazil – a conservationist view. Biodiversity and Conservation 11: 1733–1746.

Ratter J.A., Ribeiro J.F., Bridgewater S. 1997. The Brazilian cerrado vegetation and threats to its biodiversity. Annals of Botany 80: 223–230.

Renner S.S. 1989. A survey of reproductive biology in neotropical Melastomataceae and Memecylaceae. *Annals of the Missouri Botanical Garden* 76: 496–518.

Renner S.S. 1993. Phylogeny and classification of the Melastomataceae and Memecylaceae. *Nordic Journal of Botany* 13: 519–540.

Renner S.S., Triebel D., Almeda F., Stone D., Ulloa C.U., Michelangeli F.A., Goldenberg R. & Cifuentes H.M. Melastomataceae. Net. 2016. A site with information on the biodiversity of Melastomataceae. Disponível em <www. melastomataceae.net>. Acesso em 18 Mai 2016.

Renner S.S., Clausing G. & Meyer K. 2001. Historical biogeography of Melastomataceae: the roles of tertiary migration and long-distance dispersal. *American Journal of Botany* 88(7): 1290–1300.

Ribeiro P.L. 2011. Filogenia de *Minaria* (Apocynaceae) e suas implicações para biogeografia e conservação da Cadeia do Espinhaço. Tese de Doutorado. Feira de Santana, Bahia: Universidade Estadual de Feira de Santana.

Rocha M.J.R., Batista J.A.N., Guimarães P.J.F. & Michelangeli F.A. 2016. Phylogenetic relationships in the *Marcetia* alliance (Melastomeae, Melastomataceae) and implications for generic circumscription. *Botanical Journal of the Linnean Society* 181: 585–609.

Schellekens J., Horák-Terra I., Buurman P., Silva A.C. & Vidal-Torrado P. 2014. Holocene vegetation and fire dynamics in central-eastern Brazil: Molecular records from the Pau de Fruta peatland. *Organic Geochemistry* 77: 32–42.

Schaal B.A., Hayworth D.A., Olsen K.M., Rauscher J.T. & Smith W.A. 1998. Phylogeographic studies in plants: Problems and prospects. *Molecular Ecology* **7**: 465–474.

Schaal B.A. & Olsen K.M. 2000. Gene genealogies and population variation in plants. *Proceedings of the National Academy of Sciences* 97: 7024–7029.

Silva J.F., Fariñas M.R., Felfili J.M. & Klink C.A. 2006. Spatial heterogeneity, land use and conservation in the cerrado region of Brazil. *Journal of Biogeography* 33: 536–548.

Silva U.C.S. 2015. Filogeografia Comparada e Modelagem de Nicho em *Mandevilla* (Apocynaceae). Tese de Doutorado. Feira de Santana, Bahia: Universidade Estadual de Feira de Santana.

Silveira F.A.O., Negreiros D., Barbosa N.P.U., Buisson E., Carmo F.F., Carstensen D.W., Conceição A.A., Cornelissen T.G., Echternacht L., Fernandes G.W., Garcia Q.S., Guerra T.J., Jacobi C.M., Lemos-Filho J.P., Le Stradic S., Morellato L.P.C., Neves F.S. Oliveira R.S., Schaefer C.E., Viana P.L. & Lambers H. 2016. Ecology and evolution of plant diversity in the endangered campo rupestre: a neglected conservation priority. *Plant Soil* 403: 129–152.

Simon M.F., Grether R., Queiroz L.P., Skema C., Pennington R.T. & Hughes C.E. 2009. Recent assembly of the Cerrado, a neotropical plant diversity hotspot, by in situ evolution of adaptations to fire. *Proc Natl Acad Sci USA*. 106: 20359–20364.

Souza H.A.V., Collevatti R.G., Lima-Ribeiro M.S., Lemos-Filho J.P. & Lovato M.B. 2017. Um grande refúgio histórico explica padrões espaciais de diversidade genética em uma espécie de savana Neotropical. Annals of Botany 119: 239–252.

Stannard B.L. 1995. Flora of the Pico das Almas, Chapada Diamantina, Bahia, Brazil. Kew, Royal Botanic Gardens, 851p.

Telles M.P.C., Silva S.P., Ramos J.R., Soares T.N., Melo D.B., Resende L.V., Batista E.C. & Vasconcellos B.F. 2010. Estrutura Genética em Populações Naturais de *Tibouchina Papyrus* (Pau-Papel) em Áreas de Campo Rupestre no Cerrado. *Revista Brasil. Bot.* 33(2): 291–300.

Velloso A.L., Sampaio E.V.S. B. & Pareyn F.G.C. 2002. *Ecorregiões propostas para o bioma Caatinga.* Recife. Associacao Plantas do Nordeste, Instituto de Conservação Ambiental, The Nature Conservancy do Brasil, 76 p.

Volis S., Ormanbekova D. & Yermekbayev K. 2015. Role of phenotypic plasticity and population differentiation in adaptation to novel environmental conditions. *Ecology and Evolution* 5: 3818–3829.

Werneck F.P. 2011. The diversification of eastern South American open vegetation biomes: Historical biogeography and perspectives. *Quaternary Science Reviews* 30: 1630–1648.

Werneck F.P., Costa G.C., Colli G.R., Prado D.E. & Sites Jr. J.W. 2011. Revisiting the historical distribution of Seasonally Dry Tropical Forests: New insights based on palaeodistribution modelling and palynological evidence. *Global Ecology and Biogeography* 20: 272–288.

Willis K.J. & Whittaker R.J. 2002. Species diversity: Scale matters. *Science* 295: 1245–1248.

MATERIAIS E MÉTODOS GERAL

Nesse trabalho foram amostradas 27 populações (20 indivíduos em cada população, exceto POP06, com 19 indivíduos) para um total de 539 indivíduos das cinco espécies (*Pleroma rubrum*, *Tibouchina blanchetiana*, *T. carvalhoi*, *T. pereirae* e *T. velutina*) que compõem atualmente o complexo de espécies *Tibouchina pereirae*. O conjunto amostral corresponde a uma representação de toda a distribuição geográfica dessas espécies (Figura 01).

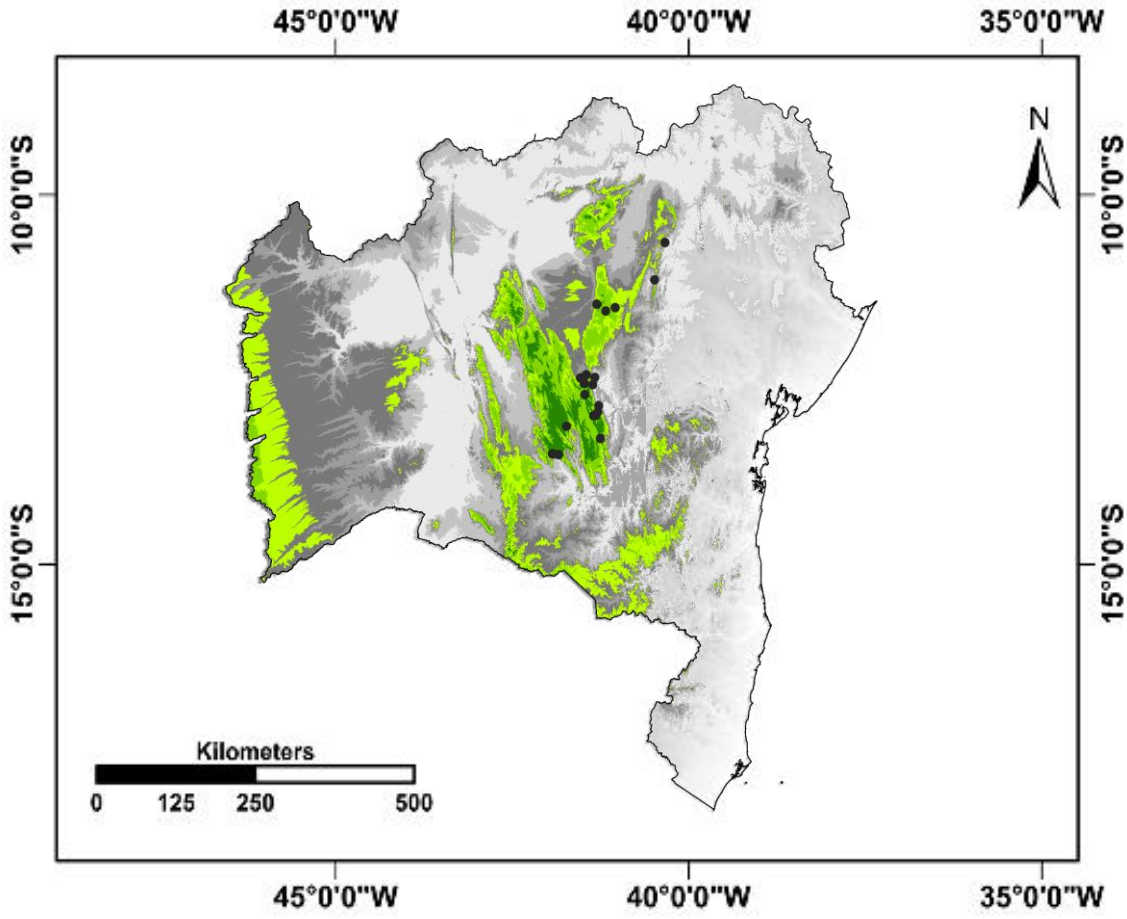

Figura 01: Pontos de coleta ao longo da distribuição geográfica do complexo *Tibouchina pereirae* nas diferentes montanhas Chapada Diamantina.

Os indivíduos de cada população foram coletados numa distância mínima de 10 m entre eles, na tentativa de evitar a coleta de indivíduos clonais. No entanto, a *simpatria* é comum entre as espécies e variedades morfológicas desse complexo, motivo pelo qual, algumas localidades de amostragem possuem uma distância menor que um quilômetro entre si (Figuras 1 e 2, Freitas 2011). Contudo, os conjuntos amostrais geográficos foram aqui assumidos como populações, buscando-se simplificar a compreensão neste trabalho. Além disso, foi coletado um indivíduo de *Tibouchinopsis mirabilis* Markgr. para ser utilizado como grupo externo, por ser a espécie mais próxima do complexo *T. pereirae* em uma filogenia prévia (Michelangeli et al. 2013). Esse conjunto de indivíduos foi usado para análises morfométricas e moleculares visando entender a variabilidade morfológica, diversidade genética e história evolutiva nesse complexo de espécies.

Para cada indivíduo, foi coletado um ramo com estruturas reprodutivas, sempre que possível. Posteriormente, os ramos foram identificados, prensados, desidratados e levados ao laboratório de taxonomia, onde foi removida uma das folhas do terceiro nó (contando-se do ápice para a base do ramo), para realização dos estudos morfométricos. Este procedimento foi rigorosamente seguido para garantir exatidão do estágio de desenvolvimento da folha em todos os indivíduos. Amostras de folhas jovens de cada um desses mesmos indivíduos foram conservadas em eppendorf's de 2 ml contendo gel de CTAB com alta concentração de sal (~0.04 g CTAB, ~0.7 g NaCl, ~1.26 ml H_2O), bem como, conservadas em filtro de papel imerso em silica gel. Ambos os conjuntos de amostras de folhas, foram mantidas em freezer até o momento da extração do DNA. Um dos ramos coletados e uma exsicata contendo uma folha de cada um dos 20 indivíduos de cada população utilizados para o estudo morfométricos, estão depositados como voucher's no herbário da Universidade Estadual de Feira de Santana (HUEFS) sob os números de registros: HUEFS224499—HUEFS224525.

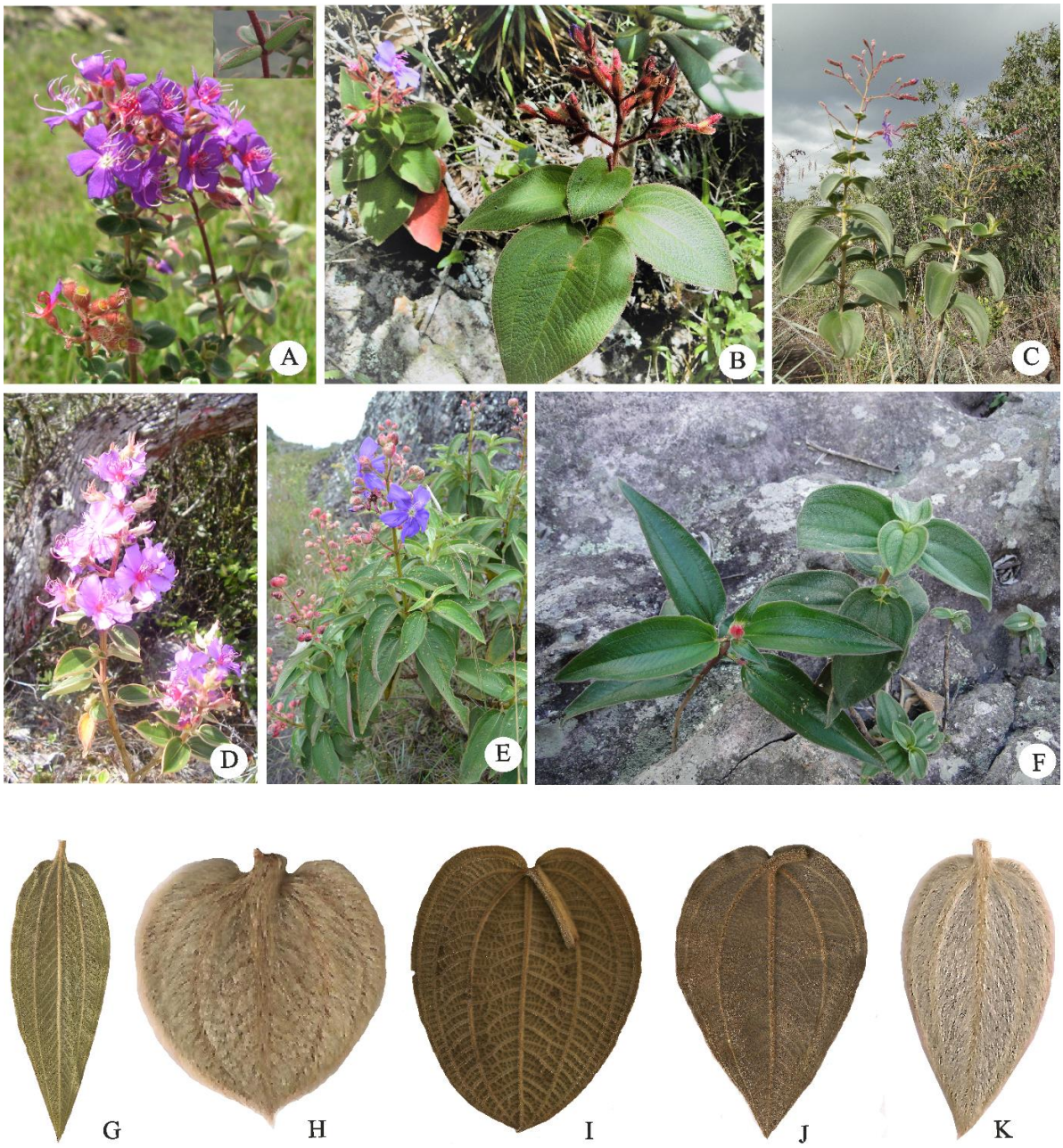

Figura 02: Representantes morfologicamente típicos do complexo de espécies *Tibouchina pereirae*. **A.** *T. blanchetiana;* **B.** *T. carvalhoi*; **C.** *T. pereirae*; **D.** *T. velutina*; **E.** *Pleroma rubrum*; **F.** Morfotipos distintos habitando o mesmo substrato; **G-K.** Imagens correspondentes a face abaxial das folhas das espécies típicas do complexo *T. pereirae*: **G.** *P. rubrum;* **H.** *T. blanchetiana;* **I.** *T. carvalhoi*; **J.** *T. pereirae*; **K.** *T. velutina*.

Obtenção dos dados referente às análises morfométricas

Uma folha de cada um dos 20 indivíduos por população, foi por vez reidratada, mergulhando-se em água fervente por cerca de dez segundos, tempo suficiente para hidratar sem comprometer a sua configuração morfológica. Após três a cinco minutos deste processo, as folhas foram digitalizadas em ambas as superfícies num scanner HP-Photosmart C4480 em resolução de 300 dpi. Porém, apenas as imagens da face abaxial foram utilizadas neste trabalho, devido a maior precisão e facilidade no posicionamento dos pontos de referência (*Landmarks*), baseando-se na localização das nervuras. Todas as folhas foram digitalizadas em escala de 1: 1. Adicionalmente, uma pequena régua foi inserida na digitalização para conferir e garantir exatidão na escala das imagens geradas.

Um total de 28 pontos de referência (*Landmarks*) digitalizados no TPSDig2 (Rohlf 2008a) foram utilizados para as análises, seguindo-se estudos anteriores (Cardozo et al. 2014, Viscosi 2015, Viscosi & Cardini 2011, Viscosi et al. 2009, entre outros). Dois pontos constituem landmarks que representam pontos homólogos (ápice e base da folha, onde a nervura principal se une ao pecíolo) e 26 pontos constituem semi-landmarks (13 em cada lado, buscando-se posicionar numa distância equivalente um do outro) para representar adequadamente a curva do esboço. Os *semi-landmaks* foram posteriormente alinhados com o processo *sliding-semilandmarks* implementado no TPSRelw (Rohlf 2008b) para otimizar a sua posição ao longo do espaço tangencial e melhor representar a sua configuração (Zelditch et al. 2012).

O processo de digitalização e medição foi realizado duas vezes, em um intervalo de dois meses entre cada procedimento, para estimar o erro de digitalização e medição. Ambas as configurações de pontos foram concatenadas em um único arquivo TPS para todas as análises posteriores, as quais foram realizadas dentro do ambiente R.

Obtenção dos dados referente às análises moleculares

O conteúdo genético (DNA) dos 20 indivíduos por cada uma das 27 populações amostradas foi extraído a partir das folhas conservadas em sílica gel. A qualidade do DNA extraído desse material mostrou-se melhor que aquele de folhas conservadas em gel CTAB (35% NaCl, 2% CTAB). O processo de extração seguiu o procedimento 2× CTAB descrito por Doyle & Doyle (1987), reescalado para 1mL e com adição de PVP-40 ao tampão CTAB.

Inicialmente, foi testada a transferabilidade de 12 *primers* de microssatélites, anteriormente desenhados para *T. papyrus* (Telles et al. 2011) e *T. pulcra* (Brito et al. 2010), na tentativa de utilizá-los como marcadores para estudar variabilidade genética no complexo *T. pereirae.* Não se obtendo resultados positivos (primer's não amplificaram para as espécies do complexo *T. pereirae*), optamos por utilizar sequências do DNA de cloroplasto e núcleo. Para isto, foram testadas dez regiões do DNA citadas na bibliografia entre as mais variáveis, para a averiguação das regiões mais propícias para o desenvolvimento deste trabalho, oito regiões do cpDNA (*rpl16, rpl32-trnL, trnQ-rps16, trnS-trnG, psbA-trnH, rps16-trnK, psbJ-petA, trnD-trnT*; Shaw et al. 2005, 2007) e duas regiões nucleares, nrETS usando os primers 18S-IGS e ETSB (Baldwin & Markos 1998) e nrITS usando os *primers* ITS17SE e ITS26SE (Baldwin et al. 1995). Foram selecionadas as duas regiões que melhor amplificaram e representam mais variações no conjunto de dados.

As reações de amplificação foram realizadas em volumes de 12µl, contendo 0,1µl de cada iniciador (*forward* e reverse), 2µl de TBT (Trialose 0,4g/mL, BSA [albumina bovina sérica] 20mg/ml^{-1}e Tris-HCL 10mM [pH 8]), 2.8µl água livre de RNAse, 5µl Top Taq Master Mix Kit (Quiagen, São Paulo Brasil), e aproximadamente 40ng de DNA para cada reação. Um único programa de PCR foi utilizado para todas as regiões do cpDNA e consistiu em: 80°C por 5 min, 30 × (95°C por 1 min, 52°C por 1 min e 65°C por 4 min), e extensão final 65°C por 5 min. Para nrITS, o programa consistiu em 94°C por 5 min, 28 × (94°C por 0,45 min, 56°C por 0,45 min e 72°C por 1 min) e extensão final 72°C por 7 min.

Na preparação para as reações de sequenciamento, os produtos da PCR foram limpos por precipitação com 11% PEG (Polietilenoglicol 8000) e álcool 70% (Paithankar & Prasad 1991). Os produtos foram posteriormente quantificados por comparação com o marcador de peso molecular *Low Mass DNA Ladder* (Invitrogen) em géis de agarose (1%). Os fragmentos purificados foram sequenciados no equipamento ABI3130XL (sequenciador em capilar), utilizando o kit de reação de sequenciamento Big Dye terminator 3.1 (Applied Biosystems, Foster city, California, U.S.A.). As reações de sequenciamento foram realizadas em um volume total de 10µl: 1,75µl do Tampão para sequenciamento (5×), 0,5µl de Big Dye e 0,5µl de cada *primer* (5µM), 0,5 a 2µl da PCR purificada contendo aproximadamente de 25 a 30ng/µl de DNA. O programa de sequenciamento foi constituído por 96°C por 3min, 35 × (96°C por 15s, 50°C por 10s, 60°C por 4min) e extensão final de 60°C por 5min. Todos os procedimentos, incluindo

extração, reações de amplificação e sequenciamento foram realizadas no Laboratório de Biologia Celular e Molecular da Universidade Estadual de Feira de Santana (LAMOL).

Foram sequenciados os primeiros 10 indivíduos de cada população, totalizando 540 sequências de cpDNA (*rpl32-trnL*) e nrDNA (ITS, incluindo ITS1, 5.8S e ITS2), pertencentes às cinco espécies do complexo *T. pereirae*. Além disso, incluiu-se uma sequência de *Tibouchinopsis mirabilis* para ambas as regiões, que foi incluído como grupo externo. As sequências obtidas foram analisadas, editadas e alinhadas utilizando-se o programa Geneious 5.3.6 (Drummond et al. 2010). Essas foram depositadas no GENBANK sob os números de acesso KY473076–KY473350 para sequencias de nrITS e KY473351–KY473625 para *rpl32-trnL* e utilizadas para a realização de todas as análises genéticas subsequentes.

A tese está estruturada em três capítulos, os quais estão formatados e editados de acordo com as normas estabelecidas pelo periódico a ser publicado: O capítulo I, consiste de uma abordagem filogeográfica englobando as cinco espécies do complexo *T. pereirae*, buscando inferir padrões filogeográficos que auxiliem no entendimento dos processos que afetaram a distribuição das linhagens, associados àqueles que determinam a diversificação, influenciando na história evolutiva dos táxons. O capítulo II, aborda o estudo dos padrões de variabilidade morfológica dentro e entre populações das espécies que compõem o complexo *T. pereirae*. A variação da forma da folha foi avaliada por meio de técnicas de Morfometria Geométrica para estimar padrões de assimetria, alometria, sinal filogenético e associação entre os padrões morfológicos e o ambiente. Através desses dados, pretendemos usar essa abordagem como um modelo para o estudo de variações morfológicas em espécies de plantas relacionadas. A sequência de análises desse estudo também pode ser usada como um guia para revelar padrões morfológicos e seu significado, uma vez que foram incluídas abordagens ainda pouco utilizadas em plantas, porém com grande potencial para determinar padrões morfológicos e associação entre espécies estreitamente relacionadas. O capítulo III, corresponde ao manuscrito de *Pleroma rubrum* J.G.Freitas, uma nova espécie, até então considerada como um morfotipo com caracteres peculiares que integra o complexo *T. pereirae*, cujo status como táxon distinto foi esclarecido através dos estudos morfométricos e moleculares apresentados no decorrer desse trabalho.

REFERÊNCIAS

Baldwin B.G. & Markos S. 1998. Phylogenetic utility of the external transcribed spacer (ETS) of 18S–26S rDNA: Congruence of ETS and ITS trees of Calycadenia (Compositae). *Molecular Phylogenetics and Evolution* 10: 449–463.

Baldwin B.G., Sanderson M.J., Porter M.J., Wjciechowski M.F., Campbell C.S. & Donoghue M.J. 1995. The ITS Region of nuclear ribosomal DNA: A valuable source of evidence on angiosperm phylogeny. Annals of the Missouri Botanical Garden. 82: 247–277.

Brito V.L G., Vigna B. B. Z. & Souza A. P. 2010. Characterization of 12 microsatellite loci from an enriched genomic library in polyploid *Tibouchina pulchra* Cogn. (Melastomataceae). *Conservation Genet Resour* 2:193–196.

Cardozo A.P., Temponi G.L., Andrade M.I., Mayo S.J. & Smidt C.E. 2014. A morphometric and taxonomic study of *Anthurium augustinum* complex (Araceae), endemic to the Brazilian Atlantic Forest. *Feddes Repertorium* 125: 43–58.

Doyle J.J. & Doyle J.L. 1987. A rapid isolation procedure for small quantities of fresh tissue. *Phytochemical Bulletin* 19: 11–15.

Drummond A.J., Ashton B., Buxton S., Cheung M., Cooper A., Heled J., Kearse M., Moir R., Stones-Havas S., Sturrock S., Thierer T. & Wilson A. 2010. Geneious v5.3. http: //www.geneious.com.

Freitas J.G. 2011. Estudos floristicos e taxonômicos em *Tibouchina* Aubl. (Melastomataceae; Melastomeae) no Estado da Bahia, Brasil. Universidade Estadual de Feira de Santana. Dissertação de Mestrado. Pp 183.

Michelangeli F.A., Guimaraes P.J.F., Penneys D.S., Almeda F. & Kriebel R. 2013. Phylogenetic relationships and distribution of New World Melastomeae (Melastomataceae). *Botanical Journal of the Linnean Society* 171: 38–60.

Paithankar, K.R. & Prasad, K.S.N. 1991. Precipitation of DNA by polyethylene glycol and ethanol. Nucleic acids research 19: 1346.

Rohlf F.J. 2008a. TpsDig2: a program for landmark development and analysis. Stony Brook, NY. Department of Ecology and Evolution, State University of New York. Available at http: //life.bio.sunysb.edu/morph/.

Rohlf F.J. 2008b. TpsRelw1.62: Relative warps. Stony Brook, NY. Department of Ecology and Evolution, State University of New York. Available at http: //life.bio.sunysb.edu/morph/.

Shaw J., Lickey E.B., Beck J.T., Farmer S.B., Liu W., Miller J., Siripun K.C, Winder C.T., Schilling E.E. & Small R.S. 2005. The tortoise and the hare II: relative utility of 21 noncoding chloroplast DNA sequences for phylogenetic analysis. *American Journal of Botany* 92: 142–166.

Shaw J., Lickey E.B., Schilling E.E. & Small R.S. 2007. Comparison of whole chloroplast genome sequences to choose noncoding regions for phylogenetic studies in angiosperms: the tortoise and the hare III. *American Journal of Botany* 94: 275–288.

Telles M.P.C., Peixoto F.P., Lima J.S., Resende L.V., Vianello R.P., Walter M.E.M.T. & Collevatti R.G. 2011. Development of microsatellite markers for the endangered Neotropical tree species *Tibouchina papyrus* (Melastomataceae). *Genetics and Molecular Research* 10 (1): 321—325.

Viscosi V. 2015. Geometric morphometrics and leaf phenotypic plasticity: assessing fluctuating asymmetry and allometry in European white oaks (*Quercus*). *Botanical Journal of the Linnean Society* 179: 335–348.

Viscosi V. & Cardini A. 2011. Leaf morphology, taxonomy and geometric morphometrics: a simplified protocol for beginners. *PloS ONE* 6: e25630.

Viscosi V., Lepais O., Gerber S. & Fortini P. 2009. Leaf morphological analyses in four European oak species (*Quercus*) and their hybrids: a comparison of traditional and geometric morphometric methods. *Plant Biosystems* 143: 564–574.

Zelditch M.L., Swiderski D.L., & Sheets H.D. 2012. Geometric Morphometrics for Biologists: A Primer, Second ed. Elsevier, Inc., London.

Capítulo I[1]

[1] Artigo formatado de acordo com as normas do periódico *PlosOne*

Genetic diversity and phylogeography of the *Tibouchina pereirae* species complex: understanding the evolutionary history of *"campos rupestres"* shrubs in the Chapada Diamantina mountain range.

Abstract— Genetic diversity assessments and evolutionary research of tropical mountaintop plant species are scarce in the literature even when some of these tropical areas are considered among the richest in species."*Campos rupestres*" are mountaintop savannas associated to the Cerrado biome with high species richness and endemism which discontinuous distribution span several mountain ranges. We analyzed the genetic diversity and evolutionary patterns of one of these endemic tropical mountaintop groups, the *Tibouchina pereirae* species complex. We assessed patterns of genetic diversity among and within species to test for species separation and spatial structure of populations using nrITS and *rpl32-trnL* markers. Furthermore, we reconstructed migration patterns and spatiotemporal dynamics for all species of the complex using Bayesian approaches to infer common patterns of evolution over the northern portion of the Espinhaço range in Bahia State, Brazil. Our results recovered genetic differentiation compatible with the separation of all the previous morphological species and suggested a strong spatial within-species population structure. As expected, most variance in the genetic component was distributed within populations (except for *P. rubrum* at nrITS and *T. blanchetiana* at *rpl32-trnL*). Estimated divergence dates for the group were congruent with establishment of several lineages associated to Cerrado savannas during the Pliocene. In addition, migration patterns and spatiotemporal reconstructions indicated that northernmost areas in the distribution could have acted as refugia during adverse climatic periods from which they expanded when temperatures rose after the Last Glacial Maximum.

Keywords: Endemic species, Evolutionary history, Hybridization, Migration analysis, Molecular dating, Phylogeography, Spatial structure, Spatiotemporal dynamics.

INTRODUCTION

Genetic diversity assessments of species are fundamental for evaluating evolutionary histories and responses to past environmental changes [1-7]. Genetic diversity assessments of plants are increasing rapidly in the literature but studies focused in the analysis of evolutionary patterns that shape this diversity are growing slowly [8-11]. These studies had promising results for understanding evolutionary patters and factors influencing the evolution on space and time at regional scales. However, they are scarce on tropical plants even when tropical areas concentrate high levels of species richness [12-17].

Tropical regions include most of the areas with highest species richness in the world even after decades of intensive human disturbance [15, 18, 19]. Thus, tropical assemblages are, in general, more complex landscapes composed by mosaics of individuals from different interacting species over a spatial and temporal framework. Consequently, ranges are not necessarily continuous and individuals or populations represent islands separated by a sea of coexisting individuals from other species or improper landscape [20, 21]. Thus, analysis of genetic diversity patterns from several species inhabiting the same areas, or closely related species, can shed light on historic processes that shape biodiversity and divergence on several scales of space and/or time [22-24]. Geographic isolation represents one of the principal causes of morphologic and genetic differentiation of plants as a result of habitat specialization and local adaptation [8, 25-28]. However, morphologic and genetic differences among populations can be fixed through several processes (acting on mutation, migration and extinction rates of lineages over time and space) that promote their divergence [29-36].

The Cerrado biogeographic province is a biodiversity hotspot harboring around 12 thousand species of plants (35% endemics). It is considered the world`s most diverse tropical savanna with a high endemism and high number of species under extinction risk [37-40]. Plants inhabiting this province present several physiognomic types but they are, in general, trees and shrubs with contorted trunks and thick barks scattered over an herbaceous layer where natural fires are frequent [41-43]. It extends over more than 1.7 million square kilometers in central Brazil and northeastern Paraguay, adjacent to seven other biogeographic provinces [37, 39, 44]. The "*campos rupestres*" are Neotropical mountaintop savannas associated to the Cerrado biome. They are antique ecosystems characterized by high species richness and endemism that extend discontinuously for more than 1200 km from northeastern to southeastern Brazil at altitudes usually above 900 m.

They also host almost five thousand species of plants (39% of them endemic) with some families reaching up to 90% of endemism [40, 45-49]. Most of the '*campos rupestres*' are along the Espinhaço range over nutrient deprived quartzite, sandstone or ironstone soils with high drainage or lixiviation and characterized by a high variation in latitude, altitude, slope, isolation, and antiquity over their extent. These characteristics create a mosaic of soil types and microclimates with an enormous variation of temperature, luminosity and moisture that limits plant distribution [45, 46].

There are two main more or less disjunct blocks of "*campos rupestres*" in the Espinhaço Range. They roughly correspond to a Northern portion in the central part of Bahia whose ranges are called Chapada Diamantina", and a Southern portion in central and northern Minas Gerais. Several mountain systems are recognized within the Chapada Diamantina ranges. At the northernmost portion, the Tombador range rises up to 1,100 m and is dominated by "caatinga" vegetation with small patches of "cerrado", a pattern also found in the Morro de Chapéu ranges. South of these mountains, the Sincorá range extends for almost 150 km on a N-S direction and rises up to 1,695 m. This range is dominated by "cerrado" and "*campos rupestres*" on the rocky outcrops and by several other forest types in the valleys and slopes. In the west, the Serra da Tromba and Serra das Almas rise up to 2,033 m on a system dominated by mountains of high elevation, vast rocky outcrops, and steep slopes. Extensive valleys, with or without isolated rocky hills, dominated by "caatinga" separate these mountain ranges from each other [50, 51].

At these open ecosystems, cycles of range expansion and contraction promoted by Pleistocene climatic oscillations transformed elevated areas into refugia at interglacial periods. Thus, population ranges contracted during warm and humid periods promoting their differentiation and expanded during cold and dry periods allowing gene flow between them [4, 38, 52, 53]. The most recent recurrent variations of dry and wet climates that greatly influenced cycles of population contraction and expansion occurred along Holocene [54-58].

Several plant species with disjunct populations on the Espinhaço range have served as study groups to assess evolutionary history, demography, genetic structure, and impact of climatic changes along time over the spatial frame of this tropical mountain range [43, 59-62]. These assessments of genetic diversity and evolutionary history in the region are only available for few groups of plants, including *Tibouchina* (Melastomataceae), and scarcer on complexes of species with restricted distributions or endemic. Studies of genetic diversity within *Tibouchina* Aubl. are scarce, we are only aware of genetic diversity

assessments in *T. papyrus* (Pohl) Toledo, *T. hatschbachii* Wurdack and *T. pulchra* Cogn. [61, 63, 64]. Nonetheless, only the former, endemic to quartzite and sandstone outcrops from the Cerrado tropical savanna, had its evolutionary history assessed [61].

Our study group, the *Tibouchina pereirae* species complex, comprises five shrub species (*Pleroma rubrum, T. blanchetiana, T. carvalhoi, T. pereirae,* and *T. velutina*) with high morphological similarity and a restricted distribution in the "*campos rupestres*" from the Chapada Diamantina mountain range on the northern portion of the Espinhaço range. They are sympatric in several localities and overlap in morphology, bringing difficulties for the correct determination of specimens [65-67]. Plants of *T. blanchetiana* and *T. pereirae* (and probably all species in the complex) develop a xylopodium (JGF per. obs.) to endure the harsh environment and the frequent natural fires of the region, a common adaptation in Cerrado plants [68, 69]. Flowers are purple and likely to be pollinated by large solitary bees (*Bombus spp., Xylocopa spp*.) as most pollen-only reward flowers in Melastomataceae and, particularly, *Tibouchina* [70]. Seeds are very small and dispersed by autochory, probably over short distances.

Here, we studied the phylogeographic patterns of all species in this complex by sequencing a nuclear and a plastid DNA region, and applying several analyses to assess genetic diversity patterns, gene flow and demography through time. Our purpose was to increase our knowledge on the evolutionary patterns of this endemic group of plants. Four main questions were addressed in this study. 1) Does genetic variation support species delimitation? 2) Are populations spatially structured within each species? 3) Are the Holocene cycles of climate variation related to the evolutionary history of each species in the *T. pereirae* complex? 4) Can we establish general patterns among the mountains within Chapada Diamantina based upon the phylogeographic patterns of each species in the *T. pereirae* complex?

MATERIAL AND METHODS

Sampling— All species from the *T. pereirae* complex (*Pleroma rubrum, T. blanchetiana, T. carvalhoi, T. pereirae, T. velutina*) were sampled. Two hundred and seventy individuals from 27 localities (hereinafter referred as populations) across their distribution range were collected. Therefore, each population consisted of ten sampled individuals that were at least ten meters apart from each other to reduce chances of sampling consanguineous individuals. Sympatry is not uncommon among species and morphological varieties thus

some populations are no more than 1 km apart. Global positioning system (GPS) coordinates were recorded for each sampling locality on site. We also collected one sample of *Tibouchinopsis mirabilis* Markgr., the sister species of the group [71], to be used as out-group for several analyses. Three young leaves for each individual were stored on silica gel on field and preserved at -4ºC until DNA extraction. DNA was isolated from the silica gel dried leaves with a rescaled 2 × CTAB protocol [72]. All isolated DNA samples were preserved at -80ºC in the DNA bank of the Laboratório de Biologia Celular e Molecular (LAMOL) at Universidade Estadual de Feira de Santana (UEFS). Herbarium specimens of each population (Supplementary material Table 1) were deposited at the UEFS herbarium (HUEFS).

Sequence amplification and analysis—PCR amplifications (12µl reactions) for nrITS (ITS1, 5.8S and ITS2) and plastid *rpl32-trnL* intergenic spacer (hereinafter referred as *rpl32-trnL*) consisted of 0.1µl of each primer (forward and reverse), 2µl of TBT (Trehalose 0.4g/mL, BSA [Bovine serum albumin] 20mg/µl, Tris-HCl 10mM [pH 8]), 5µl of TopTaq Master Mix Kit (Quiagen São Paulo Brazil), 2.8µl of RNase-free water and approximately 50 ng of DNA (2µl). The nrITS PCR amplification program consisted of 1 × 5 min at 94ºC, 28 × (45s at 94ºC, 45s at 56ºC and 1 min at 72ºC) and 1 × 7 min at 72ºC [73]. The plastid *rpl32-trnL* PCR amplification program consisted of 1 × 5 min at 80ºC, 30 × (1 min at 95ºC, 1 min at 52ºC and 4 min at 65ºC) and 1 × 5 min at 65ºC [74]. Amplified fragments were purified by precipitation using 11% PEG-8000 and 70% ethanol [75]. Purified fragments were then sequenced in an automatic ABI3130XL capillary sequencer using the Big Dye v.3.1 kit (Applied Biosystems, Foster city, California, U.S.A.) at LAMOL facilities. Forward and reverse sequenced strands were assembled and checked for sequencing errors with Geneious v.5.6 [76]. Consensus sequences were then aligned automatically with MUSCLE v.3.8 [77] and visually inspected for errors of automated alignment at indel positions. All sequences here included are available at GenBank (accession numbers: KY473076-KY473350 for nrITS and KY473351-KY473625 for plastid *rpl32-trnL*; Supplementary Material Table 1).

Genetic diversity and haplotype relationships— Preliminary results of haplotype relationships and genetic clustering of populations showed different patterns of variation between both regions thus all analyses were run for each region separately. We estimated haplotype and nucleotide diversity for all the population set and each species using Arlequin v.3.5.2.2 [78]. Then, genealogical relationships between all haplotypes were

estimated using the median joining algorithm [79] implemented in Network v.5.1 (freely available at www.fluxus-engineering.com). Tajima's D [80] and Fu's F [81] neutrality tests statistics were also estimated in Arlequin v.3.5.2.2. Both are used to test for demographic expansion of populations but Fu's F is more sensitive to population growth than Tajima's D [81]. Thus, significant D values can be interpreted as the output of bottlenecks, population expansion or heterogeneity of mutation rates while large negative F values can be interpreted as the result of sudden and significant population growth [81, 82].

Genetic differentiation— We assessed genetic differences among species with the model-based Bayesian clustering method implemented in STRUCTURE v.2.3.4 [83]. Most populations of *T. carvalhoi* and *T. pereirae* included here are in close proximity. Thus, we chose a simpler clustering method of population structure inference that does not take into account a spatial model into the genetic clusters estimation. Assignment of individuals into one to ten genetic clusters was tested assuming an admixture model with correlated allele frequencies. Each K cluster analysis consisted of 20 independent runs of 1,000,000 Markov chain Monte Carlo (MCMC) replicates after an initial burn-in of 500,000 repeats. Then, we used the delta K method of Evanno et al. (84) to select the best K (number of clusters) for data using CLUMPAK v.1.1 [85]. The optimal alignment of individuals within clusters for best K was also estimated with CLUMPAK v.1.1 using the Greedy algorithm with random input order and 100,000 repeats over all 20 replicates of best K. Optimal alignments were then plotted to graphically represent the assignment of individuals to genetic clusters.

We estimated genetic variability among species with an analysis of molecular variance [AMOVA: 86] using SPADS v.1.0 [87]. The Φ statistics from the AMOVA were used to compare genetic differentiation. G_{ST} [88] and N_{ST} [89] measures of genetic differentiation were also estimated among species with SPADS v.1.0. Statistical significance of both measures, G_{ST} and N_{ST}, were calculated with 10,000 permutations. G_{ST} and N_{ST} are both based upon haplotype frequencies but N_{ST} considers the number of mutational steps between them. Thus, N_{ST} values higher than those of G_{ST} are evidence of genetic structure among groups as closely related haplotypes are grouped together more often than those less related [89].

Spatial structuring within species— We tested for intraspecific genetic structuring using the R package "Geneland" v.4.0.6 [90]. Unlike Structure, "Geneland" allows the inclusion

of spatial locations into the Bayesian inference of population structure. Thus, it tests for spatial structuring of genetic data within species. Analysis consisted of ten independent replicates of 1,000,000 MCMC iterations; results were saved every 100 iterations (thinning = 100). The number of genetic clusters was estimated from data but restricted to a minimum of one and a maximum of five. Geographic coordinates of populations were included as Universal Transverse Mercator (UTM) coordinates and their uncertainty was set to 5 km (due to the low dispersal capability of seeds and distribution of sampling localities). Bayesian results were post-processed with a burn-in of 2,500 iterations to obtain average posterior probabilities for each run. Best run was selected based on the highest mean value of posterior probabilities.

Populations within each species were assigned to spatially predefined clusters based upon their geographic location. These spatial clusters were evaluated for genetic variability by an AMOVA within SPADS v.1.0 using 10,000 permutations and ten replicates to estimate statistical significance. Genetic differentiation between spatial groups was also estimated by G_{ST} and N_{ST} using 10,000 permutations to test for statistical significance. We also tested data for the presence of barriers to gene flow using the Monmonier's algorithm implemented in function "monmonier" from the R package "adegenet" [91]. Nuclear data is generally assumed to represent recent barriers to gene flow while plastid data is considered to represent older barriers.

Molecular dating— We calculated divergence times for Neotropical Melastomeae, including three species of the *Tibouchina pereirae* complex, with BEAST 2.3.2 [92-95]. Separate data matrices for nuclear (nrETS, nrITS1 and nrITS2) and plastid (*accd* and *psbK*) regions were built from 226 sequences of Melastomataceae available in Genbank (Supplementary Material Table 2). Independent analyses for each dataset were run assuming a relaxed lognormal clock for evolutionary rates inference and a Yule model of evolution for tree estimation. Models of sequence evolution for each DNA region were estimated with jModelTest v.2.1.17 [96] and selected using the Akaike Information Criterion (AIC). These models were set as priors of each DNA region for the estimation of divergence times. Analyses were calibrated at root (uniform prior, min= 50 ma, max= 75 ma) and Melastomeae clade (normal prior, mean= 23 ma, variance= 3 ma) with two fossils previously used for divergence time estimation in the family [97-99]. Five independent runs of 20,000,000 generations were performed for each data set (nuclear or plastid). Traces and trees were saved every 2,000 generations. We analyzed log files in Tracer v.1.6

[100] for confirmation of Estimated Sample Sizes (ESS) over 200 and evidence of convergence of traces. Log and tree files for independent runs were combined using a 25% burnin with LogCombiner v.2.3.2. Combined tree files were used to generate a consensus maximum clade credibility tree with TreeAnnotator v.2.3.2. We also estimated divergence times among all populations with BEAST v.2.3.2. We used *Tibouchinopsis mirabilis* as outgroup in the analyses following results of our Melastomeae dating analysis and the phylogenetic analysis of Michelangeli et al. (71). We assessed divergence times for all species by estimating evolutionary rates with a relaxed lognormal clock model over a tree estimated with a Coalescent Bayesian Skyline model of evolution. The root and the species complex were calibrated using a normal distribution with mean and variance encompassing the dates resulting from the Melastomeae dating analysis for both groups. We performed five independent runs of 20,000,000 generations for each region dataset. Traces and trees were saved every 2,000 generations. Convergence was estimated using same criteria as stated above for the Melastomeae analysis. Log and tree files for all runs were concatenated after a 25% burnin with LogCombiner v.2.3.2. A consensus maximum clade credibility tree was generated from these combined trees in TreeAnnotator v.2.3.2. Species were forced to be monophyletic to ensure convergence of runs [93].

Migration patterns—We used Migrate-n v.3.6.11 [101, 102] to test for different models of phylogeographic patterns, and estimate long-term mutation-scaled population sizes (θ) and mutation-scaled migration rates (M) among populations for each species in the *T. pereirae* complex. Population sizes and migration rates are modeled in Migrate-n using coalescence theory and mutation models. We ran all analyses in Bayesian mode using as priors the evolutionary rates recovered from the molecular dating analyses of the *T. pereirae* species complex. We set a uniform prior for θ (min: 0.0, max: 100.0, delta: 10.0) and M (min: 0.0, max: 1000.0, delta: 100.0). Posterior distributions were generated using the Slice sampling algorithm [103]. Parameter starting values were based on F_{ST} estimates. We used an UPGMA starting tree and static heating set to 4 chains with temperatures 1, 1.5, 3 and 1,000,000. Search strategies were set to one long chain with 200,000 genealogies recorded, a sampling increment of 100 and a burnin of 20,000. Outputs from four runs with different random seeds were compared in Tracer v1.6 to ensure convergence. Eight different models of migration patterns were run (a full migration model, two stepping-stones models, and three source models; Supplementary material Figure 1). Models were selected based on a Likelihood Bayes Factor (LBF) of the raw thermodynamic

approximation to marginal likelihoods of estimated models using the formula LBF= 2(ln *mL* (model 1) - ln *mL* (model 2). Kass and Raftery (104) argued that a difference of 3–5 log units is strong evidence favoring the better model (positive values favors model 1 and negative ones favors model 2). Immigrant numbers were estimated with equations: $Nm = [(\theta_x \times M_{y \rightarrow x})/4]$ and $Nm = [(\theta_x \times M_{y \rightarrow x})/2]$, for nrITS and *rpl32-trnL*, respectively.

Spatiotemporal dynamics— We estimated the spatiotemporal dynamics of each species using a set of models implemented in BEAST v.2.3.2 for the assessment of genealogy, migration, and demography of populations through time. Models of sequence evolution for nuclear and plastid datasets from each species were estimated independently in jModelTest v.2.1.7 and selected using the AIC (Akaike information criterion). Rates of molecular evolution from each dataset were obtained from the previous analysis of divergence time of the species complex. Genealogy and demography through time were estimated under a strict molecular clock and a coalescent Extended Bayesian Skyline Plot model of tree evolution using these models of sequence evolution and evolutionary rates [93, 105]. Migration dynamics were jointly estimated with a random walk model under a continuous-time Markov process using sampling localities (k= 3 for *P. rubrum* and *T. blanchetiana*; k= 4 for *T. velutina*; k= 6 for *T. carvalhoi*; k= 7 for *T. pereirae*) as discrete characters [106]. This mugration model infers dominant migration routes through Bayesian stochastic variable selection (BSVS), which also provides model averaging over uncertainty in the connectivity of localities. Analysis of spatiotemporal dynamics of each species consisted of two independent runs of 50,000,000 generations. Resulting trace files were manually inspected in Tracer v.1.6 for convergence of traces based on the same criteria of our previous Bayesian analyses. Trace files of both runs were combined with LogCombiner v.2.3.2 excluding 25% of generations as burnin, for subsequent analysis. Extended Bayesian Skyline Plots for each species were generated from the combined trace files of the coalescent model using the EBSPAnalyser tool of BEAST v.2.3.2. Tree files were also combined with LogCombiner v.2.3.2 excluding 25% of generations as burnin. A consensus maximum clade credibility tree was generated from these combined trees in TreeAnnotator v.2.3.2. Spatiotemporal reconstruction was then inferred using SPREAD v.1.0.6 [107]. Combined trace files and geographic coordinates were used for estimating support of transition rates (only transitions with BF > 3.0 were considered) using the Bayes factors (BF) test implemented in SPREAD v.1.0.6.

RESULTS

Sequence description, genetic diversity and haplotype relationships—We sequenced 1,109 to 1,114 bp in total from one nuclear (nrITS, including 5'-partial 18S, nrITS1, 5.8S, nrITS2 and 3'-partial 26S) and one plastid (*rpl32-trnL*) region for 270 individuals in five species. Sequences from nrITS ranged from 618 to 631 bp in extent and 62.5 to 63.3% in GC content (Table 1). Sequences from plastid *rpl32-trnL* ranged from 482 to 483 bp in extent and ranged from 28.4% to 29.6% in GC content. nrITS sequences had 22 polymorphic sites with 45 alleles and *rpl32-trnL* sequences had 18 polymorphic sites with 36 alleles (Table 1). However, haplotype diversity was similar for both regions and 33 haplotypes were present in nrITS, and 34 in *rpl32-trnL* (Table 1). Sequence descriptions and haplotype numbers for each species are summarized in Table 1. We identified eight exclusive haplotypes for *P. rubrum*, *T. blanchetiana* and *T. carvalhoi*, 21 for *T. pereirae*, and 12 for *T. velutina* (Figure 1). *Pleroma rubrum* and *T. pereirae* shared one haplotype from *rpl32-trnL*. *Tibouchina carvalhoi* and *T. pereirae* shared three haplotypes from nrITS and four from *rpl32-trnL*. *Tibouchina blanchetiana* and *T. pereirae* shared one haplotype from *rpl32-trnL*. *Tibouchina pereirae* and *T. velutina* shared two haplotypes from *rpl32-trnL* (Figure 1).

Mean values of nucleotide diversity (within all species) ranged from 0.0003 to 0.0061 in nrITS and from 0.0002 to 0.0056 in *rpl32-trnL* (Table 2). Haplotype diversity was relatively high within all species except for population 08 in *T. carvalhoi*; in addition, nrITS had higher haplotype diversity than *rpl32-trnL* in all species except for *P. rubrum* and *T. pereirae* (Table 2). However, haplotype diversity from *rpl32-trnL* was on average over 0.5 for all species except for *T. blanchetiana* (h= 0.1931, Table 2). Tajima's D neutrality test was only significant (p= <0.05) for *P. rubrum* (D= -1.5389) and the south group (population 20) of *T. velutina* (D= -1.6671*) for nrITS, and *T. blanchetiana* (D= -1.7318*) and the south group (populations 09, 21 and 24) of *T. carvalhoi* (D= -1.7316*) for *rpl32-trnL* (Table 2). On the other hand, Fu's F neutrality test was only significant (p= <0.05) for *P. rubrum* (F= -2.7159*) and the east group (populations 13 and 25) of this species (F= -1.2064*) for nrITS, and *T. blanchetiana* (F= -3.3807*), the south group (population 03) of this species (F= -1.1639*), the south group of *T. carvalhoi* (F= -2.1762*), and the east group (populations 5 and 6) of *T. velutina* (F= -2.1353*) for *rpl32-trnL* (Table 2).

Global estimates of genetic differentiation between species were significant (p= <0.01) for nrITS (Φ_{ST}= 0.9282, G_{ST}= 0.7191, N_{ST}= 0.9170, N_{ST}-G_{ST}= 0.1979; Table 3), *rpl32-trnL* (Φ_{ST}= 0.8188, G_{ST}= 0.8012, N_{ST}= 0.5883, N_{ST}-G_{ST}= 0.2129; Table 3) and combined data (Φ_{ST}= 0.8830, G_{ST}= 0.6522, N_{ST}= 0.8600, N_{ST}-G_{ST}= 0.2078). AMOVA results showed that genetic differentiation was higher within populations than between species for nrITS (Φ_{ST}= 0.9282, Φ_{CT}= 0.5757) and *rpl32-trnL* (Φ_{ST}= 0.8188, Φ_{CT}= 0.3802). Pairwise comparisons of Φ_{ST} values indicated that genetic differentiation between *T. carvalhoi* and *T. pereirae* was the smallest among species for both nrITS (Φ_{ST}= 0.1111) and *rpl32-trnL* (Φ_{ST}= 0.1051) data (Table 4). On the other hand, *P. rubrum* and *T. blanchetiana* showed the highest values of genetic differentiation for both nrITS (Φ_{ST}= 0.8398) and *rpl32-trnL* (Φ_{ST}= 0.8955) data (Table 4).

The ΔK method of Evanno et al. (84) selected K=5, for both regions, as the best cluster arrangement of all populations in the STRUCTURE analyses. Genetic clusters were mostly concordant with species definition (Figure 2). However, populations 09, 10 and 24 from *T. carvalhoi* were recovered in the genetic cluster of *T. pereirae* for both regions while populations 21 and 22 from *T. carvalhoi* were recovered within the genetic cluster of *T. pereirae* with *rpl32-trnL*; population 18 and 19 from *T. pereirae* were totally or partially recovered within the genetic cluster of *T. carvalhoi* with nrITS while populations 16 and 17 from *T. pereirae* were recovered within the genetic cluster of *P. rubrum* with nrITS but not with *rpl32-trnL*; population 14 from *T. pereirae* was recovered as an admixture of all five species with nrITS but not with *rpl32-trnL* (Figure 2). Populations 04 and 20 from *T. velutina*, population 07, 11, 12, 19, 23, and 26 from *T. pereirae*, and population 25 from *P. rubrum* were recovered as an admixture of two to five genetic clusters with *rpl32-trnL* (Figure 2).

Spatial structure within species— 'Geneland' cluster membership found only one group from nrITS and two groups (one for population 15 and one for populations 13 and 25) with *rpl32-trnL* in *P. rubrum* (Figure 3). For *T. blanchetiana*, it found two groups (one for population 02 and one for populations 01 and 03) with nrITS and only one group in *rpl32-trnL*. For *T. carvalhoi*, it found three groups with nrITS (one for population 08, one for populations 21 and 22, and one for populations 09, 10 and 24) and two groups with *rpl32-trnL* (one for population 08 and one for all other populations). For *T. pereirae*, it found four groups with nrITS (one for population 14, one for populations 16 and 17, one for population 18, and one for populations 07, 11, 12, 19, 23, 26 and 27) and three groups with

rpl32-trnL (one for populations 14, 16 and 17, one for population 18, and one for populations 07, 11, 12, 19, 23, 26 and 27). For *T. velutina*, it found three groups with nrITS (one for population 04, one for populations 05 and 06, and one for population 20) and two groups with *rpl32-trnL* (one for populations 04 and 20, and one for populations 05 and 06; Figure 3).

Global estimates of genetic differentiation in *P. rubrum* were significant only for *rpl32-trnL* (Φ_{ST}= 0.4900, G_{ST}= 0.3194, N_{ST}= 0.3951, *p*= <0.01) and AMOVA results showed that genetic differentiation was only significant within populations (Table 3). Pairwise comparisons of Φ_{ST} values among geographic areas (east– populations 13 and 25 vs. west– population 15) showed a significant genetic differentiation of regions only for *rpl32-trnL* (Φ_{ST}= 0.4839, *p*= <0.01) data (Table 5). For *T. blanchetiana*, global estimates of genetic differentiation were only significant for nrITS (Φ_{ST}= 0.5781, G_{ST}= 0.6688, N_{ST}= 0.6491, *p*= <0.01) and AMOVA results showed that genetic differentiation for nrITS was only significant among populations within regions (Φ_{SC}= 0.7375, *p*= <0.01) and within populations (Φ_{ST}= 0.7375, *p*= <0.01; Table 3). Genetic differentiation within geographic groups (north– populations 01 and 02 vs. south– population 03) in *T. blanchetiana* was only significant for nrITS (Φ_{ST}= 0.2284, *p*= <0.01) data (Table 5). For *T. carvalhoi*, global estimates of genetic differentiation were significant for both nrITS (Φ_{ST}= 0.7842, G_{ST}= 0.7019, N_{ST}= 0.7719, *p*= <0.01) and *rpl32-trnL* (Φ_{ST}= 0.8725, G_{ST}= 0.5221, N_{ST}= 0.8359, N_{ST}-G_{ST}= 0.3138, *p*= <0.01). AMOVA results showed that genetic differentiation was only significant within populations and among populations within regions for nrITS (Φ_{ST}= 0.7842, Φ_{SC}= 0.7293, *p*= <0.01) and *rpl32-trnL* (Φ_{ST}= 0.8725, Φ_{SC}= 0.2191, *p*= <0.01; Table 3). Genetic differentiation within *T. carvalhoi* was highest between central (population 08) and either north (populations 10 and 22) or south (populations 09, 21 and 24) regions for nrITS (Φ_{ST}= 0.6908-0.7025, *p*= <0.01) and *rpl32-trnL* (Φ_{ST}= 0.9156-0.9521, *p*= <0.01) while north and south populations had the lowest differentiation for plastid (Φ_{ST}= 0.1131, *p*= <0.01) data (Table 5). For *T. pereirae*, global estimates of genetic differentiation were significant for both nrITS (Φ_{ST}= 0.7842, G_{ST}= 0.7019, N_{ST}= 0.7719, N_{ST}-G_{ST}=0.2786, *p*= <0.01) and *rpl32-trnL* (Φ_{ST}= 0.7842, G_{ST}= 0.7019, N_{ST}= 0.7719, N_{ST}-G_{ST}=0.2297, *p*= <0.01; Table 3). AMOVA results showed that genetic differentiation was significant within populations, among populations within regions and among regions for nrITS (Φ_{ST}= 0.8797, Φ_{SC}= 0.7456, Φ_{CT}= 0.5270, *p*= <0.01; Table 3) but only the differentiation among regions was not significant for *rpl32-trnL* (Φ_{ST}= 0.7219, Φ_{SC}= 0.5983, *p*= <0.01; Table 3). Genetic differentiation within *T. pereirae* was higher and

significant for east (populations 14, 16 and 17) against north (populations 18, 19, 26 and 27) or south (populations 07, 11, 12, 23) regions for both nrITS (Φ_{ST}= 0.5937-0.7329, p= <0.01) and *rpl32-trnL* (Φ_{ST}= 0.4348-0.5966, p= <0.01) data (Table 5). For *T. velutina*, global estimates of genetic differentiation were significant for both nrITS (Φ_{ST}= 0.9268, G_{ST}= 0.9000, N_{ST}= 0.9180, p= <0.01) and *rpl32-trnL* (Φ_{ST}= 0.5913, G_{ST}= 0.4751, N_{ST}= 0.5461, p= <0.01). AMOVA results showed that genetic differentiation was only significant within populations and among population within regions for nrITS (Φ_{ST}= 0.9268, Φ_{ST}= 0.7959, p= <0.01) but only significant for the differentiation within populations with *rpl32-trnL* (Φ_{ST}= 0.5913, p= <0.01; Table 3). Genetic differentiation within *T. velutina* was high between all populations with nrITS (Φ_{ST}= 0.8274-0.8845, p= <0.01) but only high between east (populations 05 and 06) and either west (population 04; Φ_{ST}= 0.6102, p= <0.01) or south (population 20; Φ_{ST}= 0.7185, p= <0.01) regions with *rpl32-trnL* (Table 5).

The Monmonier algorithm identified, with nrITS and/or *rpl32-trnL*, some barriers among populations from all species except *P. rubrum* (Figure 3). For *T. blanchetiana*, only one barrier separating population 02 from populations 01 and 03 was identified with nrITS. For *T. carvalhoi*, the barriers identified with nrITS and *rpl32-trnL* separated population 8 from all other populations. For *T. pereirae*, the barriers identified with nrITS separated populations into three groups: 1) populations 07 and 14, 2) population 18, and 3) populations 16, 17, 19, 26 and 27. On the other hand, the barrier identified with *rpl32-trnL* separated populations 07 and 12 from the other nine populations. For *T. velutina*, the barriers identified with nrITS and *rpl32-trnL* separated populations into three groups: 1) population 04, 2) population 20, and 3) populations 05 and 06 (Figure 3).

Molecular clock analyses— The models of sequence evolution selected under the AIC were: F81 for nrITS and *rpl32-trnL* (reported always in this order) in *P. rubrum* and *T. blanchetiana*; F81 and HKY in *T. carvalhoi*, HKY+I and GTR for *T. pereirae*; and, F81+G and GTR for *T. velutina*. The dating analysis recovered a *Tibouchina* (*Pleroma*) clade [sensu 71] diverging from other Melastomataceae at 19.04 Ma (95%HPD= 14.06-23.94 Ma) with nuclear data and 18.22 Ma (95%HPD= 12.67-21.21 Ma) with plastid data (Supplementary Material Figures 2 and 3). The *T. pereirae* species complex diverged from *Tibouchinopsis mirabilis*, its closest relative sensu Michelangeli et al. (71), at 3.56 Ma (95%HPD= 1.91-5.37 Ma) for nuclear data and 4.82 Ma (95%HPD= 2.24-7.71 Ma) for plastid data (Figure 4, Supplementary Material Figures 2 and 3). Slightly lower mean

divergence dates were recovered from the dating analysis of population data, placing this divergence at 3.35 Ma (95%HPD= 1.63-5.15 Ma) for nuclear data and 4.49 Ma (95%HPD= 1.88-7.17 Ma) for plastid data (Figure 4). The evolutionary rates recovered (nrITS and then *rpl32-trnL*) from the dating analyses were 0.005797×10^{-6} and 0.002379×10^{-6} for *P. rubrum*, 0.005905×10^{-6} and 0.002514×10^{-6} for *T. blanchetiana*, 0.005480×10^{-6} and 0.002379×10^{-6} for *T. carvalhoi*, 0.005510×10^{-6} and 0.002390×10^{-6} for *T. pereirae*, and 0.005833×10^{-6} and 0.002377×10^{-6} for *T. velutina*.

Migration and demographic reconstruction— The likelihood Bayes factor on the migrate-n outputs selected model 6 for nrITS (LBF=-3.04) and model 5 for *rpl32-trnL* (LBF=-3.82) in *P. rubrum* (Table 6). Model 6 considered population 13 as the source for populations 15 and 25 with immigrant numbers among populations ranging from 3.74 to 6.59. Model 5 considered population 25 as the source for populations 13 and 15 with immigrant numbers ranging from 1.05 to 8.30 (Figure 3A). In *T. blanchetiana*, it was selected model 8 for nrITS (LBF=-7.16) and model 6 for *rpl32-trnL* (LBF=-7.40) data (Table 6). Model 8 considered bidirectional gene flow between populations 01 and 03, and unidirectional gene flow from population 02 to populations 01 and 03 with immigrant numbers among populations ranging from 0.62 to 0.92. Model 6 considered population 01 as the source for populations 02 and 03 with immigrant numbers among populations ranging from 2.46 to 7.63 (Figure 3B). In *T. carvalhoi*, model 7 was selected for nrITS (LBF=-15.36) and model 6 for *rpl32-trnL* (LBF=-11.42) data (Table 6). Model 7 considered bidirectional gene flow between populations 09, 21 and 24, and populations 10 and 22, and unidirectional gene flow from populations 09, 21 and 24 or populations 10 and 22 towards population 08 with immigrant numbers ranging from 0.08 to 0.32. Model 6 considered populations 10 and 22 as the source for population 08 and populations 09, 21, and 24 with immigrant numbers ranging from 0.09 to 2.35 (Figure 3C). In *T. pereirae*, model 3 was selected for nrITS (LBF=-12.00) and model 6 for *rpl32-trnL* (LBF=-16.06) data (Table 6). Model 3 considered a stepping stone route from populations 18, 19, 26 and 27 to populations 07, 11, 12 and 23, and then to populations 14, 16 and 17 with immigrant numbers ranging from 0.07 to 0.24. Model 6 considered populations 18, 19, 26 and 27 the source from populations 07, 11, 12 and 23, and populations 14, 16 and 17 with immigrant numbers ranging from 0.26 to 0.31 (Figure 3D). In *T. velutina*, model 5 was selected for nrITS (LBF=-7.42) and model 3 for *rpl32-trnL* (LBF=-15.26) data (Table 6). Model 5 considered population 04 as source for populations 05 and 06, and population 20 with

immigrant numbers ranging from 0.11 to 0.25. Model 3 considered a stepping stone route from populations 05 and 06 to population 04, and then to population 20 with immigrant numbers ranging from 0.30 to 6.29 for *rpl32-trnL* (Figure 3E).

The Bayes factor for the mugration model supported migration routes for all species except for *P. rubrum*. In *T. blanchetiana*, it supported the migration route from population 02 to population 03 (BF= 19.78, pk= 0.99). In *T. carvalhoi*, it supported the migration routes from population 24 to population 08 (BF= 2450.66, pk= 0.99), from population 22 to population 09 (BF= 5.29, pk= 0.76), from population 21 to population 09 (BF= 4.26, pk= 0.72), and from population 22 to population 21 (BF= 4.06, pk= 0.71). In *T. pereirae*, it supported the migration routes from population 19 to population 26 (BF= 10.49, pk= 0.80), from population 07 to population 23 (BF= 4.08, pk= 0.61), and from population 11 to population 26 (BF= 4.03, pk= 0.60). In *T. velutina*, it supported the migration routes from population 04 to population 20 (BF= 15.13, pk= 0.96), and from population 05 to population 06 (BF= 8.42, pk= 0.93).

Demographic estimates from the Extended Bayesian Skyline Plots resulted in similar patterns of demographic dynamics through time for all species. However, population expansion occurred at different periods in a time frame ranging from 3 to 10 ka. On the one hand, populations of *P. rubrum*, *T. blanchetiana* and *T. velutina* expanded at some time between 8 ka and 9 ka while *T. carvalhoi* expanded at some time around 5 ka. On the other hand, populations of *T. pereirae* experienced a first expansion at around 10 ka and a second expansion around 3 ka (Figure 4).

DISCUSSION

In general, results differed between nuclear and chloroplast markers for both migration models and temporal analyses. They reflected differing periods of gene flow for nrITS and cpDNA. Patterns of gene flow from pollen dispersal are inferred from nuclear data due to their high mutational rate, whereas older patterns are inferred from chloroplast markers due to their lack of recombination, low effective population size and lower mutation rates [108-111]. Thus, we assumed gene flow within the *T. pereirae* species complex was recent for nrITS and older for cpDNA.

Genetic differentiation, hybridization and species limits

Our analyses support the recognition of five groups, mostly concordant with the previous taxonomical, morphological delimitation of each species. However, the genetic composition of individuals from several populations (in all species except *T. blanchetiana*) had notorious differences in relation to their morphological assignment. This discordance between morphology and genetic clusters from nrDNA and cpDNA suggest that hybridization is playing an important role in the evolutionary dynamics of the *T. pereirae* species complex. Furthermore, some populations with introgression are more similar to one species or the other even when they shared the same nrDNA and cpDNA genetic cluster assignment. These results are in agreement of a known fact, all studies of reticulation are case studies and character expressions of offspring from hybridization events are difficult to predict [112].

Overall values of genetic differentiation (G_{ST}, N_{ST} and θ_{ST}) among species were high and significant while the positive and significant differences between N_{ST} and G_{ST} suggested that each species consists of closely related haplotypes [89]. Nonetheless, genetic differentiation between *Tibouchina pereirae* and *T. carvalhoi* was the lowest among all species pairs. This result is probably influenced by the presence of introgression at several of their populations.

These results brought about an open question on a classificatory and evolutionary issue, how should lineages resulting from reticulation events be treated? Application of species limits on these taxa is not fully straightforward. The traditional classification system disregards paraphyletic lineages and assumes species are static entities limited by sets of characters (of any kind). On the contrary, the evolutionary point of view considers species as dynamic and usually paraphyletic lineages evolving over space and time, and incorporates them into the traditional classification scheme [113-117]. Does reticulation among species in the *T. pereirae* complex imply all five entities can be subsumed into one broader entity? Not necessarily, if morphological separation among them is sound despite reticulation and results from all analyses pointed out to a complex evolutionary scenario of population expansions and contractions within this species complex. Reticulation between species has increased the genetic diversity of each species with small morphological change. Thus, the morphological species concept suits the taxonomic delimitation of the *T. pereirae* complex. Hybridization is usually regarded as a facilitator of range expansions and survival of individuals into novel environments [118, 119]. Therefore, evidence

recovered here suggests reticulation has greatly influenced actual haplotype diversity, range expansion of species and survival into probably novel environments when expanding to other mountain ranges within Chapada Diamantina.

Haplotype diversity and spatial structuring

Nucleotide and haplotype diversity of nrDNA and cpDNA within species were relatively high (compared to other species of *Tibouchina*) taking into account that only a single DNA region within each was analyzed [59, 61]. In general, nrDNA had higher haplotype diversity than cpDNA except for *P. rubrum*, where cpDNA diversity was twice that of nrDNA. It is common that nuclear markers show higher levels of haplotype diversity than cpDNA due to their higher mutation rates compared to organelle DNA [108, 111]. It was surprising that most species had high cpDNA haplotype diversity since small and aggregated plant populations with limited seed dispersal (as in our study group) are expected to have few haplotypes fixed or low genetic variation [120, 121]. On the contrary, low levels of haplotype nrDNA diversity from some populations were not expected since known pollinators (bumblebees and carpenter bees) can forage up to 10 km from their nests and increase nrDNA gene flow among populations [122, 123]. Genetic structure of populations within most species was evident from "Geneland" and "Monmonier" but not from AMOVA analyses. Haplotype distribution and AMOVA of geographic regions indicate a complex relationship among these areas. These patterns and the apparent lack of geographic barriers to gene flow among most populations suggest haplotype diversity within areas is product of population contractions and expansions. Stratigraphic records of pollen as well as organic and inorganic content suggest Late Pleistocene and Holocene in Northeastern Brazil were characterized by several contractions and expansions of dryland-associated vegetation. Thus, last 18 ka were characterized by cycles of wet (~18 to ~10 ka), dry (from ~10 to ~1.6 ka), oscillations of wet and dry (from ~1.6 to ~0.4 ka), and wet (~0.4 ka to present) conditions [54-58]. We hypothesize that populations contracted during wet conditions at early Holocene, expanded when dry conditions started to dominate the environment (~10 to ~1.6 ka), contracted again during the dry-wet oscillation period (~1.6 to 0.4 ka) and the onset of wetter conditions (~0.4 ka). This pattern allowed *rpl32-trnL* haplotypes to diverge and get fixed during first population contraction, mix haplotypes during expansion, and establish recent patterns of haplotype diversity during second contraction of populations. On the other hand, nrITS haplotypes need smaller time spans to diverge thus it is feasible that the second population contraction resulted in recent

haplotype diversity. Expansion of populations brought together individuals from different species close enough to allow gene flow between them. In fact, the spatial structure of nrITS haplotypes in *T. carvalhoi*, *T. pereirae* and *T. velutina* are apparently an artifact resulting from hybridization and introgression.

Divergence times and population temporal dynamics

Our results indicate tribe Melastomeae diverged from closest relatives at around 25.17 Ma (95%HPD= 19.76-30.84 Ma) for nuclear and 30.99 Ma (95%HPD= 25.58-36.52 Ma) for plastid data, an estimated date ca. 5 Ma older than most recently reported divergence dates for the tribe [99]. At this time, the onset of Oi-1 glaciation and the establishment of Antarctic ice sheets at the Eocene/Oligocene boundary (~34Ma) was accompanied by accelerated rates of speciation for several groups [124] and apparently tribe Melastomeae as inferred from our results (Figure 4). The onset of the Mi-1 glaciation at the Oligocene/Miocene boundary (~23Ma) and subsequent smaller glaciation brought also increased rates of speciation for certain groups of biota [124] including, as inferred from our estimated divergence dates, *Tibouchina s.l.* Divergence dates from *Tibouchina s.l.* recovered here are generally slightly older than those reported previously by other authors [97-99]. However, differences at date estimates from our analyses and those published elsewhere are probably result of considerable differences at species and DNA sampling effort [125]. The divergence of the *T. pereirae* species complex from its closest relative, *Tibouchinopsis mirabilis*, occurred sometime from 3.35 to 4.49 Ma. At this time frame (~5 Ma onwards), several other lineages of fire-adapted plants within Fabaceae and Melastomataceae diversified in the Cerrado hotspot [126]. Furthermore, it is argued that C4 grass-dominated savanna biomes (including the Cerrado) progressively expanded from 8-9 Ma with a notable expansion from 4 Ma onwards [127, 128]. Thus, several groups of plants associated to these savannas (including our study group) diversified with them. Pleistocene and Pliocene were characterized by climatic oscillations of cold and dry glacial periods separated by warm and humid interglacial epochs [129]. These climatic oscillations probably resulted in the diversification of our study group through recurrent cycles of population contraction and expansion during interglacial and glacial periods. The demographic reconstructions through time showed that populations of all species expanded greatly after the onset of the Last Glacial Maximum (LGM). In general, estimated dates of demographic expansion were placed at the beginning of a dry period that lasted ~8 ka (~10

to ~1.6 ka); nevertheless, demographic reconstructions did not recover any population contraction, a problem probably intrinsic to methodology.

Phylogeographic patterns

Patterns recovered here indicate Serra do Sincorá was an important area for the evolutionary history of *P. rubrum*, *T. carvalhoi* and *T. pereirae*. Populations of *T. carvalhoi* are restricted to this range and several of them seem to have introgression from *T. pereirae*, when both species are in close proximity. On the other hand, *P. rubrum* and *T. pereirae* have wider ranges over several mountain groups. They seem to have expanded from Serra do Sincorá to Serra das Almas where both species display evidence of introgression; nevertheless, only populations resembling typical *T. pereirae* are composed of these putative introgressed individuals. It seems that *T. blanchetiana* survived and expanded from Morro de Chapéu to Serra da Tromba when conditions allowed it. Although *T. pereirae* has been reported from Morro de Chapéu, we did not find any individual when collecting in the area. However, any population inhabiting this area should have arrived from Serra do Sincorá. Populations of *T. velutina* expanded from Serra do Tombador towards Morro de Chapéu and Serra do Sincorá where assumed introgression events with several species occurred. Thus, *P. rubrum*, *T. carvalhoi* and *T. pereirae* apparently originated at Serra do Sincorá while *T. blanchetiana* and *T. velutina* have their origin at Morro de Chapéu and Serra do Tombador, respectively. Although these mountain ranges within Chapada Diamantina are separated by biotic and abiotic factors that constrain species distributions, our study indicates that these barriers seem to be partially permeable. In addition, there is evidence that several groups of plants and animals associated to wet and dry environments have passed through them during climatic oscillations [130-132]. Our analyses suggest all species in the *T. pereirae* complex have recurrently passed these barriers several times in their evolutionary history following dry vegetation expansions.

Migration patterns among populations suggest that northernmost localities from all species served as refugia and sources for posterior expansion. Immigrant numbers estimated from our analyses suggest that populations became isolated recently after a previous expansion that was sufficient for nrITS to diverge but insufficient for *rpl32-trnL* to get fixed within populations. *Pleroma rubrum* is an exception. It has a pattern more congruent with an old expansion of populations within a time frame insufficient for nrITS and *rpl32-trnL* to get fixed within populations.

ACKNOWLEDGEMENTS

This contribution is part of the Ph.D. thesis of JGF at the Programa de Pós-graduação em Botânica from the Universidade Estadual de Feira de Santana (UEFS). We thank Dr. Hibert Huaylla for assistance during field trips. We are also grateful to PRONEX (FAPESB/CNPq PNX0014/2009) for financial support. JGF thanks Coordenação de Aperfeiçoamento de Pessoal de Nível Superior (CAPES) for a doctoral scholarship.

LITERATURE CITED

1. Meng HH, Zhang ML. Diversification of plant species in arid Northwest China: species-level phylogeographical history of *Lagochilus* Bunge ex Bentham (Lamiaceae). Molecular Phylogenetics and Evolution. 2013; 68 (3): 398-409. doi: 10.1016/j.ympev.2013.04.012.

2. Hewitt GM. Genetic consequences of climatic oscillations in the Quaternary. Philosophical transactions of the Royal Society of London. Series B, Biological sciences. 2004; 359 (1442): 183-195. doi: 10.1098/rstb.2003.1388.

3. Hewitt GM. Speciation, hybrid zones and phylogeography — or seeing genes in space and time. Molecular Ecology. 2001; 10 (3): 537-549. doi: 10.1046/j.1365-294x.2001.01202.x.

4. Hewitt GM. Quaternary phylogeography: the roots of hybrid zones. Genetica. 2011; 139 (5): 617-638. doi: 10.1007/s10709-011-9547-3.

5. Turchetto-Zolet AC, Salgueiro F, Turchetto C, Cruz F, Veto NM, Barros MJF, et al. Phylogeography and ecological niche modelling in *Eugenia uniflora* (Myrtaceae) suggest distinct vegetational responses to climate change between the southern and the northern Atlantic Forest. Botanical Journal of the Linnean Society. 2016; 182 (3): 670-688. doi: 10.1111/boj.12473.

6. Turchetto-Zolet AC, Pinheiro F, Salgueiro F, Palma-Silva C. Phylogeographical patterns shed light on evolutionary process in South America. Molecular Ecology. 2013; 22 (5): 1193-1213. doi: 10.1111/mec.12164.

7. Leal BSS, Palma da Silva C, Pinheiro F. Phylogeographic studies depict the role of space and time scales of plant speciation in a highly diverse Neotropical region. Critical Reviews in Plant Sciences. 2016; 35 (4): 215-230. doi: 10.1080/07352689.2016.1254494.

8. Hodel RG, de Souza Cortez MB, Soltis PS, Soltis DE. Comparative phylogeography of black mangroves (*Avicennia germinans*) and red mangroves

(*Rhizophora mangle*) in Florida: Testing the maritime discontinuity in coastal plants. American Journal of Botany. 2016; 103 (4): 730-739. doi: 10.3732/ajb.1500260.

9. Carstens BC, Richards CL. Integrating coalescent and ecological niche modeling in comparative phylogeography. Evolution. 2007; 61 (6): 1439-1454. doi: 10.1111/j.1558-5646.2007.00117.x.

10. Bucci G, Gonzalez-Martinez SC, Le Provost G, Plomion C, Ribeiro MM, Sebastiani F, et al. Range-wide phylogeography and gene zones in *Pinus pinaster* Ait. revealed by chloroplast microsatellite markers. Molecular Ecology. 2007; 16 (10): 2137-2153. doi: 10.1111/j.1365-294X.2007.03275.x.

11. Saeki I, Dick CW, Barnes BV, Murakami N. Comparative phylogeography of red maple (*Acer rubrum* L.) and silver maple (*Acer saccharinum* L.): Impacts of habitat specialization, hybridization and glacial history. Journal of Biogeography. 2011; 38 (5): 992-1005. doi: 10.1111/j.1365-2699.2010.02462.x.

12. Collevatti RG, Terribile LC, Diniz-Filho JA, Lima-Ribeiro MS. Multi-model inference in comparative phylogeography: an integrative approach based on multiple lines of evidence. Frontiers in Genetics. 2015; 6: 31. doi: 10.3389/fgene.2015.00031.

13. Diniz-Filho JAF, Barbosa ACOF, Collevatti RG, Chaves LJ, Terribile LC, Lima-Ribeiro MS, et al. Spatial autocorrelation analysis and ecological niche modelling allows inference of range dynamics driving the population genetic structure of a neotropical savanna tree. Journal of Biogeography. 2016; 43 (1): 167-177. doi: 10.1111/jbi.12622.

14. Vitorino LC, Lima-Ribeiro MS, Terribile LC, Collevatti RG. Demographical history and palaeodistribution modelling show range shift towards Amazon Basin for a neotropical tree species in the LGM. BMC Evolutionary Biology. 2016; 16: 213. doi: 10.1186/s12862-016-0779-9.

15. Ellis EC, Antill EC, Kreft H. All is not loss: plant biodiversity in the anthropocene. PLoS ONE. 2012; 7: e30535. doi: 10.1371/journal.pone.0030535.

16. Ribeiro PC, Lemos-Filho JP, Buzatti RSdO, Lovato MB, Heuertz M. Species-specific phylogeographical patterns and Pleistocene east–west divergence in *Annona* (Annonaceae) in the Brazilian Cerrado. Botanical Journal of the Linnean Society. 2016; 181 (1): 21-36. doi: 10.1111/boj.12394.

17. Collevatti RG, Lima-Ribeira MS, Souza-Neto AC, Franco AA, Oliveira Gd, Terribile LC. Recovering the demographical history of a Brazilian Cerrado tree species *Caryocar brasiliense*: coupling ecological niche modeling and coalescent

analyses. Natureza & Conservação. 2012; 10 (2): 169-176. doi: 10.4322/natcon.2012.024.

18. Gaston KJ. Global patterns in biodiversity. Nature. 2000; 405 (6783): 220 - 227. doi: 10.1038/35012228.

19. Kier G, Mutke J, Dinerstein E, Ricketts TH, Küper W, Kreft H, et al. Global patterns of plant diversity and floristic knowledge. Journal of Biogeography. 2005; 32 (7): 1107-1116. doi: 10.1111/j.1365-2699.2005.01272.x.

20. Gaston KJ. The structure and dynamics of geographic ranges. Oxford: Oxford University Press; 2003.

21. Pulliam HR. On the relationship between niche and distribution. Ecology Letters. 2000; 3 (4): 349-361. doi: 10.1046/j.1461-0248.2000.00143.x.

22. Avise JC, Bowen BW, Ayala FJ. In the light of evolution X: Comparative phylogeography. Proceedings of the National Academy of Sciences of the United States of America. 2016; 113 (29): 7957-7961. doi: 10.1073/pnas.1604338113.

23. Francoso E, Zuntini AR, Carnaval AC, Arias MC. Comparative phylogeography in the Atlantic Forest and Brazilian savannas: Pleistocene fluctuations and dispersal shape spatial patterns in two bumblebees. BMC Evolutionary Biology. 2016; 16: 267. doi: 10.1186/s12862-016-0803-0.

24. Bagley JC, Johnson JB. Phylogeography and biogeography of the lower Central American neotropics: Diversification between two continents and between two seas. Biological Reviews. 2014; 89 (4): 767-790. doi: 10.1111/brv.12076.

25. Schaal BA, Olsen KM. Gene genealogies and population variation in plants. Proceedings of the National Academy of Sciences. 2000; 97 (13): 7024-7029. doi: 10.1073/pnas.97.13.7024.

26. Schaal BA, Hayworth DA, Olsen KM, Rauscher JT, Smith WA. Phylogeographic studies in plants: problems and prospects. Molecular Ecology. 1998; 7 (4): 465-474. doi: 10.1046/j.1365-294x.1998.00318.x.

27. Avise JC. Phylogeography: The history and formation of species. Cambridge: Harvard University Press; 2000.

28. Cramer MD, Verboom GA. Measures of biologically relevant environmental heterogeneity improve prediction of regional plant species richness. Journal of Biogeography. 2017; 44 (3): 579-591. doi: 10.1111/jbi.12911.

29. Willis KJ, Whittaker RJ. Species Diversity: Scale Matters. Science. 2002; 295 (5558): 1245-1248. doi: 10.1126/science.1067335.

30. Wang Y, Yan G. Molecular phylogeography and population genetic structure of *O. longilobus* and *O. taihangensis* (*Opisthopappus*) on the Taihang mountains. PLoS ONE. 2014; 9 (8): e104773. doi: 10.1371/journal.pone.0104773.

31. Fuchs J, Ericson PG, Bonillo C, Couloux A, Pasquet E. The complex phylogeography of the Indo-Malayan *Alophoixus bulbuls* with the description of a putative new ring species complex. Molecular Ecology. 2015; 24 (21): 5460-5474. doi: 10.1111/mec.13337.

32. Chavez-Pesqueira M, Nunez-Farfan J. Genetic diversity and structure of wild populations of *Carica papaya* in Northern Mesoamerica inferred by nuclear microsatellites and chloroplast markers. Annals of Botany. 2016; 118 (7): 1293-1306. doi: 10.1093/aob/mcw183.

33. Volis S, Ormanbekova D, Yermekbayev K. Role of phenotypic plasticity and population differentiation in adaptation to novel environmental conditions. Ecology and Evolution. 2015; 5 (17): 3818-3829. doi: 10.1002/ece3.1607.

34. Kawecki TJ, Ebert D. Conceptual issues in local adaptation. Ecology Letters. 2004; 7 (12): 1225-1241. doi: 10.1111/j.1461-0248.2004.00684.x.

35. Knowles LL, Carstens BC. Delimiting species without monophyletic gene trees. Systematic Biology. 2007; 56 (6): 887-895. doi: 10.1080/10635150701701091.

36. Knowles LL, Carstens BC, Keat ML. Coupling genetic and ecological-niche models to examine how past population distributions contribute to divergence. Current Biology. 2007; 17 (11): 940-946. doi: 10.1016/j.cub.2007.04.033.

37. Myers N, Mittermeier RA, Mittermeier CG, da Fonseca GAB, Kent J. Biodiversity hotspots for conservation priorities. Nature. 2000; 403 (6772): 853-858. doi: 10.1038/35002501.

38. Werneck FP, Nogueira C, Colli GR, Sites JW, Costa GC. Climatic stability in the Brazilian Cerrado: Implications for biogeographical connections of South American savannas, species richness and conservation in a biodiversity hotspot. Journal of Biogeography. 2012; 39 (9): 1695-1706. doi: 10.1111/j.1365-2699.2012.02715.x.

39. Werneck FP, Costa GC, Colli GR, Prado DE, Sites Jr JW. Revisiting the historical distribution of Seasonally Dry Tropical Forests: New insights based on palaeodistribution modelling and palynological evidence. Global Ecology and Biogeography. 2011; 20 (2): 272-288. doi: 10.1111/j.1466-8238.2010.00596.x.

40. BFG. Growing knowledge: An overview of seed plant diversity in Brazil. Rodriguésia. 2015; 66 (4): 1-29. doi: 10.1590/2175-7860201566411.

41. Ratter JA, Ribeiro JF, Bridgewater S. The Brazilian Cerrado vegetation and threats to its biodiversity. Annals of Botany. 1997; 80 (3): 223-230. doi: 10.1006/anbo.1997.0469.

42. Furley PA. Tropical savannas and associated forests: Vegetation and plant ecology. Progress in Physical Geography. 2007; 31 (2): 203-211. doi: 10.1177/0309133307076107.

43. Souza HA, Collevatti RG, Lima-Ribeiro MS, Lemos-Filho JP, Lovato MB. A large historical refugium explains spatial patterns of genetic diversity in a Neotropical savanna tree species. Annals of Botany. 2017; 119 (2): 239-252. doi: 10.1093/aob/mcw096.

44. Morrone JJ. Biogeographical regionalisation of the Neotropical region. Zootaxa. 2014; 3782 (1): 1-110. doi: 10.11646/zootaxa.3782.1.1.

45. Fernandes GW, editor. Ecology and conservation of mountaintop grasslands in Brazil. New York: Springer; 2016.

46. Silveira FAO, Negreiros D, Barbosa NPU, Buisson E, Carmo FF, Carstensen DW, et al. Ecology and evolution of plant diversity in the endangered campo rupestre: a neglected conservation priority. Plant and Soil. 2016; 403 (1): 129-152. doi: 10.1007/s11104-015-2637-8.

47. Rapini A, Ribeiro PL, Lambert S, Pirani JR. A flora dos campos rupestres da Cadeia do Espinhaco. Megadiversidade. 2008; 4 (1-2): 15-23.

48. Conceição AA, Pirani JR. Delimitação de habitats em campos rupestres na Chapada Diamantina, Bahia: Substratos, composição florística e aspectos estructurais. Boletim de Botânica da Universidade de São Paulo. 2005; 23 (1): 85-111. doi: 10.11606/issn.2316-9052.v23i1p85-111.

49. de Carvalho F, Godoy EL, Lisboa FJG, Moreira FMdS, de Souza FA, Berbara RLL, et al. Relationship between physical and chemical soil attributes and plant species diversity in tropical mountain ecosystems from Brazil. Journal of Mountain Science. 2014; 11 (4): 875-883. doi: 10.1007/s11629-013-2792-4.

50. Stannard BL. Flora of the Pico das Almas, Chapada Diamantina, Bahia, Brazil. London: Kew Royal Botanic Gardens; 1995.

51. Funch LS. Florestas da região norte do Parque Nacional da Chapada Diamantina e seu entorno. In: Funch LS, Funch RR, Queiroz LP, editors. Serra do Sincorá – Parque Nacional da Chapada Diamantina. Feira de Santana: Radam; 2008. p. 63-77.

52. Werneck FP. The diversification of eastern South American open vegetation biomes: Historical biogeography and perspectives. Quaternary Science Reviews. 2011; 30 (13-14): 1630-1648. doi: 10.1016/j.quascirev.2011.03.009.

53. Bueno ML, Pennington RT, Dexter KG, Kamino LHY, Pontara V, Neves DM, et al. Effects of Quaternary climatic fluctuations on the distribution of neotropical savanna tree species. Ecography. 2017; 40 (3): 403-414. doi: 10.1111/ecog.01860.

54. de Oliveira PE, Barreto AMF, Suguio K. Late Pleistocene/Holocene climatic and vegetational history of the Brazilian caatinga: The fossil dunes of the middle São Francisco River. Palaeogeography Palaeoclimatology Palaeoecology. 1999; 152 (3-4): 319-337. doi: 10.1016/S0031-0182(99)00061-9.

55. Harrison SP, Kutzbach JE, Liu Z, Bartlein PJ, Otto-Bliesner B, Muhs D, et al. Mid-Holocene climates of the Americas: A dynamical response to changed seasonality. Climate Dynamics. 2003; 20 (7): 663 - 688. doi: 10.1007/s00382-002-0300-6.

56. Horák-Terra I, Martínez Cortizas A, da Luz CFP, Rivas López P, Silva AC, Vidal-Torrado P. Holocene climate change in central–eastern Brazil reconstructed using pollen and geochemical records of Pau de Fruta mire (Serra do Espinhaço Meridional, Minas Gerais). Palaeogeography, Palaeoclimatology, Palaeoecology. 2015; 437 (1): 117-131. doi: 10.1016/j.palaeo.2015.07.027.

57. Pessenda LCR, Gouveia SEM, Ribeiro AdS, de Oliveira PE, Aravena R. Late Pleistocene and Holocene vegetation changes in northeastern Brazil determined from carbon isotopes and charcoal records in soils. Palaeogeography, Palaeoclimatology, Palaeoecology. 2010; 297 (3-4): 597-608. doi: 10.1016/j.palaeo.2010.09.008.

58. Schellekens J, Horák-Terra I, Buurman P, Silva AC, Vidal-Torrado P. Holocene vegetation and fire dynamics in central-eastern Brazil: Molecular records from the Pau de Fruta peatland. Organic Geochemistry. 2014; 77 (1): 32-42. doi: 10.1016/j.orggeochem.2014.08.011.

59. Telles MPdC, da Silva SP, Ramos JR, Soares TN, Melo DB, Resende LV, et al. Estrutura genética em populações naturais de *Tibouchina papyrus* (pau-papel) em áreas de campo rupestre no cerrado. Revista Brasileira de Botânica. 2010; 33 (2): 291-300. doi: 10.1590/S0100-84042010000200010.

60. Barbosa AR, Fiorini CF, Silva-Pereira V, Mello-Silva R, Borba EL. Geographical genetic structuring and tangled morpho-anatomical variation in the *Vellozia hirsuta* (Velloziaceae) ochlospecies complex. American Journal of Botany. 2012; 99 (9): 1477-1488. doi: 10.3732/ajb.1200070.

61. Collevatti RG, de Castro TG, de Souza Lima J, de Campos Telles MP. Phylogeography of *Tibouchina papyrus* (Pohl) Toledo (Melastomataceae), an

endangered tree species from rocky savannas, suggests bidirectional expansion due to climate cooling in the Pleistocene. Ecology and Evolution. 2012; 2 (5): 1024-1035. doi: 10.1002/ece3.236.

62. Collevatti RG, Rabelo SG, Vieira RF. Phylogeography and disjunct distribution in *Lychnophora ericoides* (Asteraceae), an endangered cerrado shrub species. Annals of Botany. 2009; 104 (4): 655-664. doi: 10.1093/aob/mcp157.

63. da Maia FR, Sujii PS, Goldenberg R, da Silva-Pereira V, Zucchi MI. Development and characterization of microsatellite markers for *Tibouchina hatschbachii* (Melastomataceae), an endemic and habitat-restricted shrub from Brazil. Acta Scientiarum. Biological Science. 2016; 38 (3): 327-332. doi: 10.4025/actascibiolsci.v38i3.31496.

64. Brito VLG, Mori GM, Vigna BBZ, Azevedo-Silva M, Souza AP, Sazima M. Genetic structure and diversity of populations of polyploid *Tibouchina pulchra* Cogn. (Melastomataceae) under different environmental conditions in extremes of an elevational gradient. Tree Genetics & Genomes. 2016; 12: 101. doi: 10.1007/s11295-016-1059-y.

65. Freitas JG. Estudos floristicos e taxonômicos em *Tibouchina* Aubl. (Melastomataceae; Melastomeae) no Estado da Bahia, Brasil: Universidade Estadual de Feira de Santana; 2011.

66. Freitas JG, dos Santos AKA, Guimarães PJF, Oliveira RP. Flora da Bahia: Melastomataceae – *Tibouchina* s.l. Sitientibus série Ciências Biológicas. 2016; 16: 10.13102/scb11111. doi: 10.13102/scb1111.

67. Freitas JG, van den Berg C. A new species of *Pleroma* (Melastomataceae) endemic to Chapada Diamantina, Bahia, Brazil. Phytotaxa. 2016; 288 (3): 249-257. doi: 10.11646/phytotaxa.288.3.5.

68. Simon MF, Pennington T. Evidence for adaptation to fire regimes in the tropical savannas of the Brazilian Cerrado. International Journal of Plant Sciences. 2012; 173 (6): 711-723. doi: 10.1086/665973.

69. Appezzato-da-Glória B, Cury G, Kasue Misaki Soares M, Rocha R, Hissae Hayashi A. Underground systems of Asteraceae species from the Brazilian Cerrado. The Journal of the Torrey Botanical Society. 2008; 135 (1): 103-113. doi: 10.3159/07-ra-043.1.

70. Renner SS. A survey of reproductive biology in neotropical Melastomataceae and Memecylaceae. Annals of the Missouri Botanical Garden. 1989; 76 (2): 496-518. doi: http://www.jstor.org/stable/2399497.

71. Michelangeli FA, Guimaraes PJF, Penneys DS, Almeda F, Kriebel R. Phylogenetic relationships and distribution of New World Melastomeae (Melastomataceae). Botanical Journal of the Linnean Society. 2013; 171 (1): 38-60. doi: 10.1111/j.1095-8339.2012.01295.x.

72. Doyle JJ, Doyle JL. A rapid DNA isolation procedure for small quantities of fresh leaf tissue. Phytochemical Bulletin of the Botanical Society of America. 1987; 19 (1): 11-15.

73. White TJ, Bruns T, Lee S, Taylor J. Amplification and direct sequencing of fungal ribosomal RNA genes for phylogenetics. In: Innis MA, Gelfand DH, Sninsky JJ, White TJ, editors. PCR protocols: A guide to methods and Applications. San Diego: Academic Press, Inc.; 1990. p. 315-322.

74. Shaw J, Lickey EB, Schilling EE, Small RL. Comparison of whole chloroplast genome sequences to choose noncoding regions for phylogenetic studies in angiosperms: The tortoise and the hare III. American Journal of Botany. 2007; 94 (3): 275 - 288. doi: 10.3732/ajb.94.3.275.

75. Paithankar KR, Prasad KSN. Precipitation of DNA by polyethylene glycol and ethanol. Nucleic Acids Research. 1991; 19 (6): 1346.

76. Drummond AJ, Ashton B, Buxton S, Cheung M, Cooper A, Heled J, et al. Geneious v5.3. Available from http://www.geneious.com. 2010.

77. Edgar RC. MUSCLE: Multiple sequence alignment with high accuracy and high throughput. Nucleic Acids Research. 2004; 32 (5): 1792-1797. doi: 10.1093/nar/gkh340.

78. Excoffier L, Lischer HEL. Arlequin suite ver 3.5: A new series of programs to perform population genetics analyses under Linux and Windows. Molecular Ecology Resources. 2010; 10 (3): 564-567. doi: 10.1111/j.1755-0998.2010.02847.x.

79. Bandelt H-J, Forster P, Röhl A. Median-joining networks for inferring intraspecific phylogenies. Molecular Biology and Evolution. 1999; 16 (1): 37-48. doi: 10.1093/oxfordjournals.molbev.a026036.

80. Tajima F. Statistical method for testing the neutral mutation hypothesis by DNA polymorphism. Genetics. 1989; 123 (3): 585-595.

81. Fu Y-X. Statistical tests of neutrality of mutations against population growth, hitchhiking and background selection. Genetics. 1997; 147 (2): 915-925.

82. Tajima F. The amount of DNA polymorphism maintained in a finite population when the neutral mutation rate varies among sites. Genetics. 1996; 143 (3): 1457-1465.

83. Pritchard JK, Stephens M, Donnelly P. Inference of population structure using multilocus genotype data. Genetics. 2000; 155 (2): 945-959.

84. Evanno G, Regnaut S, Goudet J. Detecting the number of clusters of individuals using the software STRUCTURE: A simulation study. Molecular Ecology. 2005; 14 (8): 2611-2620. doi: 10.1111/j.1365-294X.2005.02553.x.

85. Kopelman NM, Mayzel J, Jakobsson M, Rosenberg NA, Mayrose I. Clumpak: A program for identifying clustering modes and packaging population structure inferences across K. Molecular Ecology Resources. 2015; 15 (5): 1179-1191. doi: 10.1111/1755-0998.12387.

86. Excoffier L, Smouse PE, Quattro JM. Analysis of molecular variance inferred from metric distances among DNA haplotypes: Application to human mitochondrial DNA restriction data. Genetics. 1992; 131 (2): 479-491.

87. Dellicour S, Mardulyn P. Spads 1.0: A toolbox to perform spatial analyses on DNA sequence data sets. Molecular Ecology Resources. 2014; 14 (3): 647-651. doi: 10.1111/1755-0998.12200.

88. Pons O, Petit RJ. Estimation, variance and optimal sampling of gene diversity I. Haploid locus. Theoretical and Applied Genetics. 1995; 90 (3): 462-470. doi: 10.1007/BF00221991.

89. Pons O, Petit RJ. Measuring and testing genetic differentiation with ordered versus unordered alleles. Genetics. 1996; 144 (3): 1237-1245.

90. Guillot G, Renaud S, Ledevin R, Michaux J, Claude J. A unifying model for the analysis of phenotypic, genetic, and geographic data. Systematic Biology. 2012; 61 (6): 897-911. doi: 10.1093/sysbio/sys038.

91. Jombart T. Adegenet: A R package for the multivariate analysis of genetic markers. Bioinformatics. 2008; 24 (11): 1403-1405. doi: 10.1093/bioinformatics/btn129.

92. Drummond AJ, Rambaut A. BEAST: Bayesian evolutionary analysis by sampling trees. BMC Evolutionary Biology. 2007; 7: 214. doi: 10.1186/1471-2148-7-214.

93. Drummond AJ, Bouckaert RR. Bayesian evolutionary analysis with BEAST 2. Cambridge: Cambridge University Press; 2015.

94. Drummond AJ, Suchard MA, Xie D, Rambaut A. Bayesian phylogenetics with BEAUti and the BEAST 1.7. Molecular Biology and Evolution. 2012; 29 (8): 1969-1973. doi: 10.1093/molbev/mss075.

95. Bouckaert R, Heled J, Kuhnert D, Vaughan T, Wu CH, Xie D, et al. BEAST 2: a software platform for Bayesian evolutionary analysis. Plos Computational Biology. 2014; 10 (4): e1003537. doi: 10.1371/journal.pcbi.1003537.

96. Posada D, Crandall KA. MODELTEST: Testing the model of DNA substitution. Bioinformatics. 1998; 14 (9): 817-818. doi: 10.1093/bioinformatics/14.9.817.

97. Renner SS, Meyer K. Melastomeae come full circle: Biogeographic reconstruction and molecular clock dating. Evolution. 2001; 55 (7): 1315-1324. doi: 10.1111/j.0014-3820.2001.tb00654.x.

98. Renner SS, Clausing G, Meyer K. Historical biogeography of Melastomataceae: The roles of Tertiary migration and long-distance dispersal. American Journal of Botany. 2001; 88 (7): 1290-1300.

99. Berger BA, Kriebel R, Spalink D, Sytsma KJ. Divergence times, historical biogeography, and shifts in speciation rates of Myrtales. Molecular Phylogenetics and Evolution. 2016; 95 (1): 116-136. doi: 10.1016/j.ympev.2015.10.001.

100. Rambaut A, Suchard MA, Xie D, Drummond AJ. Tracer v1.6, Available from http://beast.bio.ed.ac.uk/Tracer. 2014.

101. Beerli P, Felsenstein J. Maximum-likelihood estimation of migration rates and effective population numbers in two populations using a coalescent approach. Genetics. 1999; 152 (2): 763-773.

102. Beerli P, Felsenstein J. Maximum likelihood estimation of a migration matrix and effective population sizes in n subpopulations by using a coalescent approach. Proceedings of the National Academy of Sciences of the United States of America. 2001; 98 (8): 4563-4568. doi: 10.1073/pnas.081068098.

103. Neal RM. Slice sampling. The Annals of Statistics. 2003; 31 (3): 705-767. doi: http://www.jstor.org/stable/3448413.

104. Kass RE, Raftery AE. Bayes Factors. Journal of the American Statistical Association. 1995; 90 (430): 773-795. doi: 10.2307/2291091.

105. Heled J, Drummond AJ. Bayesian inference of population size history from multiple loci. BMC Evolutionary Biology. 2008; 8: 289. doi: 10.1186/1471-2148-8-289.

106. Lemey P, Rambaut A, Drummond AJ, Suchard MA. Bayesian Phylogeography Finds Its Roots. Plos Computational Biology. 2009; 5 (9): e1000520. doi: 10.1371/journal.pcbi.1000520.

107. Bielejec F, Rambaut A, Suchard MA, Lemey P. SPREAD: Spatial phylogenetic reconstruction of evolutionary dynamics. Bioinformatics. 2011; 27 (20): 2910-2912. doi: 10.1093/bioinformatics/btr481.

108. Petit RJ, Vendramin GG. Plant phylogeography based on organelle genes: An introduction. In: Weiss S, Ferrand N, editors. Phylogeography of Southern European Refugia. London: Springer; 2007. p. 23-97.

109. Hamilton MB, Miller JR. Comparing Relative Rates of Pollen and Seed Gene Flow in the Island Model Using Nuclear and Organelle Measures of Population Structure. Genetics. 2002; 162 (4): 1897-1909.

110. Petit RJ, Duminil J, Fineschi S, Hampe A, Salvini D, Vendramin GG. Comparative organization of chloroplast, mitochondrial and nuclear diversity in plant populations. Molecular Ecology. 2005; 14 (3): 689-701. doi: 10.1111/j.1365-294X.2004.02410.x.

111. Sork VL, Gugger PF, Chen JM, Werth S. Evolutionary lessons from California plant phylogeography. Proceedings of the National Academy of Sciences of the United States of America. 2016; 113 (29): 8064-8071. doi: 10.1073/pnas.1602675113.

112. Wissemann V. Plant evolution by means of hybridization. Systematics and Biodiversity. 2007; 5 (3): 243-253. doi: 10.1017/s1477200007002381.

113. Hörandl E. Paraphyletic versus monophyletic taxa—evolutionary versus cladistic classifications. Taxon. 2006; 55 (3): 564-570. doi: 10.2307/25065631.

114. Hörandl E. Beyond cladistics: Extending evolutionary classifications into deeper time levels. Taxon. 2010; 59 (2): 345-350. doi: http://www.jstor.org/stable/25677594.

115. Hörandl E, Stuessy TF. Paraphyletic groups as natural units of biological classification. Taxon. 2010; 59 (6): 1641-1653. doi: http://www.jstor.org/stable/41059863.

116. Stuessy TF, Hörandl E. The importance of comprehensive phylogenetic (evolutionary) classification—A response to Schmidt-Lebuhn's commentary on paraphyletic taxa. Cladistics. 2014; 30 (3): 291-293. doi: 10.1111/cla.12038.

117. Schmidt-Lebuhn AN. Fallacies and false premises—A critical assessment of the arguments for the recognition of paraphyletic taxa in botany. Cladistics. 2012; 28 (2): 174-187. doi: 10.1111/j.1096-0031.2011.00367.x.

118. Pfennig KS, Kelly AL, Pierce AA. Hybridization as a facilitator of species range expansion. Proceedings of the Royal Society B: Biological Sciences. 2016; 283 (1839): 20161329. doi: 10.1098/rspb.2016.1329.

119. Canestrelli D, Porretta D, Lowe WH, Bisconti R, Carere C, Nascetti G. The tangled evolutionary legacies of range expansion and hybridization. Trends in Ecology & Evolution. 2016; 31 (9): 677-688. doi: 10.1016/j.tree.2016.06.010.

120. Ray C. Maintaining genetic diversity despite local extinctions: Effects of population scale. Biological Conservation. 2001; 100 (1): 3-14. doi: 10.1016/S0006-3207(00)00202-0.

121. Harrison S, Hastings A. Genetic and evolutionary consequences of metapopulation structure. Trends in Ecology & Evolution. 1996; 11 (4): 180-183. doi: 10.1016/0169-5347(96)20008-4.

122. Pasquet RS, Peltier A, Hufford MB, Oudin E, Saulnier J, Paul L, et al. Long-distance pollen flow assessment through evaluation of pollinator foraging range suggests transgene escape distances. Proceedings of the National Academy of Sciences. 2008; 105 (36): 13456-13461. doi: 10.1073/pnas.0806040105.

123. Goulson D, Stout JC. Homing ability of the bumblebee *Bombus terrestris* (Hymenoptera: Apidae). Apidologie. 2001; 32 (1): 105-111. doi: 10.1051/apido:2001115.

124. Zachos J. Trends, rhythms, and aberrations in global climate 65 Ma to present. Science. 2001; 292 (5517): 686-693. doi: 10.1126/science.1059412.

125. Rutschmann F. Molecular dating of phylogenetic trees: A brief review of current methods that estimate divergence times. Diversity and Distributions. 2006; 12 (1): 35-48. doi: 10.1111/j.1366-9516.2006.00210.x.

126. Simon MF, Grether R, de Queiroz LP, Skema C, Pennington RT, Hughes CE. Recent assembly of the Cerrado, a neotropical plant diversity hotspot, by in situ evolution of adaptations to fire. Proceedings of the National Academy of Sciences of the United States of America. 2009; 106 (48): 20359-20364. doi: 10.1073/pnas.0903410106.

127. Cerling TE, Harris JM, MacFarden BJ, Leakey MG, Quade J, Eisenmann V, et al. Global vegetation change through the Miocene/Pliocene boundary. Nature. 1997; 389 (6647): 153-158. doi: 10.1038/38229.

128. Hoorn C, Bogotá-A. GR, Romero-Baez M, Lammertsma EI, Flantua SGA, Dantas EL, et al. The Amazon at sea: Onset and stages of the Amazon River from a marine record, with special reference to Neogene plant turnover in the drainage basin. Global and Planetary Change. In press. doi: 10.1016/j.gloplacha.2017.02.005.

129. Lisiecki LE, Raymo ME. A Pliocene-Pleistocene stack of 57 globally distributed benthic $\delta^{18}O$ records. Paleoceanography. 2005; 20 (1): PA1003. doi: 10.1029/2004pa001071.

130. Thomé MTC, Sequeira F, Brusquetti F, Carstens B, Haddad CFB, Rodrigues MT, et al. Recurrent connections between Amazon and Atlantic forests shaped diversity in Caatinga four-eyed frogs. Journal of Biogeography. 2016; 43 (5): 1045-1056. doi: 10.1111/jbi.12685.

131. Magalhães IL, Oliveira U, Santos FR, Vidigal TH, Brescovit AD, Santos AJ. Strong spatial structure, Pliocene diversification and cryptic diversity in the Neotropical dry forest spider *Sicarius cariri*. Molecular Ecology. 2014; 23 (21): 5323-5336. doi: 10.1111/mec.12937.

132. Pinheiro F, Cozzolino S, Draper D, de Barros F, Félix LP, Fay MF, et al. Rock outcrop orchids reveal the genetic connectivity and diversity of inselbergs of northeastern Brazil. BMC Evolutionary Biology. 2014; 14 (49): 49. doi: 10.1186/1471-2148-14-49.

Table 1: Sequence description of the five species of the T. *pereirae* complex analyzed herein. *Allele numbers.

Species	Sequence length		GC content (%)		Gaps		Polymorphic sites		Haplotypes	
	nrITS	*rpl32-trnL*	nrITS	*rpl32-trnL*	nrITS	*rpl32-trnL*	nrITS	*rpl32-trnL*	nrITS	*rpl32-trnL*
P. rubrum	626	482–483	63.1–63.3	28.4–28.6	0	1	3 (6*)	4 (8*)	4	5
T. blanchetiana	626	483	62.5–62.8	28.6–29.0	0	0	6 (12*)	3 (6*)	5	4
T. carvalhoi	628–631	483	62.9–63.2	28.4–29.4	0–3	0	7 (14)*	11 (22*)	7	8
T. pereirae	618–631	483	62.8–63.2	28.4–29.6	0–13	0	11 (23*)	12 (24*)	14	17
T. velutina	626	483	62.9–63.3	28.4–29.2	0	0	7 (15*)	9 (18*)	6	8
Total	618–631	482–483	62.5–63.3	28.4–29.6	0–13	0–1	22 (45*)	18 (36*)	33	34

Table 2: Summary of genetic diversity and neutrality tests (Tajima's D and Fu's F) from five species of the *T. pereirae* species complex. Pop prefix=population; nr= nuclear ITS; pl= plastid *rpl32-trnL* intergenic spacer; Haps= Haplotype number; P= Polymorphic sites; *h*=haplotype diversity; π= nucleotide diversity; N= north; S= south; C= central; E= east; W= west.

	Haps		P		*h*		π		Tajima's D		Fu's F	
Species	**nr**	**pl**	**nr**	**pl**	**nr**	**pl**	**nr**	**pl**	**nr**	**pl**	**nr**	**pl**
T. blanchetiana	5	4	6	3	0.6736+/-0.0549	0.1931+/-0.0951	0.0023+/-0.0016	0.0004+/-0.0006	-0.1854	-1.7318*	0.3019	-3.3807*
N (Pop01, 02)	2	1	1	0	0.5263+/-0.0363	0.1000+/-0.0880	0.0008+/-0.0008	0.0002+/-0.0004	1.5650	-1.1644	1.4860	-0.8793
S (Pop03)	3	3	5	2	0.6444+/-0.1012	0.3778+/-0.1813	0.0027+/-0.0019	0.0008+/-0.0009	-0.2286	-1.4008	1.5464	-1.1639*
T. carvalhoi	7	8	9	11	0.7836+/-0.0278	0.5706+/-0.0672	0.0029+/-0.0019	0.0038+/-0.0024	-0.4600	-0.6314	0.2608	-0.4692
C (Pop08)	2	1	1	0	0.2000+/-0.1541	0	0.0003+/-0.0005	0	-1.1117	0	-0.3393	0
N (Pop10, 22)	4	4	5	3	0.7211+/-0.0584	0.5947+/-0.0977	0.0034+/-0.0022	0.0014+/-0.0013	0.6324	-0.5098	2.0161	-0.8647
S (Pop09, 21, 24)	5	4	7	4	0.6046+/-0.0856	0.2506+/-0.1017	0.0018+/-0.0013	0.0007+/-0.0008	-0.6501	-1.7316*	-0.2840	-2.1762*
T. pereirae	14	17	27	18	0.7880+/-0.0329	0.8414+/-0.0258	0.0061+/-0.0034	0.0056+/-0.0033	-0.0063	-0.5860	0.0111	-3.8916
S (Pop07, 11, 12, 23)	3	6	4	9	0.5423+/-0.0558	0.5256+/-0.0738	0.0024+/-0.0016	0.0037+/-0.0024	-0.5635	-0.4522	3.2004	0.4635
E (Pop14, 16, 17)	6	3	7	3	0.7448+/-0.0562	0.7563+/-0.0575	0.0041+/-0.0025	0.0030+/-0.0021	1.3738	-0.1118	1.2261	-0.5445
N (Pop18, 19, 26, 27)	6	6	15	6	0.6474+/-0.0662	0.7910+/-0.0317	0.0023+/-0.0016	0.0045+/-0.0028	-0.5103	1.4521	-0.2017	1.1132
P. rubrum	4	5	3	4	0.2506+/-0.1017	0.5678+/-0.0905	0.0004+/-0.0005	0.0016+/-0.0013	-1.5389*	-0.7173	-2.7159*	-1.3335
W (Pop13, 25)	3	4	2	3	0.2789+/-0.1235	0.4368+/-0.1295	0.0005+/-0.0006	0.0013+/-0.0012	-1.1407	-1.1407	-1.2064*	-1.0615
E (Pop15)	2	2	1	1	0.2000+/-0.1541	0.5333+/-0.0947	0.0003+/-0.0005	0.0011+/-0.0011	-1.1117	1.3027	-0.3393	1.0292
T. velutina	6	8	7	9	0.7923+/-0.0212	0.7256+/-0.0517	0.0038+/-0.0024	0.0028+/-0.0019	1.2756	-1.0755	1.4639	-2.2203
W (Pop04)	2	2	1	2	0.2000+/-0.1541	0.3556+/-0.1591	0.0003+/-0.0005	0.0015+/-0.0014	-1.1117	0.0189	-0.3393	1.5235
E (Pop05, 06)	2	4	1	3	0.5263+/-0.0363	0.3632+/-0.1309	0.0008+/-0.0008	0.0008+/-0.0009	1.5650	-1.4407	1.4860	-2.1353*
S (Pop20)	2	4	4	5	0.2000+/-0.1541	0.6444+/-0.1518	0.0013+/-0.0011	0.0027+/-0.0021	-1.6671*	-1.0353	1.7441	-0.3121

Table 3: Summary of genetic differentiation estimates from all species in the *T. pereirae* complex. *Not significant at p= 0.01.

		All	***P. rubrum***	***T. blanchetiana***	***T. carvalhoi***	***T. pereirae***	***T. velutina***
Nuclear							
	G_{ST}	0.7191	-0.0510*	0.6688	0.7019	0.5808	0.9000
	N_{ST}	0.9170	-0.0256*	0.6491	0.7719	0.8595	0.9180
	N_{ST}-G_{ST}	0.1979	0.0254*	-0.0197*	0.0700*	0.2786	0.0180*
	Φ_{SC}	0.8307	-0.0667*	0.7375	0.7293	0.7456	0.7959
	Φ_{ST}	0.9282	-0.0063*	0.5781	0.7842	0.8797	0.9268
	Φ_{CT}	0.5757	0.0566*	-0.6068*	0.2029*	0.5270	0.6413*
Plastid							
	G_{ST}	0.5883	0.3194	0.0038*	0.5221	0.4667	0.4751
	N_{ST}	0.8012	0.3951	-2.2E-16*	0.8359	0.6964	0.5461
	N_{ST}-G_{ST}	0.2129	0.0756*	-0.0038*	0.3138	0.2297	0.0710*
	Φ_{SC}	0.7077	0.0364*	-0.0526*	0.2191	0.5983	-0.0138*
	Φ_{ST}	0.8188	0.4900	0.0244*	0.8725	0.7219	0.5913
	Φ_{CT}	0.3802	0.4707*	0.0732*	0.8367*	0.3078*	0.5968*

Table 4: Pairwise estimates of genetic differentiation between species: above diagonal plastid, F_{ST} values and below diagonal nuclear F_{ST} values. All values were statistically significant at p= 0.01.

Species	*P. rubrum*	*T. blanchetiana*	*T. carvalhoi*	*T. pereirae*	*T. velutina*
P. rubrum	—	0.8955	0.8068	0.5502	0.7388
T. blanchetiana	0.8398	—	0.8237	0.7164	0.7741
T. carvalhoi	0.6569	0.7070	—	0.1051	0.6495
T. pereirae	0.4220	0.4705	0.1111	—	0.5370
T. velutina	0.5586	0.6130	0.6028	0.3611	—

Table 5: Pairwise comparison of genetic differentiation (F_{ST} estimates) between groups within each species in the *T. pereirae* complex. Above diagonal plastid *rpl32-trnL* intergenic spacer, F_{ST} values and below diagonal nuclear ITS F_{ST} values. * Not significant at p=0.01. Group composition by species — *Pleroma rubrum*: East – 13 and 25, West – 15; *T. blanchetiana*: North – 1 and 2, South – 3; *T. carvalhoi*: North – 10 and 22, Central – 8, South – 9, 21 and 24; *T. pereirae*: North – 18, 19, 26 and 27, South – 7, 11, 12, and 23, East – 14, 16 and 17; *T. velutina*: East – 5 and 6, West – 4, South – 20.

Species	**Groups**	**Groups**		
P. rubrum		East	West	
	East	—	0.4839	
	West	0.0111*	—	
T. blanchetiana		North	South	
	North	—	0.0380*	
	South	0.2284	—	
T. carvalhoi		North	Central	South
	North	—	0.9156	0.1131
	Central	0.6908	—	0.9521
	South	0.0152*	0.7025	—
T. pereirae		North	South	East
	North	—	0.1423	0.4348
	South	0.2271	—	0.5966
	East	0.5937	0.7329	—
T. velutina		East	West	South
	East	—	0.7185	0.6102
	West	0.8845	—	0.2673
	South	0.8274	0.8276	—

Table 6: Likelihood Bayes factor of migration models estimated with Migrate-n v.3.6 for each species of the *T. pereirae* complex *Best migration model.

	P. rubrum		***T. blanchetiana***		***T. carvalhoi***		***T. pereirae***		***T. velutina***	
	nuclear	plastid	nuclear	plastid	nuclear	plastid	nuclear	plastid	nuclear	plastid
Model 1	-1.40	-0.14	-2.24	-4.40	-8.86	-0.90	-0.54	0.00	-1.56	-7.84
Model 2	-1.80	0.00	-1.04	0.00	0.00	-3.26	-6.88	-8.08	-1.68	-8.88
Model 3	-1.70	-2.06	0.00	-4.16	-1.16	-4.82	-12.00*	-14.60	-6.52	-15.26*
Model 4	-2.34	-2.22	-4.72	-3.36	-12.26	-10.68	0.00	-7.26	-2.94	0.00
Model 5	-0.58	-3.82*	-3.10	-4.98	-2.52	0.00	-10.18	-6.94	-7.42*	-7.24
Model 6	-3.04*	-3.76	-6.84	-7.40*	-12.56	-11.42*	-11.36	-16.06*	-0.30	-6.62
Model 7	0.00	-2.04	-6.68	-6.26	-15.36*	-8.32	-8.28	-6.82	-4.56	-12.62
Model 8	-1.42	-2.14	-7.16*	-5.36	-13.76	-9.56	-9.74	-7.18	0.00	-5.72

Supplementary material Table 1: Population numbers, geographic locations, herbarium vouchers, and GenBank accession numbers of nrITS and *rpl32-trnL* sequences from the populations of each species in the *T. pereirae* complex analyzed herein.

Population	Species	Mountain range	Geographic location (latitude / longitude)	Collector number (voucher HUEFS)	Genbank accession numbers nrITS	Genbank accession numbers *rpl32-trnL*
Pop 01	*T. blanchetiana*	Morro do Chapéu	-11.544012 / 41.071793	JG Freitas 791(224499)	KY473081-KY473090	KY473356-KY473365
Pop 02	*T. blanchetiana*	Morro do Chapéu	-11.590269 / 41.207386	JG Freitas 792 (224500)	KY473091-KY473100	KY473366-KY473375
Pop 03	*T. blanchetiana*	Serra da Tromba	-13.150838 / 41.765007	JG Freitas 801(224501)	KY473101-KY473110	KY473376-KY473385
Pop 04	*T.velutina*	Morro do Chapéu	-11.500004 / 41.332506	JG Freitas 793 (224502)	KY473111-KY473120	KY473386-KY473395
Pop 05	*T.velutina*	Serra do Tombador	-11.169701 / 40.511145	JG Freitas 842 (224503)	KY473121-KY473130	KY473396-KY473405
Pop 06	*T.velutina*	Serra do Tombador	-10.665892 / 40.363834	JG Freitas 843 (224504)	KY473131-KY473140	KY473406-KY473415
Pop 07	*T. pereirae*	Serra do Sincorá	-13.314274 / 41.284381	JG Freitas 815 (224505)	KY473141-KY473150	KY473416-KY473425
Pop 08	*T. carvalhoi*	Serra do Sincorá	-12.723895 / 41.506946	JG Freitas 822 (224506)	KY473151-KY473160	KY473426-KY473435
Pop 09	*T.carvalhoi*	Serra do Sincorá	-12.958375 / 41.320275	JG Freitas 814 (224507)	KY473161-KY473170	KY473436-KY473445
Pop 10	*T. carvalhoi*	Serra do Sincorá	-12.455019 / 41.482509	JG Freitas 796 (224508)	KY473171-KY473180	KY473446-KY473455
Pop 11	*T. pereirae*	Serra do Sincorá	-12.998419 / 41.348890	JG Freitas 817 (224509)	KY473181-KY473190	KY473456-KY473465
Pop 12	*T. pereirae*	Serra do Sincorá	-13.000982 / 41.347218	JG Freitas 818 (224510)	KY473191-KY473200	KY473466-KY473475
Pop 13	*P. rubrum*	Serra do Sincorá	-12.998419 / 41.34889	JG Freitas 816 (224511)	KY473201-KY473210	KY473476-KY473485
Pop 14	*T. pereirae*	Serra das Almas	-13.533733 / 41.877499	JG Freitas 838 (224512)	KY473211-KY473220	KY473486-KY473495
Pop 15	*P. rubrum*	Serra das Almas	-13.524427 / 41.956023	JG Freitas 839 (224513)	KY473221-KY473230	KY473496-KY473505
Pop 16	*T. pereirae*	Serra das Almas	-13.522437 / 41.965468	JG Freitas 841 (224514)	KY473231-KY473240	KY473506-KY473515
Pop 17	*T. pereirae*	Serra das Almas	-13.524691 / 41.969567	JG Freitas 840 (224515)	KY473241-KY473250	KY473516-KY473525
Pop 18	*T. pereirae*	Serra do Sincorá	-12.588334 / 41.391389	JG Freitas 803 (224516)	KY473251-KY473260	KY473526-KY473535
Pop 19	*T. pereirae*	Serra do Sincorá	-12.489776 / 41.362092	JG Freitas 800 (224517)	KY473261-KY473270	KY473536-KY473545
Pop 20	*T. velutina*	Serra do Sincorá	-12.872387 / 41.307149	JG Freitas 813 (224518)	KY473271-KY473280	KY473546-KY473555
Pop 21	*T. carvalhoi*	Serra do Sincorá	-12.992717 / 41.348937	JG Freitas 795 (224519)	KY473281-KY473290	KY473556-KY473565
Pop 22	*T. carvalhoi*	Serra do Sincorá	-12.497249 / 41.567415	JG Freitas 794 (224520)	KY473291-KY473300	KY473566-KY473575
Pop 23	*T. pereirae*	Serra do Sincorá	-13.009476 / 41.379928	JG Freitas 820 (224521)	KY473301-KY473310	KY473576-KY473585
Pop 24	*T. carvalhoi*	Serra do Sincorá	-13.008825 / 41.376033	JG Freitas 819 (224522)	KY473311-KY473320	KY473586-KY473595
Pop 25	*P. rubrum*	Serra do Sincorá	-13.006396 / 41.375835	JG Freitas 821 (224523)	KY473321-KY473330	KY473596-KY473605
Pop 26	*T. pereirae*	Serra do Sincorá	-12.5697 / 41.516791	JG Freitas 894 (224524)	KY473331-KY473340	KY473606-KY473615
Pop 27	*T. pereirae*	Serra do Sincorá	-12.571619 / 41.514474	JG Freitas 802 (224525)	KY473341-KY473350	KY473616-KY473625

Supplementary material Table 2: GenBank accession numbers of nrDNA (nrITS, nrETS) and cpDNA (*accd-psaI*, *psbK-psbL*) from 226 specimens of Melastomataceae used in the BEAST v.2.3.2 divergence dating analyses.

Species	ITS	accd	psbK	ETS
Acanthella sprucei Hook	JQ730036	JQ730247	JQ730456	KF462811
Aciotis acuminifolila (Mart. ex DC.) Triana	JQ730037	JQ730248	JQ730457	—
Aciotis circaeifolia (Bonpl.) Triana	JQ730038	JQ730249	JQ730458	KF462812
Aciotis indecora (Bonpl.) Triana	JQ730039	JQ730250	JQ730459	KF462813
Aciotis paludosa (Mart. ex DC.) Triana	JQ730040	JQ730251	JQ730460	KF462814
Aciotis purpurascens (Aubl.) Triana	JQ730041	JQ730252	JQ730461	KF462815
Aciotis rubricaulis (Mart. ex DC.) Triana	JQ730042	JQ730253	JQ730462	KF462816
Acisanthera alsinaefolia (DC.) Triana	JQ730043	JQ730254	JQ730463	KF462817
Acisanthera hedyotidea (C.Presl.) Triana	JQ730044	JQ730255	JQ730464	KF462818
Acisanthera quadrata Persl.	JQ730045	JQ730256	JQ730465	KF462819
Amphorocalyx multiflorus Baker	JQ730046	JQ730257	JQ730466	—
Amphorocalyx rupestris H.Perrier	JQ730047	JQ730258	JQ730467	—
Appendicularia thymifolia (Bonpl.) Triana	JQ730049	JQ730260	JQ730468	KF462820
Arthrostemma primaevum Almeda	JQ730050	JQ730261	JQ730469	KF462821
Brachyotum benthamianum Triana	JQ730051	JQ730262	JQ730470	KF462822
Brachyotum confertum (Bonpl.) Triana	JQ730052	JQ730263	JQ730471	KF462823
Brachyotum fictum Wurdack	JQ730053	JQ730264	JQ730472	KF462824
Brachyotum fraternum Wurdack	JQ730054	JQ730265	JQ730473	—
Brachyotum harlingii Wurdack	JQ730055	JQ730266	JQ730474	KF462825
Brachyotum incrassatum E.Cotton	JQ730056	JQ730267	JQ730475	KF462826
Brachyotum ledifolium (Desr.) Triana	JQ730057	JQ730268	JQ730476	KF462827
Brachyotum lindenii Cogn.	JQ730058	JQ730269	JQ730477	—
Brachyotum microdon (Naudin) Triana	JQ730059	JQ730270	JQ730478	KF462828
Brachyotum rostratum (Naudin)	JQ730060	JQ730271	JQ730479	—
Bucquetia glutinosa DC.	JQ730061	JQ730272	JQ730480	—
Cambessedesia espora (A.St.Hil. Ex Bonpl.) DC.	JQ730062	JQ730273	JQ730481	KF462834
Cambessedesia hilariana (A.St.Hil. ex Bonpl.) DC.	JQ730063	JQ730274	JQ730482	KF462835
Castratella piloseloides (Bonpl.) Naudin	JQ730064	JQ730275	JQ730483	KF462836
Centradenia grandifolia (Schltdl.) Endl. Ex Walp.	JQ730065	JQ730276	—	KF462837
Centradenia inaequilateralis (Schltdl. & Cham.) G.Don	JQ730066	JQ730277	JQ730484	KF462838
Chaetolepis cufodontisii Standl.	JQ730067	JQ730278	JQ730485	—
Chaetolepis microphylla (Bonpl.) Miq.	JQ730068	JQ730279	JQ730486	—
Chaetostoma armatum (Spreng.) Cogn.	JQ730069	JQ730280	JQ730487	—
Comolia microphylla Benth.	JQ730070	JQ730281	JQ730488	KF462841
Comolia sertularia (DC.) Triana	JQ730071	JQ730282	JQ730489	KF462842
Comolia vernicosa (Benth.) Triana	JQ730072	JQ730283	JQ730490	KF462843
Desmoscelis villosa (Aubl.) Naudin	JQ730073	JQ730284	JQ730491	KF462844
Dichaetanthera africana Jacq-Fél.	JQ730074	JQ730285	JQ730492	KF462845
Dichaetanthera oblongifolia Baker	JQ730075	JQ730286	JQ730493	—
Dionycha bojeri Naudin	JQ730076	JQ730287	JQ730494	—
Dissotis cf. phaeotricha Harv.	JQ730078	JQ730289	JQ730496	—
Dissotis multiflora (Sm.) Triana	JQ730077	JQ730288	JQ730495	KF462846
Eriocnema fulva Naudin	EF418811	JQ730291	JQ730497	—
Ernestia confertiflora Wurdack	JQ730079	JQ730292	JQ730498	—
Ernestia glandulosa Gleason	JQ730080	JQ730293	JQ730499	KF462847
Ernestia pullei Gleason	JQ730081	JQ730294	JQ730500	KF462848
Ernestia tenella (Bonpl.) DC.	JQ730082	JQ730295	JQ730501	—
Fritzschia erecta Cham.	JQ730083	JQ730296	JQ730502	KF462849
Graffenrieda latifolia (Naudin) Triane	AY460450	JQ730297	JQ730503	—
Graffenrieda moritziana Triana	AY460451	JQ730298	JQ730504	—
Heterocentron elegans (Schltdl.) Kuntze	JQ730085	JQ730299	JQ730506	KF462850
Heterocentron muricatum Gleason	JQ730086	JQ730300	JQ730507	KF462851
Heterocentron subtriplinervium (Link & Otto) A.Braun & C.D.Bouché	JQ730087	JQ730301	JQ730508	KF462852

Species	ITS	accd	psbK	ETS
Heterotis decumbens (P.Beauv.) Trian	JQ730088	JQ730302	JQ730509	KF462853
Itatiaia cleistopetala Ule	JQ730090	JQ730303	JQ730510	KF462854
Lavoisiera imbricata (Thunb.) DC.	JQ730091	JQ730304	JQ730511	—
Lavoisiera mucorifera Mart. Ex Schrank ex DC.	JQ730092	JQ730305	JQ730512	—
Lavoisiera pulchella Cham.	JQ730093	JQ730306	JQ730513	KF462857
Macairea radula (Bonpl.) DC.	JQ730095	JQ730307	JQ730514	KF462859
Macairea thyrsiflora DC.	JQ730096	JQ730308	JQ730515	KF462860
Marcetia eimeriana A.B.Martins & E.M.Woodgyer	JQ730098	JQ730309	JQ730517	—
Marcetia ericoides Cogn.	JQ730099	JQ730310	JQ730518	—
Marcetia taxifolia (A.St.Hil.) DC.	JQ730102	JQ730311	JQ730521	—
Melastoma candidum D.Don	JQ730103	JQ730312	JQ730522	—
Melastoma denticulatum Labill.	JQ730104	JQ730313	JQ730523	KF462861
Melastoma malabathrichum L.	JQ730105	JQ730314	JQ730524	—
Melastoma sanguineum Sims	JQ730106	JQ730315	JQ730525	—
Meriania brevipedunculata Judd & Skean	KJ933971	KJ933883	KJ934024	KJ933924
Meriania ekmanii Urb.	KJ933972	KJ933884	KJ934025	KJ933925
Meriania longifolia (Naudin) Cogn.	AY460454	JQ730316	JQ730526	—
Meriania parvifolia Judd & Skean	KJ933973	KJ933885	KJ934026	KJ933926
Meriania squamulosa Urb. & Ekman	KJ933974	KJ933886	KJ934027	KJ933927
Miconia dodecandra (Desr.) Cogn.	AY460506	JQ730317	JQ730527	—
Miconia rubrisetulosa Ionta, Judd & Skean	KJ934005	KJ933906	KJ934058	KJ933952
Miconia schlimii Triana	KM893625	KM886962	KM893648	KM893560
Miconia sp.	KJ934006	KJ933907	KJ934059	KJ933953
Miconia tomentosa (Rich.) D.Don ex DC.	EF418905	JQ730318	JQ730528	—
Miconia uninervis Alain	KM893638	KM886987	KM893679	KM893459
Miconia woodsii (Judd & Skean) Ionta, Judd & Skean	KJ934007	KJ933908	KJ934060	KJ933954
Microlepis oleaefolia (DC.) Triana	JQ730107	JQ730319	JQ730529	KF462862
Monochaetum bonplandii (Kunth.) Naudin	JQ730108	JQ730320	JQ730530	—
Monochaetum discolor H. Karst. Ex Triana	JQ730109	JQ730321	JQ730531	KF462863
Monochaetum humboldtianum Walp.	JQ730110	JQ730322	JQ730532	KF462864
Monochaetum meridense Naudin	JQ730111	JQ730323	JQ730533	—
Monochaetum polyneuron Triana	JQ730112	JQ730324	JQ730534	—
Monochaetum uribei Wurdack	JQ730113	JQ730325	JQ730535	KF462866
Monochaetum volcanicum Cogn.	JQ730114	JQ730326	JQ730536	KF462867
Nepsera aquatica (Aubl.) Naudin	JQ730115	JQ730327	JQ730537	—
Osbeckia australiana Naudin	JQ730116	JQ730328	JQ730538	KF462868
Osbeckia nepalensis Hook.	JQ730118	JQ730329	JQ730539	—
Osbeckia stellata Buch.-Ham. ex Ker Gawl	JQ730119	JQ730330	JQ730540	—
Pachyloma huberioides (Naudin) Triana	JQ730120	JQ730331	JQ730541	KF462870
Physeterostemon tomasii Amorim, Michelangeli & Goldenb.	JQ730121	JQ730332	JQ730542	—
Pilocosta campanensis (Almeda & Whiffin) Almeda	JQ730122	JQ730333	JQ730543	KF462871
Pilocosta nana (Standl.) Almeda & Whiffin	JQ730123	JQ730334	JQ730544	KF462872
Pilocosta nubicola Almeda	JQ730124	JQ730335	JQ730545	KF462873
Pilocosta oerstedii (Triana) Almeda & Whiffin	JQ730125	JQ730336	JQ730546	KF462874
Pterogastra divaricata (Bonpl.) Naudin	JQ730126	JQ730337	JQ730547	AY460434
Pterogastra minor Naudin	JQ730127	JQ730338	JQ730548	—
Pterolepis alpestris (DC.) Triana	JQ730128	JQ730339	JQ730549	—
Pterolepis glomerata (Rottb.) Miq.	JQ730129	JQ730340	JQ730550	KF462876
Pterolepis parnasiifolia (DC.) Triana	JQ730130	JQ730341	JQ730551	—
Pterolepis repanda (DC.) Triana	JQ730131	JQ730342	JQ730552	—
Pterolepis rotundifolia Wurdack	JQ730132	JQ730343	JQ730553	—
Pterolepis sp.	JQ730133	JQ730344	JQ730554	KF462877
Rhexia aristosa Britton	JQ730134	JQ730345	JQ730555	KF462878
Rhexia virginica L.	JQ730136	JQ730346	JQ730557	KF462879
Rhynchanthera bracteata Triana	JQ730137	JQ730347	JQ730558	KF462880
Rhynchanthera grandiflora (Aubl.) DC	JQ730138	JQ730348	JQ730559	KF462881

Species	ITS	accd	psbK	ETS
Rhynchanthera serrulata (Rich.) DC.	AY460435	JQ730349	JQ730560	—
Rousseauxia andringitrensis (H.Perrier) Jacq.-Fél.	JQ730139	JQ730350	JQ730561	—
Rousseauxia minimifolia (Jum. & H.Perrier) Jacq.-Fél.	JQ730140	JQ730351	JQ730562	—
Sandemania hoehnei (Cogn.) Wurdack	JQ730141	JQ730352	JQ730563	KF462882
Siphanthera hostmanii Cogn.	JQ730142	JQ730353	JQ730564	KF462883
Svitramia hatschbachii Wurdack	JQ730143	JQ730354	JQ730565	KF462886
Svitramia minor R.Romero & A.B.Martins	JQ730144	JQ730355	JQ730566	KF462887
Svitramia pulchra Cham.	JQ730145	JQ730356	JQ730567	KF462888
Svitramia sp. 1	KF463036	KF407969	KF463011	KF462884
Svitramia sp. 2	KF463037	KF407970	KF463012	KF462885
Svitramia wurdackiana R.Romero & A.B.Martins	JQ730148	JQ730359	JQ730570	KF462889
Tibouchina aemula (Triana) Cogn.	JQ730149	JQ730360	JQ730572	KF462891
Tibouchina alpestris Cogn.	JQ730150	JQ730361	JQ730573	—
Tibouchina angustifolia (Naudin) Cogn.	JQ730151	JQ730362	JQ730574	KF462892
Tibouchina arborea (Gardn.) Cogn.	JQ730152	JQ730363	JQ730575	KF462893
Tibouchina arenaria Cogn.	JQ730153	JQ730364	JQ730576	KF462894
Tibouchina aspera Aubl.	JQ730154	JQ730365	JQ730577	KF462895
Tibouchina aspera var asperima Cogn.	JQ730155	JQ730366	JQ730578	KF462896
Tibouchina axillaris Cogn.	JQ730156	JQ730367	JQ730579	KF462897
Tibouchina barnebyana Wurdack	JQ730157	JQ730368	—	KF462898
Tibouchina benthamiana (Gardn.) Cogn.	JQ730158	JQ730369	JQ730580	KF462899
Tibouchina bicolor (Naudin) Cogn.	JQ730159	JQ730370	JQ730581	KF462900
Tibouchina bipenicillata (Naudin) Cogn.	JQ730160	JQ730371	JQ730582	KF462901
Tibouchina blanchetiana Cogn.	JQ730161	JQ730372	—	KF462902
Tibouchina boudetii P.J.F.Guim. & Goldenb.	JQ730162	JQ730373	JQ730583	KF462903
Tibouchina breedlovei Wurdack	JQ730163	JQ730374	JQ730584	KF462904
Tibouchina brevisepala Cogn.	KF463039	KF407972	—	KF462905
Tibouchina calycina Cogn.	KF463040	KF407973	—	KF462906
Tibouchina candolleana (DC.) Cogn.	JQ730164	JQ730375	JQ730585	KF462907
Tibouchina cardinalis (Bonpl.) Cogn.	JQ730165	JQ730376	JQ730586	KF462908
Tibouchina castellensis Brade	JQ730166	JQ730377	JQ730587	KF462909
Tibouchina cerastifolia (Naudin) Cogn.	JQ730167	—	JQ730588	KF462910
Tibouchina chamaecistus (Naudin) Cogn.	JQ730168	JQ730378	JQ730589	—
Tibouchina ciliaris (Vent.) Cogn.	JQ730169	—	JQ730590	KF462911
Tibouchina cinerea Cogn.	JQ730170	JQ730379	JQ730591	KF462912
Tibouchina citrina (Naudin) Cogn.	JQ730171	JQ730380	JQ730592	KF462913
Tibouchina clavata (Pers.) Wurdack	JQ730172	JQ730381	JQ730593	KF462914
Tibouchina clidemiodes (O.Berg ex Triana) Cogn.	JQ730173	JQ730382	—	KF462915
Tibouchina clinopodifolia (DC.) Cogn.	JQ730174	JQ730383	JQ730594	KF462916
Tibouchina confertiflora (Naudin) Cogn.	JQ730175	JQ730384	JQ730595	—
Tibouchina corymbosa (Raddi) Cogn.	JQ730176	JQ730385	JQ730596	KF462918
Tibouchina cristata Brade	JQ730177	JQ730386	JQ730597	KF462919
Tibouchina cryptadena Gleason	JQ730178	JQ730387	JQ730598	KF462920
Tibouchina dimorphylla Gleason	KF463044	—	KF463017	KF462921
Tibouchina dubia (Cham.) Cogn.	JQ730179	JQ730388	JQ730599	KF462923
Tibouchina estrellensis (Raddi) Cogn.	JQ730180	JQ730389	JQ730600	KF462924
Tibouchina fissinervia DC.	JQ730181	JQ730390	JQ730601	KF462925
Tibouchina fothergillae (Schrank & Mart. ex DC.) Cogn.	JQ730182	JQ730391	JQ730602	KF462926
Tibouchina foveolata Cogn.	JQ730183	JQ730392	JQ730603	KF462927
Tibouchina fraterna N.E.Br.	JQ730184	JQ730393	JQ730604	KF462928
Tibouchina frigidula (DC.) Cogn.	JQ730185	JQ730394	JQ730605	KF462929
Tibouchina gardneriana (Triana) Cogn.	JQ730186	JQ730395	JQ730606	KF462930
Tibouchina gayana (Naudin) Cogn.	JQ730187	JQ730396	JQ730607	KF462931
Tibouchina geitneriana (Schltdl.) Cogn.	JQ730188	JQ730397	JQ730608	—
Tibouchina gleasoniana Wurdack	JQ730189	—	JQ730609	KF462932
Tibouchina gracilis (Bonpl.) Cogn.	JQ730190	JQ730398	JQ730610	KF462933
Tibouchina granulosa (Desr.) Cogn.	JQ730191	JQ730399	JQ730611	KF462934

Species	ITS	accd	psbK	ETS
Tibouchina grossa (L.f.) Cogn.	JQ730192	JQ730400	JQ730612	KF462935
Tibouchina heteromalla (D.Don) Cogn.	JQ730193	JQ730401	JQ730613	KF462936
Tibouchina hieracioides (DC.) Cogn.	JQ730194	JQ730402	JQ730614	KF462937
Tibouchina hospita (DC.) Cogn.	JQ730195	JQ730403	JQ730615	KF462938
Tibouchina inopinata Wurdack	JQ730196	JQ730404	JQ730616	KF462939
Tibouchina itatiaiae Cogn.	JQ730197	JQ730405	JQ730617	KF462940
Tibouchina kleinii Wurdack	JQ730198	JQ730406	JQ730618	KF462941
Tibouchina laevicaulis Wurdack	JQ730199	JQ730407	JQ730619	KF462942
Tibouchina laxa (Desr.) Cogn.	JQ730200	JQ730408	JQ730620	—
Tibouchina lepidota (Bonpl.) Baill.	JQ730201	JQ730409	JQ730621	KF462943
Tibouchina lindeniana Cogn.	JQ730202	JQ730410	JQ730622	KF462944
Tibouchina llanorum Wurdack	JQ730203	JQ730411	JQ730623	KF462945
Tibouchina longifolia (Vahl) Baill.	JQ730204	JQ730412	JQ730624	—
Tibouchina macrochiton (Mart. Ex DC) Cogn.	JQ730205	JQ730413	JQ730625	KF462946
Tibouchina manicata Cogn.	JQ730206	JQ730414	JQ730626	KF462947
Tibouchina mariae Wurdack	KF463046	KF407979	KF463019	KF462948
Tibouchina martialis (Cham.) Cogn.	JQ730207	JQ730415	JQ730627	KF462950
Tibouchina martiusiana (DC.) Cogn.	JQ730208	JQ730416	JQ730628	KF462951
Tibouchina melanocalyx R.Romero, P.J.F. Guimaraes & Leoni	JQ730209	JQ730417	JQ730629	KF462952
Tibouchina microphylla Cogn. Ex Schwacke	JQ730210	JQ730418	JQ730630	KF462953
Tibouchina minor Cogn.	JQ730211	JQ730419	JQ730631	KF462954
Tibouchina mollis (Bonpl.) Cogn.	JQ730212	JQ730420	JQ730632	KF462955
Tibouchina mutabilis Cogn.	JQ730213	JQ730421	JQ730633	KF462957
Tibouchina naudiniana (Decne) Cogn.	JQ730214	JQ730422	JQ730634	KF462958
Tibouchina nodosa Wurdack	JQ730215	JQ730423	JQ730635	KF462959
Tibouchina octopetala Cogn.	JQ730216	JQ730424	JQ730636	—
Tibouchina oreophilla Wurdack	JQ730217	JQ730425	JQ730637	KF462960
Tibouchina ornata (Sw.) Baill.	JQ730218	JQ730426	JQ730638	KF462961
Tibouchina papyrus (Pohl) Toledo	JQ730219	JQ730427	JQ730639	KF462962
Tibouchina pendula Cogn.	JQ730220	JQ730428	JQ730640	KF462963
Tibouchina pereirae Brade & Markgr.	JQ730221	JQ730429	JQ730641	KF462964
Tibouchina pleromoides J.F.Macbr.	KF463047	KF407980	KF463020	—
Tibouchina pulchra (Cham.) Cogn.	JQ730222	JQ730430	JQ730642	KF462965
Tibouchina radula Markgr.	JQ730223	JQ730431	JQ730643	—
Tibouchina ramboi Brade	JQ730224	JQ730432	JQ730644	KF462966
Tibouchina salviifolia Cogn.	JQ730225	JQ730433	JQ730645	KF462967
Tibouchina saxosa Gleason	KF463048	KF407981	KF463021	KF462968
Tibouchina sebastianopolitana (Raddi) Cogn.	JQ730226	JQ730434	JQ730646	KF462969
Tibouchina sellowiana Cogn.	JQ730227	JQ730435	JQ730647	KF462970
Tibouchina semidecandra (Schrank & Mart. ex DC.) Cogn.	JQ730228	JQ730436	JQ730648	KF462971
Tibouchina sp. 1	JQ730231	JQ730439	JQ730651	KF462972
Tibouchina sp. 2	JQ730232	JQ730440	JQ730652	—
Tibouchina sp. 3	JQ730229	JQ730437	JQ730649	KF462949
Tibouchina sp. 4	KF463050	KF407982	KF463022	KF462974
Tibouchina sp. 5	KF463051	KF407983	KF463023	—
Tibouchina stenocarpa (DC.) Cogn.	JQ730233	JQ730441	JQ730653	KF462976
Tibouchina striphnocalyx (DC.) Pittier	JQ730234	JQ730442	JQ730654	KF462977
Tibouchina trichopoda (DC.) Baill.	JQ730235	JQ730443	JQ730655	KF462978
Tibouchina trinervia Cogn.	—	JQ730444	JQ730656	KF462979
Tibouchina urceolaris (DC.) Cogn.	JQ730236	JQ730445	JQ730657	KF462980
Tibouchina ursina (Cham.) Cogn.	JQ730237	JQ730446	JQ730658	KF462982
Tibouchina valtheri Cogn.	JQ730238	JQ730447	JQ730659	KF462983
Tibouchina velutina (Naudin) Cogn.	JQ730239	JQ730448	JQ730660	KF462984
Tibouchina wurdackii Almeda & Todzia	JQ730240	JQ730449	JQ730661	KF462985
Tibouchinopsis mirabilis Brade & Marckgr.	JQ730241	JQ730450	JQ730662	KF462986
Trembleya parviflora Cogn.	JQ730242	JQ730451	JQ730663	KF462987
Tristemma coronatum Benth.	JQ730243	JQ730452	JQ730664	—

Species	ITS	accd	psbK	ETS
Tristemma hirtum P. Beauv.	JQ730244	JQ730453	JQ730665	KF462988
Tristemma littorale Benth.	JQ730245	JQ730454	JQ730666	KF462989
Tristemma mauritianum J.F.Gmel.	JQ730246	JQ730455	JQ730667	—

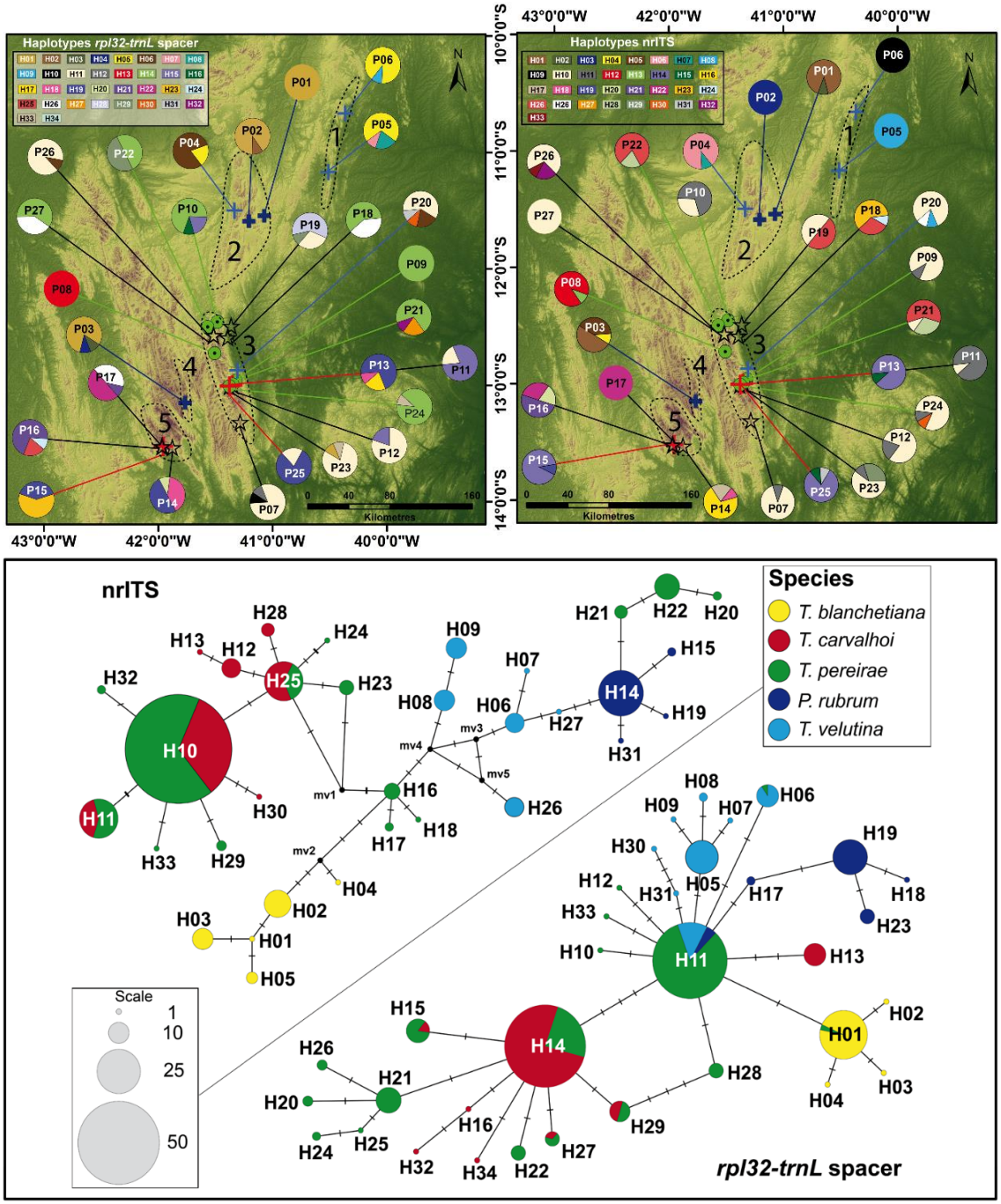

Figure 1: Above, diversity of haplotypes and geographic distribution of each of them in each population and species in the *T. pereirae* complex for both nrITS and *rpl32-trnL* data. The dotted lines represent groups of populations in the areas of each mountain in the Chapada Diamantina. **1.** Serra do Tombador, **2.** Morro do Chapéu, **3.** Serra do Sincorá, **4.** Serra da Tromba, **5.** Serra das Almas. Below, phylogenetic relationships among the haplotypes of each species, obtained through Network.

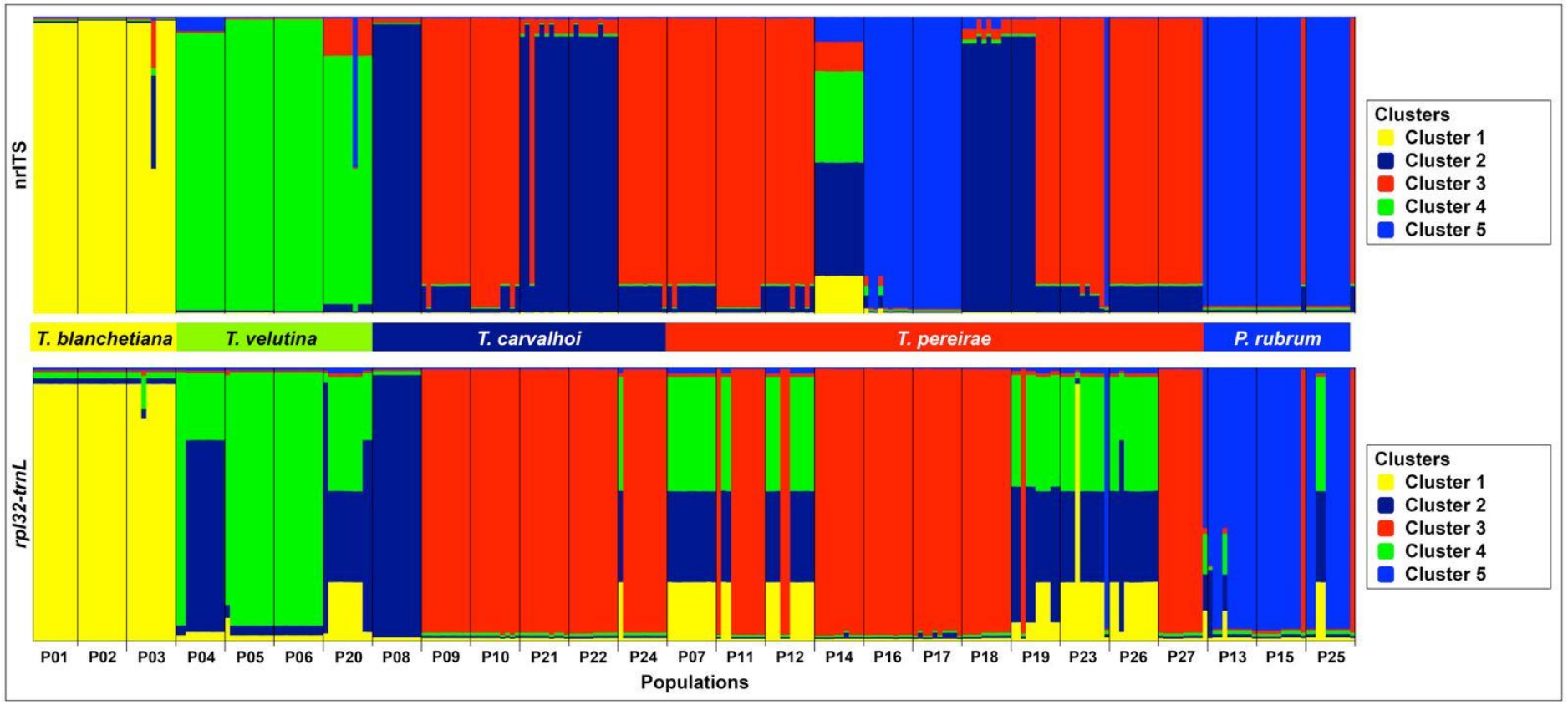

Figure 2: Structuring of genetic diversity in the *T. pereirae* complex, optimal alignment of individuals using nrITS and *rpl32-trnL* data, with the best number of genetic clusters obtained from the analyzes performed in STRUCTURE v.2.3.4 and CLUMPAK v.1.1., Comparing with the traditional morphological delimitation of the species of the complex.

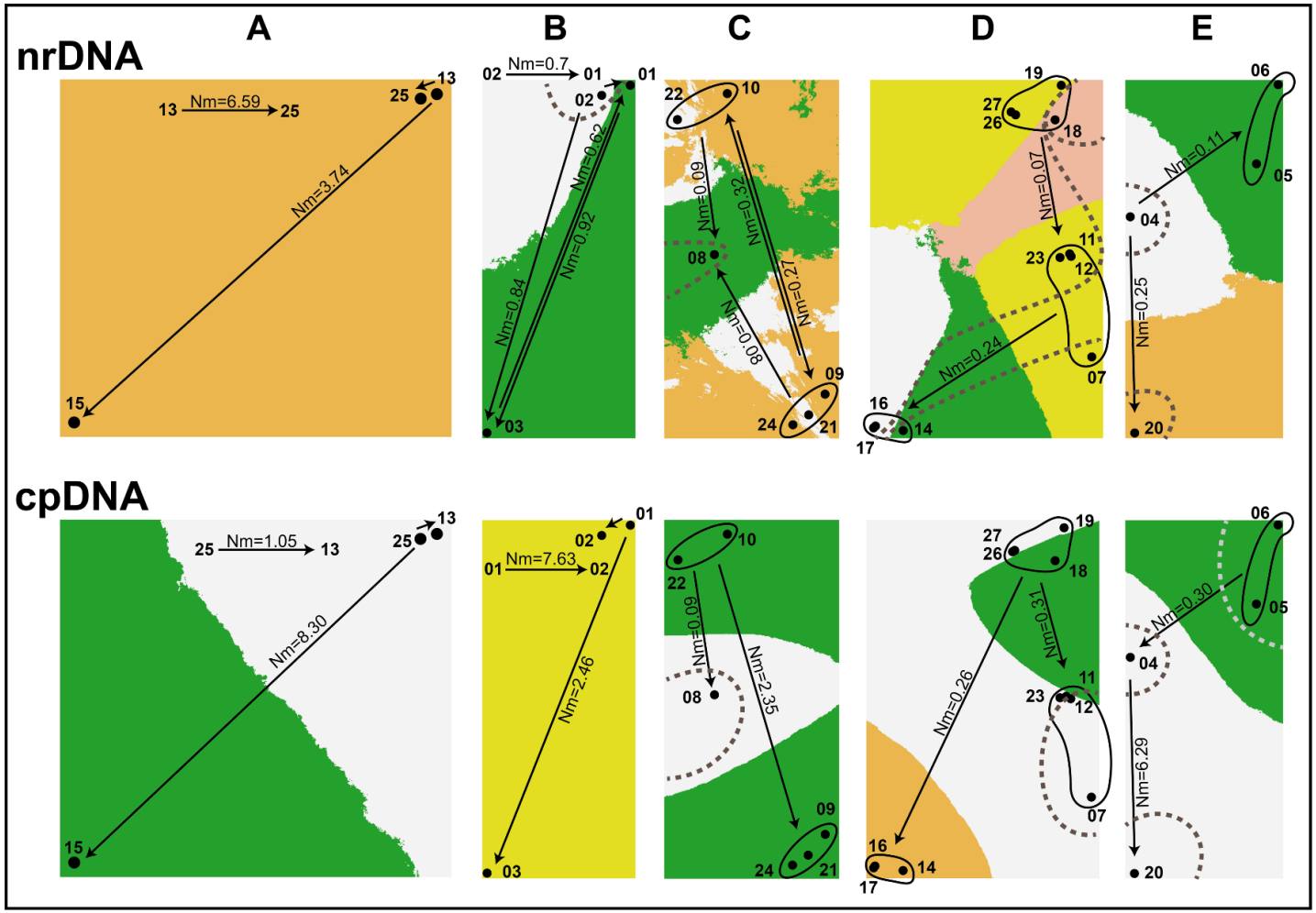

Figure 3: Spatial structure of the populations in each species of the *T. pereirae* complex, through the "Geneland" analyzes (colored background); Migration patterns obtained through Migrate-n analysis (continuous line drawings); And barriers to gene flow, estimated from the Monmonier analysis (gray dotted lines). **A.** *Pleroma rubrum*; **B.** *Tibouchina blanchetiana*; **C.** *T. carvalhoi*; **D.** *T. pereirae* and **E.** *T. velutina*; **Nm** = estimated number of immigrants.

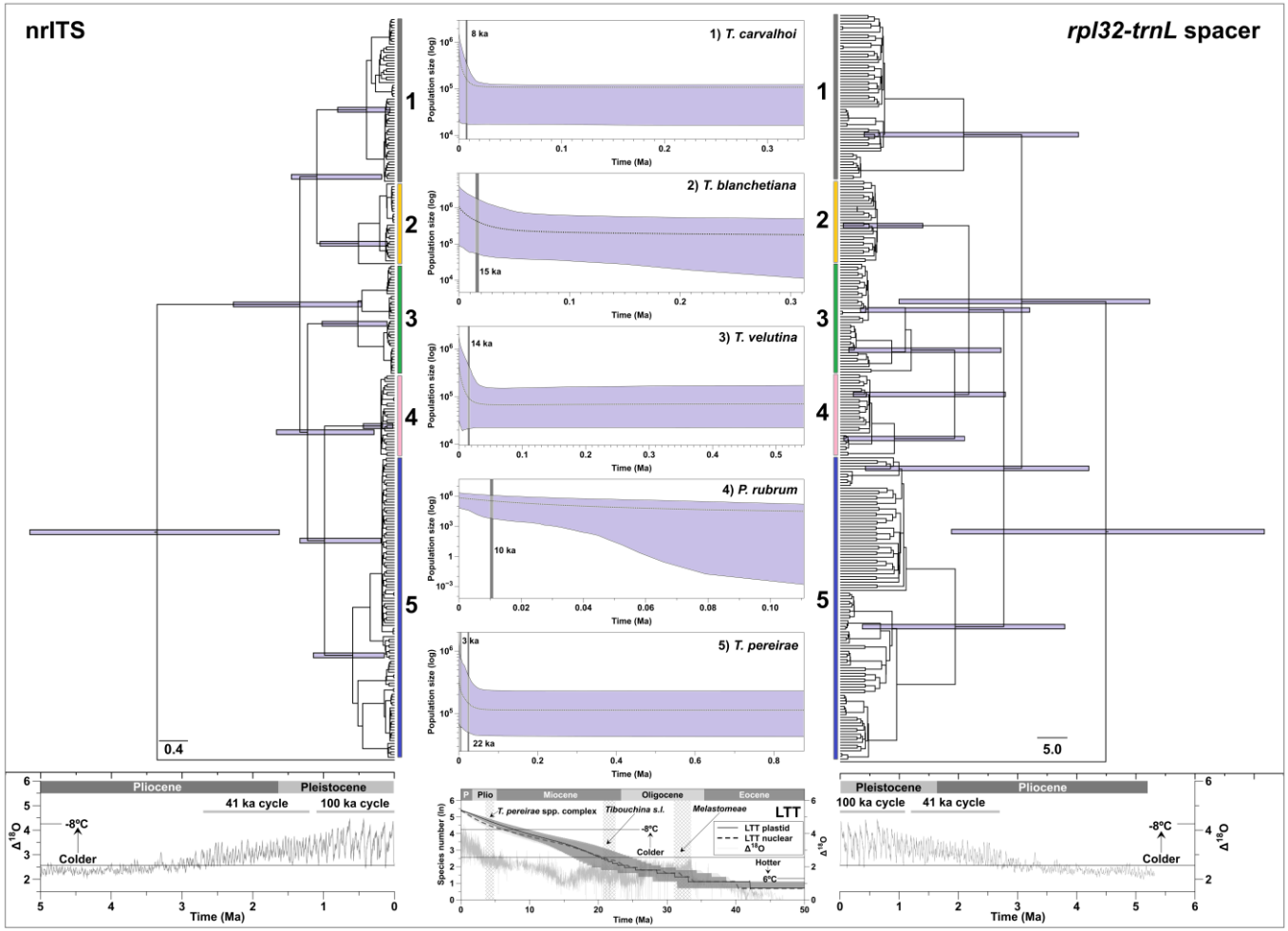

Figure 4: Graphical representations of divergence times estimated by analysis in BEAST v.2.3.2 with population data using nrITS and *rpl32-trnL*, inference of lineages through time (LTT) by means of Melastomeae dating analyzes and demographic reconstructions (Extended Bayesian Skyline Plots) for each species in the *T. pereirae* complex.

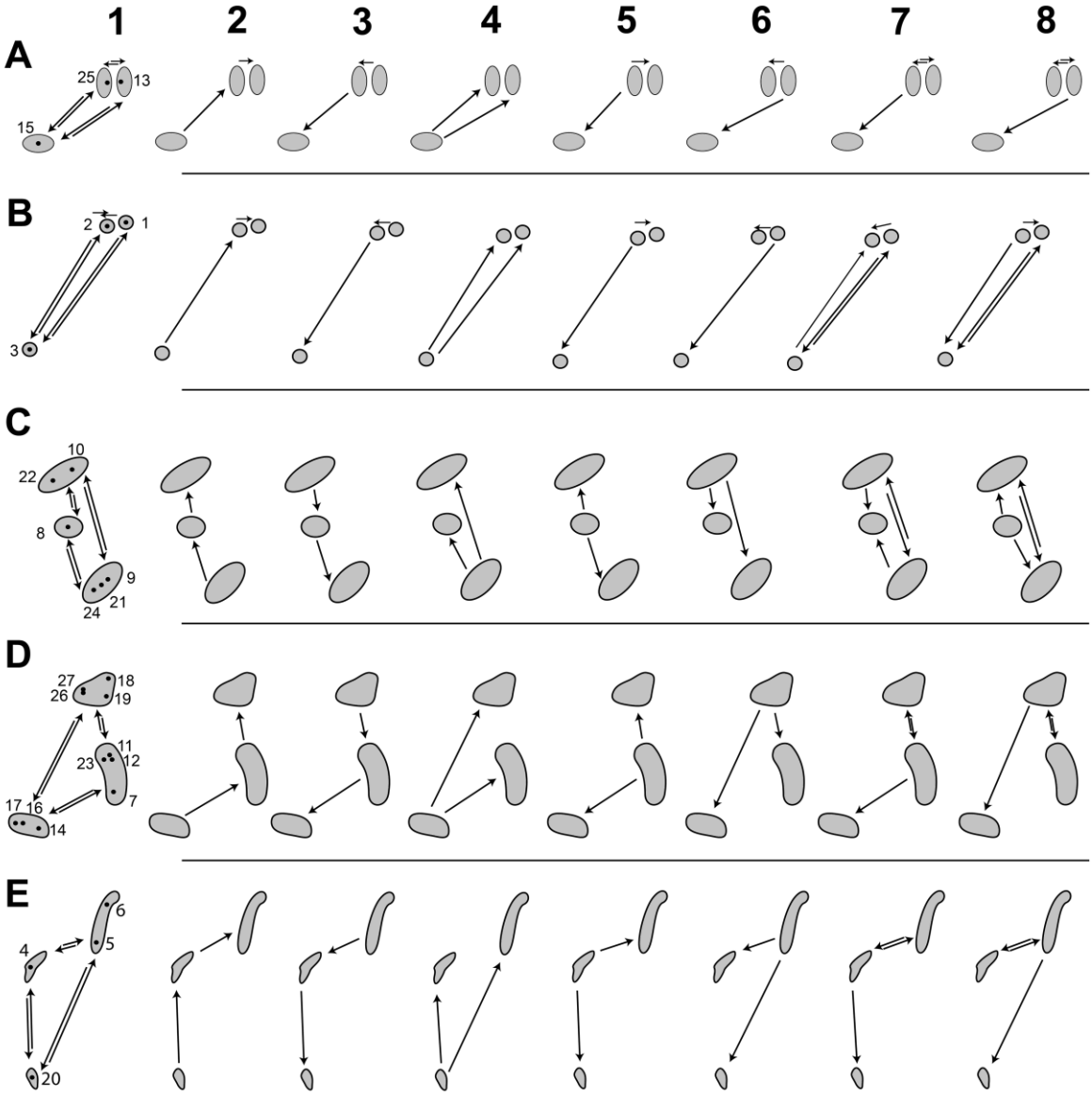

Supplementary material figure 1: The eight migration models evaluated in the Migrate-n analysis of each species in the *T. pereirae* complex. Circles correspond to groups of populations in different mountains, single arrows indicate the unidirectional genetic flow, double arrows indicate bi-directional gene flow. **A**. *Pleroma rubrum*; **B**. *Tibouchina blanchetiana*; **C**. *T. carvalhoi*; **D**. *T. pereirae*; **E**. *T. velutina*.

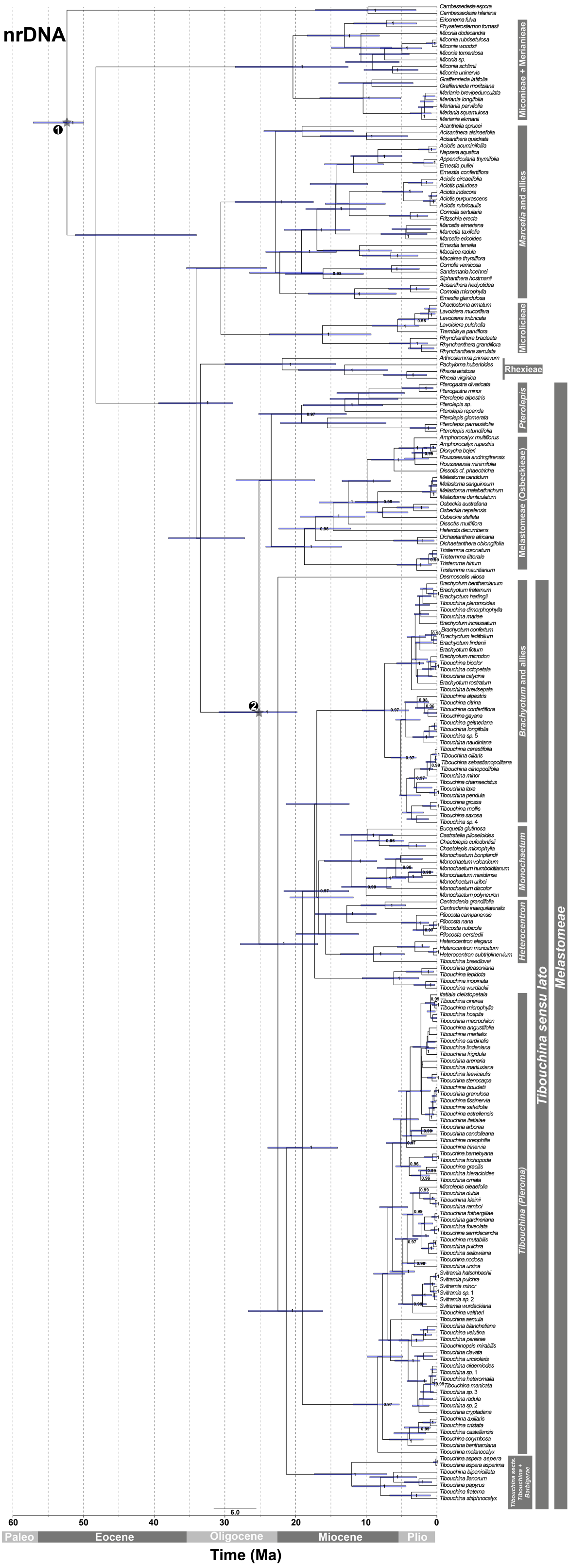

Supplementary material Figure 2: Maximum credibility Bayesian tree estimated with BEAST v2.3.2 from nrDNA (nrITS– nrITS1, 5.8S, and nrITS2; and nrETS) data from 226 specimens of Melastomataceae. Stars indicate fossil calibrating points in the analysis: 1) Melastomataceae fossil leaves ~50 Ma; 2) Melastomeae-like cochleate seeds ~23 Ma.

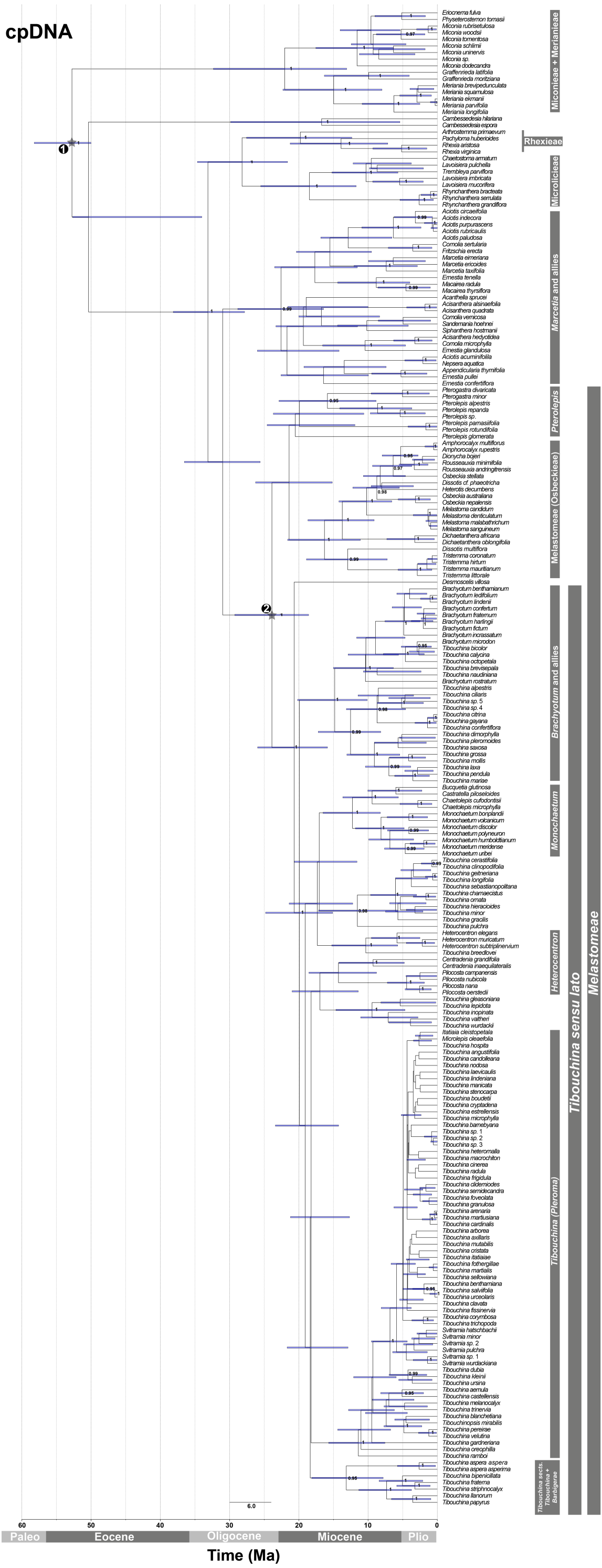

Supplementary material Figure 3: Maximum credibility Bayesian tree estimated with BEAST v2.3.2 from cpDNA (*accd-psaI* and *psbK-psbL*) data from 226 specimens of Melastomataceae. Stars indicate fossil calibration points: 1) Melastomataceae fossil leaves ~50 Ma; 2) Melastomeae-like cochleate seeds ~23 Ma.

Capítulo II[2]

[2] Artigo formatado de acordo com as normas do periódico *Annals of Botany*

Leaf shape and size variation in the *T. pereirae* species complex: species separation and phylogenetic signal

Background and aims: Leaf symmetry, shape and size variation in several groups of plants is far for being accounted. Leaf variation has been proved useful for answering taxonomic or evolutionary questions and has recently been analysed with a diverse set of geometric morphometrics tools. *Tibouchina* is one of the most diverse lineages of Melastomataceae in Brazil and, particularly, of the Espinhaço mountain range of Bahia and Minas Gerais states. Several species are endemic to this mountain region. Among them, the *Tibouchina pereirae* species complex inhabits the northern part (Chapada Diamantina). Leaf variation among species and populations within the group was evident from field prospections. Thus, an account of leaf shape and size variation from these species is here presented to address questions on the taxonomic utility and phylogenetic signal of leaf traits in this group. **Methods:** We analysed leaf shape, size, and symmetry through geometric morphometrics in all five species of the *T. pereirae* species complex. A group of species that inhabits the harsh environments of the *campos rupestres* of Bahia. Five hundred and thirty nine individuals from 27 localities spanning most of their distribution range were collected and analysed. The leaves of these individuals were analysed with a diverse set of geometric morphometrics tools to determine patterns of variation in shape, symmetry, and size. These traits were also analysed for their taxonomic utility and phylogenetic signal. **Key Results:** Leaf shape variation in this group of species was complex. Size was correlated with shape and statistically significant for explaining shape variation. Each species had different allometric trends with separate intercepts. There was evidence of three kinds of asymmetry in the species group, directional asymmetry (DA), fluctuating asymmetry (FA) and antisymmetry (AS). Directional asymmetry and FA were statistically significant for all species. Patterns of asymmetry within species revealed populations with left- or right-handed DA, or antisymmetry (AS). Within-species differentiation was obvious for shape and size traits as well as asymmetry patterns but they were discordant. Species separation from Canonical Variate Analysis (CVA) analyses of size-corrected of the shape was supported by multi-response permutation procedure (MRPP) analyses with high statistical significance. However, size was not negligible for species differentiation. These leaf and size traits had no phylogenetic signal and were not correlated with phylogenetic distance except for a positive correlation on one of the shape

traits (CV2) for small phylogenetic distances. **Conclusions:** Size was correlated with shape variation in the *T. pereirae* species complex. The differences of allometric trends between species were probably a result of distinct environmental pressures on each species; the most variable species were precisely the ones with wide distribution ranges. Size-corrected shape was sufficient for species differentiation. Limits of *T. pereirae* with *T. carvalhoi* and *T. velutina* were diffuse but supported by MRPP analysis. However, accounting for size variation lead to a more conspicuous species differentiation. Leaf shape and size in this species group were apparently evolving toward diverging morphospaces. Thus, phylogenetic distance was not correlated to shape (CV1) or size and there was no significant phylogenetic signal of any leaf trait.

Keywords: Antisymmetry, Brazil, Directional asymmetry, Fluctuating asymmetry, Leaf geometric morphometrics, Melastomeae, Phylogenetic signal, Phylomorphospace, *Tibouchina pereirae* species complex.

INTRODUCTION

Plants respond to environmental heterogeneity by either local adaptation or phenotypic plasticity. The first implies possible genetic modifications and population differentiation whereas the second involves optimal phenotype expression on each environment without genetic differentiation (Kawecki and Ebert, 2004; Pfennig *et al*., 2010; Palacio-López *et al*., 2015; Volis *et al*., 2015). Local adaptation and phenotypic plasticity can have diffuse limits, lead to similar results, and be not mutually exclusive (Kawecki and Ebert, 2004; Pfennig *et al*., 2010; Volis *et al*., 2015). Furthermore, both processes produce patterns of variation among populations and species, and contribute to generating new species or adaptive radiations (Kawecki and Ebert, 2004; Pfennig *et al*., 2010).

Thus, character variation in plants and, possibly, population or species divergence can be driven by environmental heterogeneity through local adaptation or phenotypic plasticity (Kawecki and Ebert, 2004; Pfennig *et al*., 2010; Glennon and Cron, 2015). Leaf shape and size are important characters for plant fitness and its variation is regulated by similar genetic architectures (Andres *et al*., 2014; Dkhar and Pareek, 2014; Ichihashi *et al*., 2014; Vlad *et al*., 2014; Ferris *et al*., 2015). Leaf symmetry, shape or size variations among closely related species are reported as responses to genetic factors, environmental heterogeneity or biological pressures. This leaf variation among individuals, populations, and species has been studied extensively in search for ecological or evolutionary meaning (Glennon and Cron, 2015; Viscosi, 2015).

Bilateral symmetry is generally divided in matching symmetry and object symmetry; the first one denotes symmetry between two corresponding objects, e.g. the wings of a fly; the second one indicates symmetry within an object, e.g. a leaf (Mardia *et al*., 2000). There are three types of deviations from perfect symmetry: directional asymmetry, fluctuating asymmetry and antisymmetry (Klingenberg, 2015). Directional asymmetry is related to the systematic differences between left-right sides, thus being consistent among individuals; it has been reported few times in plant leaves and there is not a clear biological meaning for this variation (Baranov, 2014). Fluctuating asymmetry refers to small changes in symmetry and it has been reported many times on plant leaves. This variation on symmetry has been associated to developmental instabilities product of environmental or biological pressures and it is characterized by a bell-shaped frequency distribution of the asymmetry with mean zero (van Valen, 1962; Klingenberg and

McIntyre 1998; Palmer, 2005; Viscosi, 2015; Fernandes *et al*., 2016). Antisymmetry is a pattern characterized by an admixture of left and right asymmetric individuals, thus asymmetry has a bimodal frequency distribution; furthermore, the direction of asymmetry is random and, with few exceptions, not inherited (Palmer, 2005; Chitwood *et al*., 2012; Silva *et al*., 2012; Klingenberg, 2015).

Allometry is defined as the covariation of size and shape by the Gould-Mosimann school of thought in allometry (Klingenberg, 1998, 2016). It is usually analysed through a multivariate regression of shape on size (Klingenberg, 1998, 2016; Monteiro, 1999; Strelin *et al*., 2016). Shape is defined as: 'information left when size, position, and orientation are removed from coordinates data' (Rohlf and Slice, 1990; Mardia *et al*., 2000). This is usually achieved through a Procrustes superimposition of individual coordinates. However, shape is not fully free of size influence and it is necessary the use of a size-correction methodology. Residuals from a multivariate regression of shape on size (centroid size or its log-transformed values) are generally used as size-corrected shape data (Klingenberg, 1998, 2016; Monteiro, 1999; Strelin *et al*., 2016). Thus, plotting this size-corrected shape against size (log-transformed centroid size) provides a good estimate of allometric trends between species (Drake and Klingenberg, 2008).

Species are abstract units delimited by sets of characters particular to hypothesis of independently evolving lineages (de Queiroz, 2007). These sets of characters are prone to variation due to environmental and genetic factors. Character variation has been quantified using several measurement and analysis tools through time. Over the last decades, geometric morphometrics has gained importance in the analysis of character variation through multivariate analysis of bi- and three-dimensional structures (Zelditch *et al*., 2012; Ocakoglu and Ercan, 2013; Mcnulty and Vinyard, 2015). Geometric morphometrics has proved to be a useful tool to estimate different types of character variation, and its association with environmental or evolutionary factors (Viscosi *et al*., 2009a, 2009b; Klingenberg *et al*., 2012; Klingenberg and Marugán-Lobón, 2013; Benítez *et al*., 2014; Viscosi, 2015; Lemic *et al*., 2016). It has been extensively applied to analyse character shape variation in animals (Pauers and McMillan, 2014; Ruane, 2015). In plants, it has been applied in a limited extent to study shape variation of leaves and flower structures (Viscosi and Cardini, 2011; Savriama *et al*., 2012, Gómez *et al*., 2014, 2016; Wang *et al*., 2015; Reginato and Michelangeli, 2016).

The analysis of shape variation through geometric morphometrics has been successful on taxonomic grounds and it has been widely applied on animals (e.g.

Mitrovski-Bogdanović *et al*., 2014; Qubaiova *et al*., 2015; Karanovic *et al*., 2016) and, in some cases, plants (e.g. Shipunov and Bateman, 2005; Duminil *et al*., 2012; Innangi and Izzo, 2014; Kabátová *et al*., 2014; Baleeiro *et al*., 2016) for species delimitation and recognition. Shape by itself is important in species differentiation but sometimes size is also needed for adequate determination (Glennon and Cron, 2015; Viscosi, 2015). Many plant species lack detailed studies on their morphological variation and determination can pose a difficult task for closely related species. Attempts for implementation of an automated system for plant identification is still limited to some well-known groups (Cope *et al*., 2012).

Melastomataceae is one of the ten most diverse plant families of Brazil; it includes more than 1,300 species with over 65 per cent of endemism. Three genera are the most species rich: *Miconia* Ruiz & Pav., *Leandra* Raddi, and *Tibouchina* Aubl., with over 650 species (BFG, 2015). Recently, these genera have experienced taxonomic rearrangements as a consequence of revisions and phylogenetic analyses but they are far from being completed (Michelangeli *et al*., 2013; Gamba and Almeda, 2014; Reginato and Michelangeli, 2015).

The genus *Tibouchina* is particularly diverse in the Brazilian North-eastern Region (Michelangeli *et al*., 2013); within this region, the mountains of the Espinhaço range are one of the most important areas due to its high plant diversity and endemism (Fernandes, 2016). There are at least 25 species of *Tibouchina*, ten of which endemic, distributed in the northern portion of this mountain range in Bahia state. Five of those endemic species are closely related and considered to be the '*Tibouchina pereirae* species complex'; it comprises *Pleroma rubrum* J.G.Freitas, *T. blanchetiana* Cogn., *T. carvalhoi* Wurdack, *T. pereirae* and *T. velutina* Cogn. (Freitas, 2011; Freitas & van den Berg, In press). *Tibouchina* is undergoing taxonomic rearrangements and most of their species will belong to *Brachyotum*, *Chaetogastra* or *Pleroma* (Michelangeli *et al*., 2013; Meyer, 2016). In fact, all but one species of *Tibouchina* from Bahia will belong to *Pleroma* (Guimarães et al., unpubl. res.). The *Tibouchina pereirae* species complex is a monophyletic group and belongs to the *Pleroma* clade. Thus, at the nomenclatural level, it is waiting for taxonomic combinations that will be associated with the publication of phylogenetic data (Michelangeli *et al*., 2013, Freitas *et al*., unpubl. res.).

Freitas (2011) highlighted the morphological similarities among the species of this complex, and the problems regarding species delimitation. Many morphological characters in the group overlap and pose an identification challenge for those not familiar with their

variation. She also remarked the variation in leaf morphology of these species across the heterogeneous and harsh environments of their geographical range.

The aim of this study is to assess variation on leaf shape configurations in all five species of the *Tibouchina pereirae* species complex and to test it for taxonomic value, population differentiation, allometric trends, and phylogenetic signal. We proposed four main questions based on the previous knowledge stated above. 1) Does leaf size influence leaf shape variation? 2) Are the patterns of variation from leaf shape and size useful to determine species membership? 3) Is there evidence in leaf shape variation for population differentiation within species? 4) Is there phylogenetic signal on leaf shape variation and size? These questions are addressed by using a wide set of tools for geometric morphometric analyses of shape and size variation as well as different tools for analysing phylogenetic signal on continuous characters, all of them described on detail ahead.

MATERIAL AND METHODS

Study group and sampling

A total of 539 individuals from 27 populations of the five species recognized within the *Tibouchina pereirae* complex have been sampled for comparisons of leaf variation among geographic samples and species (Fig. 1, Supplementary Information Table S1). Sympatry is common between the species and morphological varieties; therefore some sampling localities (seven) are no more than one kilometre apart (Fig. 2). However, for simplicity every geographical sample was treated as a single population. Each population consisted of 20 individuals, except for POP06 where no more than 19 individuals were found (Table S1). A branch from every individual was collected, with reproductive structures whenever possible; these were later pressed, identified and deposited at the herbarium of the 'Universidade Estadual de Feira de Santana' (HUEFS). From each branch, one of the two leaves (leaves are opposed for all species except *T. blanchetiana*) from the third node (from apex to base) was picked for using in the morphometric analyses. This was rigorously followed to ensure samples represented the same leaf developmental stage in all individuals. The twenty leaves of each population were then mounted on dried herbarium sheets, annotated and deposited as vouchers at the HUEFS as a reference material for reproducibility (Table S1).

Landmark and semi-landmark digitizing

All leaves were soaked individually into boiling water during 10s for rehydration (enough to rehydrate them without compromising their morphological configuration). Then, leaves were scanned within three to five minutes after rehydration (the abaxial surface uppermost) with a HP Photosmart C4480 scanner at a 300 dpi resolution. All leaves were scanned at a 1: 1 scale but a small ruler was added at scanning to ensure every image was at the same scale for digitizing.

Two landmarks and 26 semi-landmarks (13 on each half) were digitized on the contour of every leaf scanned to quantify shape and symmetric variation (Fig. 1). All landmarks and semi-landmarks for each leaf were digitized using TPSDig2 (Rohlf, 2008a) after all images were checked for being at the same scale with the aid of the scanned rules on the images. Two landmarks were selected to represent homologous points on simple leaves (apex and base of leaf, where the main vein joins the petiole), as a common practice in other studies (Viscosi *et al*., 2009b; Viscosi and Cardini, 2011; Cardozo *et al*., 2014; Viscosi, 2015). Thirteen semi-landmarks on each side were chosen to adequately represent the outline curve, along the leaf margin, between the two original landmarks; they were selected after plotting different number of points and visually analysing them; thus, the final number of points was regarded as the best array of points to depict outline between landmarks. The semi-landmarks were digitized on an approximate equal distribution along the leaf margin and automatically aligned with the sliding semi-landmarks procedure implemented in TPSRelw (Rohlf, 2008b) to optimize their position along the tangential space and better represent their configuration (Zelditch *et al*., 2012). The process was done twice, with an interval of two months between each, to estimate digitizing error of landmarks and semi-landmarks; both sets of landmarks were concatenated in a single TPS file for all posterior analyses.

All morphometric analyses were performed within the R environment using the ‘geomorph’ (Adams and Otárola-Castillo, 2013), ‘Morpho’ (Schlager, 2016), and ‘shapes’ (Dryden, 2015) packages. Other additional analyses for morphometric data were performed using the ‘vegan’ (Oksanen et al., 2016), ‘phylosignal’ (Keck *et al*., 2016), and ‘phytools’ (Revell, 2012) packages. The TPS file with raw coordinates of specimens was imported to R using the function *readland.tps* from ‘geomorph’; they were then projected to Procrustes coordinates with the Procrustes superimposition method using function *procSym* from ‘Morpho’. The resulting data file contained a centroid size list, and a matrix

of rotated and scaled coordinates. The latter matrix fulfilled definition of shape: 'information left when size, position, and orientation are removed from data' (Rohlf and Slice, 1990; Mardia *et al*., 2000). A separate matrix with categorical variables was imported into R for subsequent multivariate analysis. These variables separated the specimens into different factors (*i.e*. populations, species, and replicates).

Asymmetry

We then tested whether Directional Asymmetry (hereinafter, DA) and/or Fluctuating Asymmetry (hereinafter, FA) were driving leaf shape variation between and within species. We also tested whether this variation was significant. For these analyses, the function *bilat.symmetry* ('geomorph') was applied on aligned coordinates for overall data and each species assuming object symmetry in the sense of Mardia *et al*. (2000), and incorporating individuals, sides, and replicates as categorical variables. This function decomposed variation of shape symmetry into variation between individuals, sides (DA), and the interaction individuals × side (FA). We used a Procrustes multivariate ANOVA to analyse these components of shape symmetric variation and permutation methods (residual randomization permutation procedure, RRPP) to assess the significance of model effects on shape variation. The function used type I sum of squares for testing significance of the model, a desirable quality for unbalanced sampling designs like ours (Zelditch *et al*., 2012). The replicate variable was used to estimate measurement error for all analyses (Viscosi and Cardini, 2011; Adams and Otárola-Castillo, 2013). All analyses of shape symmetric variation were performed with 10,000 iterations using RRPP. Antisymmetry (hereinafter, AS) was tested on all species by Canonical Variate Analysis (CVA) of the asymmetric component of shape from all samples and using species as categorical variable (Silva *et al*., 2012).

The mean squares from analyses were used to estimate repeatability, a ratio of among individuals and measurement error variances usually accounted as an estimate of error (Zelditch *et al*., 2012). First, the value for individual variance (σ_{Ind}) was estimated by the equation $\sigma_{Ind} = (MS_{Ind}-MS_{ME})/k$ where MS_{Ind} equals individual mean squares, MS_{ME} equals measurement error mean squares, and k equals number of replicates. Second, the total variance (σ_{total}) was calculated by adding σ_{Ind} to MS_{ME}. Last, the values of repeatability were estimated by dividing σ_{Ind} by σ_{total} (Zelditch *et al*., 2012).

Allometry

A first coarse measurement of shape variation between species was obtained by computing the Mahalanobis distances from shape coordinates of each individual to grand mean shape coordinates; these distances were later box-plotted by species to visually represent shape variation between them. Size variation was also first estimated roughly by box-plotting the centroid size variation of each species.

Covariation between size and shape was analysed with the function *procD.allometry* from 'geomorph'. This function produced estimates for three different approaches of covariation of size and shape. The first, the common allometric component (CAC), was an estimate of the common trend between groups; therefore, plotting CAC against the log centroid size helped identifying differences between allometric trajectories (Mitteroecker *et al*., 2004; Adams *et al*., 2013). The second, the 'RegScore', was an estimate of shapes scores from the regression of shape on size; consequently, plotting these scores against log centroid size helped identifying trends between groups (Drake and Klingenberg, 2008). The last, the 'PredLine', was an estimate of predicted values from the regression of shape on size; thus, correlation lines from CAC against log centroid size represented allometric trajectories for each species (Adams and Nistri, 2010). The proportion of shape variation explained by size, species, and replicates was estimated by fitting these variables to a linear model on a Procrustes multivariate ANOVA. Significance of the variation of model components was calculated through 10,000 iterations using RRPP (Collyer *et al*., 2015).

Shape and species separation

Shape was defined as the component left after aligning, rotating and scaling were applied to landmark configurations (Rohlf and Slice, 1990; Mardia *et al*., 2000). This was carried out through a Procrustes superimposition. However, shape was not fully free of size influence; therefore, residuals from a multivariate regression of shape against size were used as an approach for size correction (Klingenberg, 2016; Monteiro, 1999; Strelin *et al*., 2016). These residuals (hereinafter, size-corrected shape) were used to estimate shape variation among species. For this, shape was fitted to a linear model with several factors depending on whether they were evaluated as a whole (species, populations, individuals, and replicates) or as separate species (populations, individuals, and replicates). The

significance of the Procrustes multivariate ANOVA of this model was estimated through 10,000 iterations using RRPP.

A CVA analysis was performed to evaluate the importance of shape for species differentiation within the *T. pereirae* complex. This analysis was obtained by running function *CVA* ('Morpho') on size-corrected shape while employing species as categorical variable. Statistical significance of group differences in mean shapes was assessed with permutation tests (10,000 permutations per run) and Jackknife cross-validation using Mahalanobis distances on the CVA analysis. These distances were later plotted as dendrograms. Shape and size differences for main groups within each species were computed with function *plotRefToTarget* ('geomorph') and plotted as displacement vectors between corresponding landmarks from non-scaled coordinates (Procrustes superimposition coordinates without scaling to unit centroid size). Thus, each plot represented variation of groups regarding to mean shape and size of a species.

Within- versus among-groups dissimilarities were computed using the multi-response permutation procedure (MRPP) implemented in function *mrpp* from 'vegan' (Oksanen *et al.*, 2016). This is a permutation test that allows estimating the significance between within- and among-group distances (Mielke and Berry, 2007). This procedure was used to test overlap of distances in the first two CV spaces from the CVA of size-corrected shape among all pairwise comparisons of the five species. Significance of MRPP's delta statistic was assessed after 10,000 permutations.

Phylomorphospace and phylogenetic signal

The relationship between shape, size and phylogenetic distances was estimated by plotting a Bayesian phylogenetic tree of the species (Freitas *et al*. unpubl. res.) onto a morphospace of leaf shape and size. This morphospace was determined by the species' mean values from first two CV spaces of CVA on size-corrected shape. On the other hand, the size morphospace was described by the species' mean value of log-transformed centroid size. This phylomorphospace plot was generated through function *phylomorphospace3d* from 'phytools' (Revell, 2012). Furthermore, several indices of phylogenetic signal were tested to estimate correlation between morphospace and phylogenetic distance. The Moran's I index (Moran, 1948, 1950), the Cmean index (Abouheif, 1999), the Blomberg's K and K* indices (Blomberg *et al*., 2003) and Pagel's lambda index (Pagel, 1999) were estimated using function *phyloSignal* from 'phylosignal' (Keck *et al*., 2016). These indices were tested against a null hypothesis of absence of

signal through either randomization (I, Cmean, K, and K*) or likelihood ratio tests (λ) by doing 10,000 replicates within analyses. These indices were estimated for the morphospace traits plus a simulated trait. The latter was generated under a Brownian motion (BM) model of evolution based on the phylogenetic tree through function *rTraitContWeight* ('phylosignal'). Finally, a phylogenetic correlogram for each character was built with function *phyloCorrelogram* ('phylosignal') by generating 1,000 points; confidence intervals for each of these correlograms were estimated with 10,000 bootstrap replicates.

RESULTS

Asymmetry

The multivariate ANOVA of leaf asymmetry analyses resulted in no statistical significance of variation among individuals (p = 0.963) when all species were treated as a unit (Table 1). However, it represented the highest source of variation in the lineal model (R^2 = 0.866). Directional asymmetry (R^2 = 0.040) and FA (R^2 = 0.089) explained less than 15 per cent of the variation in the model but were statistically significant (p = 0.001). Leaf symmetry analyses for each species resulted in no statistical significance (p-values ranged from 0.989 to 1) of symmetric variation among individuals (Table 1). Nevertheless, variation among individuals was the main source of symmetric variation for all species (R^2 ranged from 0.553 to 0.702) except *P. rubrum* (R^2 = 0.396) where the major source of variation was the interaction between individuals and size (R^2 = 0.489, Table 1). Variation in symmetry between leaf sides (representing DA) was significant for all species (p = 0.001) and represented less than 20 per cent (R^2 ranged from 0.086 to 0.19) of leaf symmetric variation (Table 1). Variation in symmetry due to the interaction of individuals and sides (representing FA) was also significant for all species (p = 0.001) and represented less than 30 per cent of leaf symmetric variation for all species (R^2 ranged from 0.193 to 0.286) except *P. rubrum* (R^2 = 0.489, Table 1). Symmetric and asymmetric components of shape were plotted for all species to represent symmetric variation graphically; furthermore, we plotted thin-plate spline (TPS) deformation grids for representing DA and FA variation within species (Fig. 3A-F).

CVA analysis of the asymmetric component of shape from all samples resulted in the recognition of asymmetry trends between and within species (Fig. 4). *Tibouchina blanchetiana* was predominantly left-handed (Fig. 5A). *Pleroma rubrum* and *T. velutina*

were predominantly right-handed (Fig. 5D, E). *Tibouchina carvalhoi* and *T. pereirae* had an admixture of left-handed, right-handed, or antisymmetric populations (Fig. 5B,C). *Tibouchina carvalhoi* had a complex pattern of asymmetry. Northern populations were right-handed (POP08 and POP10) or antisymmetric (POP22) and southern populations were antisymmetric (POP09, POP21 and POP24). *Tibouchina pereirae* had also a complex pattern of asymmetry. Northern populations were either right-handed (POP18, POP26 and POP27) or antisymmetric (POP19). Southern populations were left-handed (POP07, POP11, POP12 and POP23). Western populations were either right-handed (POP14) or left-handed (POP16 and POP17).

Overall, the repeatability values were high for the asymmetry analysis; the computed value from all samples was 0.995 while those for each species ranged from 0.932 to 0.996 (Table 1). Digitizing error between replicates was low for all samples (R^2 = 0.004) and each species (R^2 ranged from 0.003 to 0.038). Box-plotting of the computed Mahalanobis distances of shape and size helped at identifying outliers. There were several outliers when considering shape and few with size (Fig. 6); thus, they were not removed from analysis due to the fact that those samples could represent hybrids or variation in allometric trends among species.

Allometry

The effect of size was significant ($p < 0.001$) for shape variation in the Procrustes multivariate ANOVA of allometry. However, it represented less than 15 per cent (R^2 = 0.109) of shape variation in the linear model (Table 2). Variation among species represented most of the variance in the lineal model (R^2 = 0.598) and it was statistically significant ($p < 0.001$). The interaction between log-centroid size and species had the lowest variance (R^2 = 0.025) in the model but it was statistically significant ($p < 0.001$). Thus, the residual component of the model represented a little more than 25 per cent of the variance in the model (Table 2).

Allometric analyses showed that the residual shape component varied little in relation to the common allometric component for all species. Only two species, *P. rubrum* and *T. blanchetiana*, had no strong overlapping distributions of these two components (Fig. 7A). Species were more clearly separated when the common allometric component was plotted against log-centroid size (Fig. 7B). This pattern was also observed at the plotting of the shape regression score against size (Fig. 7C). Correlations between common allometric component and log-centroid size for *P. rubrum* and *T. blanchetiana* were negative (-0.208

and -0.104, respectively). On the other hand, *T. carvalhoi*, *T. pereirae*, and *T. velutina* had positive correlations (0.211, 0.661 and 0.484, respectively) between the common allometric component and log-centroid size. Thus, all five species had different trends in shape and size correlations (Fig. 7D).

Shape and species separation

The effect of species, populations, and individuals in the variation of size-corrected shape were statistically significant ($p < 0.001$) in the Procrustes multivariate ANOVA (Table 3). Most of the variance was explained by variation among individuals ($R^2 = 0.726$) whereas variation among species and populations contributed less than 15 per cent each ($R^2 = 0.137$, 0.115, respectively) to the variance of the model (Table 3). Within species, shape variation had a similar pattern and differences among individuals represented most of the variance (R^2 ranged from 0.722 in *T. velutina* to 0.909 in *P. rubrum*) in the lineal model (Table 3).

The CVA of size-corrected shape coordinates had an overall classification accuracy of 68.74%. This accuracy was lower for *T. carvalhoi* (41.67%) and *T. velutina* (61%), and higher for *T. blanchetiana* (74.17%), *T. pereirae* (79.55%) and *P. rubrum* (87.5%). The first two CV scores of the CVA explained 92.29% of variation (Fig. 8). *Tibouchina pereirae* overlapped strongly with *T. carvalhoi* and *T. velutina*. All other species had partially overlapping distributions (Fig. 8). All MRPP pairwise comparisons were statistically significant with *p* values lower than 0.001 (Table 4). Two pairs had the lower A values, *T. carvalhoi-T. pereirae* (A = 0.04751) and *T. pereirae-T. velutina* (A = 0.09159), from the MRPP tests (Table 4).

The CVA analyses within species provided evidence of population differentiation for all of them. The dendrograms from Mahalanobis' distances of non-scaled coordinates showed differentiation in size and shape among populations for each species (Fig. 9A-E). *Tibouchina blanchetiana* was arranged in two groups that differed mainly in size; populations POP02 and POP03 had relatively bigger leaves than population POP01 (Fig. 9A). *Tibouchina carvalhoi* had a similar pattern of variation in size but more pronounced; populations POP21, POP22 and POP24 had comparatively smaller leaves than populations POP08, POP09, and POP10 (Fig. 9B). The groups in *T. pereirae* were strikingly different in size; populations POP07, POP11, POP12, POP19 and POP23 had considerably smaller leaves than populations POP14, POP16, POP17, POP18, POP26 and POP27 (Fig. 9C). A similar pattern was found in *P. rubrum* where population POP13 had smaller leaves than

populations POP15 and POP25 (Fig. 9D). Finally, *T. velutina* had two different groups with differing size and shape; one group (POP05, POP06 and POP20) had the closer size and shape to the mean for the species while the other population was bigger and more elongated (POP04) than the mean (Fig. 9E).

Phylomorphospace and phylogenetic signal

The phylomorphospace highlighted a general trend of separate patterns of leaf shape and size evolution among species (Fig. 10). Species diverged from each other on their leaf shape and size morphospace independently of their phylogenetic relationships (Fig. 10). All phylogenetic signal indices were not statistically significant (*p*-values ranged from 0.193 to 1) for the traits analysed except for the BM simulated trait (Table 5). The correlograms of traits and phylogenetic distances resulted in no significant correlation for traits CV1 and size, and significant positive correlation at the shortest phylogenetic distances for trait CV2 (Fig. 11A-C). However, the BM simulated trait showed significant correlation at either short (positive) or long (negative) phylogenetic distances (Fig. 11D).

DISCUSSION

Results from our analyses provided evidence to answer our four main questions regarding the trends in shape and size within the *Tibouchina pereirae* species complex. First, it was observed that leaf size influenced leaf shape variation. The analysis of allometry supported different positive or negative trends of shape variation related to size for all species. Although *Tibouchina pereirae* and *T. velutina* presented parallel and positive allometric trajectories with similar slopes, the intercepts were different (Fig. 7D). *Tibouchina carvalhoi* had also a positive allometric trajectory but with a more gradual slope and a different intercept. *Tibouchina blanchetiana* and *P. rubrum* showed slightly negative allometric trajectories with similar slopes but separate intercepts (Fig. 7D). Species differences in correlations of leaf shape and size are common in other groups of plants (Albarrán-Lara *et al*. 2010; Viscosi, 2015). However, a pattern observed in this study is that the leaf shape of *P. rubrum*, *T. blanchetiana* and *T. carvalhoi* is less correlated to size than those of *T. pereirae* and *T. velutina* (Fig. 7D).

In response to the question about the utility of variation patterns of leaf shape and size to determine species separation, the results show that the relatively low overall

classification accuracy (68%) of the CVA indicated that shape in itself serves only as a moderate measure of differentiation between species; however, accuracy values for *P. rubruma*, *T. blanchetiana* and *T. pereirae* ranged from 74% to 87.5%. The results of MRPP analyses from size-corrected shape were significant ($p < 0.001$) for all pairwise comparisons in the species complex. However, the differences in shape between species were greater that the differences within species. *Tibouchina pereirae* had the lowest values of between-group separation at comparisons with *T. carvalhoi* and *T. velutina*. Thus, the MRPP results supported thet the leaf shape is a useful trait to determine species membership. However, CVA and MRPP results indicated a possible problem at separating *T. pereirae* from *T. carvalhoi* and *T. velutina* using leaf shape alone. On the other hand, the correlation of shape and size showed a clearer group differentiation (smaller overlap between groups) than CVA ordination. Thus, size is not negligible for species differentiation (Fig. 7A-D).

The search for evidence of leaf shape variation for the differentiation of populations within species indicates complex patterns of symmetric variations in the *T. pereirae* species complex. Directional asymmetry explained less than 20 per cent (R^2 ranged from 0.086 to 0.19) of symmetric variation within each species but was statistically significant ($p = 0.001$). All populations within *P. rubrum*, *T. blanchetiana* and *T. velutina* showed a distribution of asymmetry components typical of DA. *Tibouchina blanchetiana* had left-handed DA while *P. rubrum* and *T. velutina* had right-handed DA. *Tibouchina carvalhoi* and *T. pereirae* were composed of populations dominated by either right-handed or left-handed individuals, or an admixture of both. Furthermore, there was some population differentiation in the asymmetry components of leaf shape (Fig. 5B-C). Northern populations of *T. carvalhoi* were either right-handed or antisymmetric while southern ones were antisymmetric. A similar pattern of regional subdivision was present in *T. pereirae*; northern populations were right-handed or antisymmetric; southern populations were left-handed; and, western populations were either right-handed or left-handed. However, there are few studies of plant leaf asymmetry and available ones usually found DA statistically not significant for leaf symmetric variation (Albarrán-Lara *et al*., 2010; Baranov, 2014; Ivanov *et al*., 2015; Viscosi, 2015; Telhado *et al*., in press). Directional asymmetry had been reported in Melastomataceae for *Lavoisiera campospotoana* Barreto and discarded from *Trembleya laniflora* Cogn., *T. parviflora* Cogn., and *Tibouchina heteromalla* Cogn. using traditional morphometrics (Telhado *et al*., in press). Graham *et al*. (1993) argued that DA could represent a biased AS pattern affected by environment; an event reported for

Convolvulus L., *Solanum lycopersicum* L., and *Arabidopsis thaliana* (L.) Heynh. for left-right asymmetric variations due to phyllotaxis (Graham *et al*., 1993; Chitwood *et al*., 2012). In summary, the biological significance of DA or AS is unclear but one thing is for sure they are widely present in animals and plants (Palmer, 2005; Klingenberg, 2015). The dendrograms from Mahalanobis distances of non-scaled shape coordinates showed some differentiation among populations of all species (Fig. 8). However, there was sign of association between these within-species separation and geographic location only in *T. pereirae* (except for POP19). It is clear, therefore, the need for more comprehensive studies to explain these patterns of internal variation in leaf shape.

The phylogenetic signal on leaf shape and size variation is not evident. The plotted phylogeny of the group in the morphospace defined by shape and size indicated there was no phylogenetic signal in leaf traits for the evolution of these species. However, the phylogenetic signal indices supported this first impression. No index was capable of identifying phylogenetic signal for leaf shape and size on the group. Blomberg *et al*. (2003) pointed out measurement error and/or deviation from a Brownian motion evolution as causes for absence of phylogenetic signal. They considered three sources of measurement error: errors in tip data measurements, errors in branch lengths, and errors in tree topology. Measurement error for tip data represented, in general, less than five per cent of the variation for each species. Branch length and tree topology errors were not evaluated; however, the simulated trait under Brownian motion was significant for phylogenetic signal, indicating there was no problem with branch lengths and tree topology for traits to evolve under Brownian motion. Thus, deviations from a Brownian motion pattern were regarded as species evolving in different trait spaces. Correlograms supported a phylogenetic signal for the CV2 trait at short phylogenetic distances. However, none of the phylogenetic signal indices was statistically significant for this trait and *p*-values were no lower than 0.19 (Table 5). Thus, the correlation between this trait and phylogenetic distance can be explained by its somewhat conserved variation between related species (Fig. 10).

Fluctuating asymmetry (FA) was widespread within all species in the complex and represented over 19 per cent of leaf shape variation for each species. It has been associated to developmental instability due to environmental disturbances (Graham *et al*., 1993; Klingenberg, 2015). All five species in the *T. pereirae* complex inhabit the *campos rupestres* of the northern Espinhaço Range; there, they have to cope with the harsh conditions typical of the area, e.g. nutrient impoverished soils with high drainage or

leaching, herbivory, and frequent fires (Fernandes, 2016). Most of our collection localities had signs of damage by fire and all plants had evidence of herbivory (JGF pers. obs.). Thus, it was not surprising that FA represented a large percent amount of variation in shape. Telhado *et al*. (In press) found a statistically significant FA in the leaves of *T. heteromalla* resulting probably from environmental stress or herbivory in similar environments to those inhabited by the species analysed here. We need more detailed analyzes of the symmetry components of the leaves, before drawing any conclusion on the nature of asymmetric variation. For example, Procrustes multivariate ANOVA of asymmetric components assigned more variation in symmetry to FA than to DA. However, plots of the CVA from asymmetric components showed contrasting patterns of asymmetry. These plots indicated DA as the main source of variation in symmetry and, in minor degree, AS. It seemed that some variation assigned to FA by the Procrustes multivariate ANOVA refers in fact to DA.

In summary, allometric trends within the *T. pereirae* species complex were independent for each species. Size is not a negligible character for species differentiation in this group. Population divergence is evident from leaf shape and size, and asymmetry patterns. Furthermore, there is no correlation between location and group separation for all species as it occurred with the asymmetry components. This could be the result of complex evolutionary scenarios or random patterns of shape and size variation within species. There is no phylogenetic signal from shape and size in this group of species.

ACKNOWLEDGMENTS

This contribution is part of the Ph.D. thesis of JGF at the Programa de Pós-graduação em Botânica from the Universidade Estadual de Feira de Santana (UEFS). We thank Dr. Hibert Huaylla for assistance during field trips and Dr. Tiago A. Pontes for training at geometric morphometrics. We are also grateful to PRONEX (FAPESB/CNPq PNX0014/2009) for financial support. JGF thanks Coordenação de Aperfeiçoamento de Pessoal de Nível Superior (CAPES) for a doctoral scholarship. LNPF thanks Consejo Nacional de Ciencia y Tecnología (CONACyT) for grants (204216 and 239018) to fulfill a two-year postdoctoral fellowship at UEFS, and CvdB thanks CNPq for a productivity scholarship (PQ-1B).

LITERATURE CITED

Abouheif E. 1999. A method for testing the assumption of phylogenetic independence in comparative data. *Evolutionary Ecology Research* **1**: 895–909.

Adams DC, Nistri A. 2010. Ontogenetic convergence and evolution of foot morphology in European cave salamanders (family: Plethodontidae). *BMC Evolutionary Biology* **10**: 216. doi: 10.1186/1471-2148-10-21.

Adams DC, Otárola-Castillo E. 2013. geomorph: an r package for the collection and analysis of geometric morphometric shape data. *Methods in Ecology and Evolution* **4**: 393–399. doi: 10.1111/2041-210X.12035.

Adams DC, Rohlf FJ, Slice DE. 2013. A field comes of age: geometric morphometrics in the 21st century. *Hystrix* **24**: 7–14. doi: 10.4404/hystrix-24.1-6283.

Albarrán-Lara AL, Mendoza-Cuenca L, Valencia-Avalos S, González-Rodríguez A, Oyama K. 2010. Leaf fluctuating asymmetry increases with hybridization and introgression between *Quercus magnoliifolia* and *Quercus resinosa* (Fagaceae) through an altitudinal gradient in Mexico. *International Journal of Plant Sciences* **171**: 310–322. doi: 10.1086/650317.

Andres RJ, Bowman DT, Kaur B, Kuraparthy V. 2014. Mapping and genomic targeting of the major leaf shape gene (L) in Upland cotton (*Gossypium hirsutum* L.). *Theoretical and applied genetics* **127**: 167–177. doi: 10.1007/s00122-013-2208-4.

Baleeiro PC, Jobson RW, Sano PT. 2016. Morphometric approach to address taxonomic problems: the case of *Utricularia* sect. *Foliosa* (Lentibulariaceae). *Journal of Systematics and Evolution* **54**: 175–186. doi: 10.1111/jse.12186.

Baranov SG. 2014. Use of morphogeometric method for study fluctuating asymmetry in leaves *Tilia cordata* under industrial pollution. *Advances in Environmental Biology* **8**: 2391–2398.

Benítez HA, **Püschel T, Lemic D, Čačija M, Kozina A, Bažok R. 2014.** Ecomorphological variation of the wireworm cephalic capsule: studying the interaction of environment and geometric shape. *PLoS ONE* **9**: 102059. doi: 10.1371/journal.pone.0102059.

BFG. 2015. Growing knowledge: an overview of seed plant diversity in Brazil. *Rodriguésia* **66**: 1–29. doi: 10.1590/2175-7860201566411.

Blomberg SP, Garland TJr, Ives AR. 2003. Testing for phylogenetic signal in comparative data: behavioral traits are more labile. *Evolution* **57**: 717–745. doi: 10.1111/j.0014-3820.2003.tb00285.x.

Cardozo AP, Temponi LG, Andrade IM, Mayo SJ, Smidt EC. 2014. A morphometric and taxonomic study of *Anthurium augustinum* complex (Araceae), endemic to the Brazilian Atlantic Forest. *Feddes Repertorium* **125**: 43–58. doi: 10.1002/fedr.201400025.

Chitwood DH, Headland LR, Ranjan A, *et al*. 2012. Leaf asymmetry as a developmental constraint imposed by auxin-dependent phyllotactic patterning. *The Plant Cell* **24**: 2318–2327. doi: 10.1105/tpc.112.098798.

Collyer ML, Sekora DJ, Adams DC. 2015. A method for analysis of phenotypic change for phenotypes described by high-dimensional data. *Heredity* **115**: 357–365. doi: 10.1038/hdy.2014.75.

Cope JS, Corney D, Clark JY, Remagnino P, Wilkin P. 2012. Plant species identification using digital morphometrics: a review. *Expert Systems with Applications* **39**: 7562–7573. doi: 10.1016/j.eswa.2012.01.073.

de Queiroz K. 2007. Species concepts and species delimitation. *Systematic Biology* **56**: 879–886. doi: 10.1080/10635150701701083.

Dkhar J, Pareek A. 2014. What determines a leaf's shape. *EvoDevo* **5**: 47. doi: 10.1186/2041-9139-5-47.

Drake AG, Klingenberg CP. 2008. The pace of morphological change: historical transformation of skull shape in St Bernard dogs. *Proceedings of the Royal Society B, Biological Sciences* **275**: 71–76. doi: 10.1098/rspb.2007.1169.

Dryden IL. 2015. *shapes: statistical shape analysis*. R package version 1.1-11. https: //CRAN.R-project.org/package=shapes.

Duminil J, Kenfack D, Viscosi V, Grumiau L, Hardy OJ. 2012. Testing species delimitation in sympatric species complexes: the case of an African tropical tree, *Carapa spp*. (Meliaceae). *Molecular Phylogenetics and Evolution* **62**: 275–285. doi: 10.1016/j.ympev.2011.09.020.

Fernandes GW. 2016. The megadiverse rupestrian grassland. In: Fernandes GW, ed. *Ecology and Conservation of Mountaintop Grasslands in Brazil*. New York: Springer, 3–14. doi: 10.1007/978-3-319-29808-5_1.

Fernandes GW, Oliveira SC, Campos IR, Barbosa M, Soares LA, Cuevas-Reyes P. 2016. Leaf fluctuating asymmetry and herbivory of *Tibouchina heteromalla* in

restored and natural environments. *Neotropical Entomology* **45**: 44–49. doi: 10.1007/s13744-015-0342-1.

Ferris KG, Rushton T, Greenlee AB, Toll K, Blackman BK, Willis JH. 2015. Leaf shape evolution has a similar genetic architecture in three edaphic specialists within the *Mimulus guttatus* species complex. *Annals of Botany* **116**: 213–223. doi: 10.1093/aob/mcv080.

Freitas JG. 2011. *Estudos floristicos e taxonômicos em* Tibouchina *Aubl. (Melastomataceae; Melastomeae) no estado da Bahia, Brasil*. Tésis de Mestrado, Universidade Estadual de Feira de Santana, Brasil.

Freitas JG, van den Berg, C. In press. A new species of *Pleroma* D.Don (Melastomataceae) endemic to Chapada Diamantina, Bahia, Brazil. *Phytotaxa.*

Gamba D, Almeda F. 2014. Systematics of the Octopleura clade of *Miconia* (Melastomataceae: Miconieae) in Tropical America. *Phytotaxa* **179**: 1–174. doi: 10.11646/phytotaxa.179.1.1.

Gómez JM, Torice R, Lorite J, Klingenberg CP, **Perfectti F. 2014.** The role of pollinators in the evolution of corolla shape variation, disparity and integration in a highly diversified plant family with a conserved floral bauplan. *Annals of Botany* **117**: 889–904. doi: 10.1093/aob/mcv194.

Gómez JM, Perfectti F, **Klingenberg CP. 2016.** The role of pollinator diversity in the evolution of corolla-shape integration in a pollination-generalist plant clade. *Philosophical Transactions of the Royal Society B, Biological Sciences* **369**: 20130257. doi: 10.1098/rstb.2013.0257.

Glennon KL, Cron GV. 2015. Climate and leaf shape relationships in four *Helichrysum* species from the Eastern Mountain Region of South Africa. *Evolutionary Ecology* **29**: 657–678. doi: 10.1007/s10682-015-9782-7.

Graham JH, Freeman DC, Emlen JM. 1993. Antisymmetry, directional asymmetry, and dynamic morphogenesis. *Genetica* **89**: 121–137. doi: 10.1007/BF02424509.

Ichihashi Y, Aguilar-Martinez JA, Farhi M, *et al*. 2014. Evolutionary developmental transcriptomics reveals a gene network module regulating interspecific diversity in plant leaf shape. *Proceedings of the National Academy of Sciences of the United States of America* **111**: E2616–E2621. doi: 10.1073/pnas.1402835111.

Innangi M, Izzo A. 2014. *Pinguicula lavalvae* (Lentibulariaceae), a new endemic butterwort from southern Italy diagnosed with the aid of geometric morphometrics. *Plant Biosystems* **149**: 990–999. doi: 10.1080/11263504.2014.920426.

Ivanov VP, Ivanov YV, Marchenko SI, Kuznetsov VV. 2015. Application of fluctuating asymmetry indexes of silver birch leaves for diagnostics of plant communities under technogenic pollution. *Russian Journal of Plant Physiology* **62**: 340–348. doi: 10.1134/S1021443715030085.

Kabátová K, Vít P, Suda J. 2014. Species boundaries and hybridization in central-European *Nymphaea* species inferred from genome size and morphometric data. *Preslia* **86**: 131–154.

Karanovic T, Djurakic M, Eberhard SM. 2016. Cryptic species or inadequate taxonomy? Implementation of 2D geometric morphometrics based on integumental organs as landmarks for delimitation and description of copepod taxa. *Systematic Biology* **65**: 304–327. doi: 10.1093/sysbio/syv088.

Kawecki TJ, Ebert D. 2004. Conceptual issues in local adaptation. *Ecology Letters* **7**: 1225–1241. doi: 10.1111/j.1461-0248.2004.00684.x.

Keck F, Rimet F, Bouchez A, Franc A. 2016. phylosignal: an R package to measure, test, and explore the phylogenetic signal. *Ecology and Evolution* **6**: 2774–2780. doi: 10.1002/ece3.2051.

Klingenberg CP. 1998. Heterochrony and allometry: the analysis of evolutionary change in ontogeny. *Biological Reviews* **73**: 79–123. doi: 10.1111/j.1469-185X.1997.tb00026.x.

Klingenberg CP. 2015. Analyzing fluctuating asymmetry with geometric morphometrics: concepts, methods, and applications. *Symmetry* **7**: 843–934. doi: 10.3390/sym7020843.

Klingenberg CP. 2016. Size, shape, and form: concepts of allometry in geometric morphometrics. *Development Genes and Evolution* **226**: 113–137. doi: 10.1007/s00427-016-0539-2.

Klingenberg CP, McIntyre GS. 1998. Geometric morphometrics of developmental instability: analyzing patterns of fluctuating asymmetry with Procrustes methods. *Evolution* **52**: 1363–1375. http: //www.jstor.org/stable/2411306.

Klingenberg CP, Duttke S, Whelan S, Kim M. 2012. Developmental plasticity, morphological variation and evolvability: a multilevel analysis of morphometric integration in the shape of compound leaves. *Journal of Evolutionary Biology* **25**: 115–129. doi: 10.1111/j.1420-9101.2011.02410.x.

Klingenberg CP, Marugán-Lobón J. 2013. Evolutionary covariation in geometric morphometric data: analyzing integration, modularity and allometry in a phylogenetic context. *Systematic Biology* **62**: 591–610. doi: 10.1093/sysbio/syt025.

Lemic D, Benítez HA, Püschel T, Gašparić HV, Šatvar M, Bažok R. 2016. Ecological morphology of the sugar beet weevil Croatian populations: evaluating the role of environmental conditions on body shape. *Zoologischer Anzeiger* **260**: 25–32. doi: 10.1016/j.jcz.2015.11.003.

Mardia KV, Bookstein FL, Moreton IJ. 2000. Statistical assessment of bilateral symmetry of shapes. *Biometrika* **87**: 285–300. doi: 10.1093/biomet/87.2.285.

Mcnulty KP, Vinyard CJ. 2015. Morphometry, geometry, function, and the future. *The Anatomical Record* **298**: 328–333. doi: 10.1002/ar.23064.

Meyer FS. 2016. *Estudos sitemáticos no clado de Chaetogastra DC. e gêneros aliados* (*Melastomataceae: Melastomeae*). PhD Thesis, Universidade Estadual de Campinas, Brasil.

Michelangeli FA, Guimaraes PJF, Penneys DS, Almeda F, Kriebel R. 2013. Phylogenetic relationships and distribution of New World Melastomeae (Melastomataceae). *Botanical Journal of the Linnean Society* **171**: 38–60. doi: 10.1111/j.1095-8339.2012.01295.x.

Mielke PW, Berry KJ. 2007. *Permutation methods: a distance function approach*, 2nd edition. New York: Springer.

Mitrovski-Bogdanović A, Tomanović Ž, Mitrović M, *et al*. 2014. The *Praon dorsale-yomenae s.str*. complex (Hymenoptera, Braconidae, Aphidiinae): species discrimination using geometric morphometrics and molecular markers with description of a new species. *Zoologischer Anzeiger* **253**: 270–282. doi: 10.1016/j.jcz.2014.02.001.

Mitteroecker P, Gunz P, Bernhard M, Schaefer K, Bookstein FL. 2004. Comparison of cranial ontogenetic trajectories among great apes and humans. *Journal of Human Evolution* **46**: 679–697. doi: 10.1016/j.jhevol.2004.03.006.

Monteiro, LR. 1999. Multivariate regression models and geometric morphometrics: the search for causal factors in the analysis of shape. *Systematic Biology* **48**: 192–199. doi: 10.1080/106351599260526.

Moran PAP. 1948. The interpretation of statistical maps. *Journal of the Royal Statistical Society. Series B (Methodological)* **10**: 243–251. http: //www.jstor.org/stable/2983777.

Moran PAP. 1950. Notes on continuous stochastic phenomena. *Biometrika* **37**: 17–23. http: //www.jstor.org/stable/2332142.

Ocakoglu G, Ercan I. 2013. Traditional and modern morphometrics: review. *Turkiye Klinikleri Journal of Biostatistics* **5**: 37–41.

Oksanen J, Blanchet F, Kindt R, *et al*. 2016. vegan: community ecology package. R package version 2.3-5. https: //CRAN.R-project.org/package=vegan.

Pagel M. 1999. Inferring the historical patterns of biological evolution. *Nature* **401**: 877–884. doi: 10.1038/44766.

Palacio-López K, Beckage B, Scheiner S, Molofsky J. 2015. The ubiquity of phenotypic plasticity in plants: a synthesis. *Ecology and Evolution* **5**: 3389–3400. doi: 10.1002/ece3.1603.

Palmer AR. 2005. Antisymmetry. In: Hallgrímsson B, Hall BK, eds. *Variation*. San Diego: Academic Press, 359-398. doi: 10.1016/B978-012088777-4/50018-1.

Pauers MJ, McMillan SA. 2014. Geometric morphometrics reveals surprising diversity in the Lake Malawi cichlid genus *Labeotropheus*. *Hydrobiologia* **748**: 145–160. doi: 10.1007/s10750-014-1941-2.

Pfennig DW, Wund MA, Snell-Rood EC, Cruickshank T, Schlichting CD, Moczek AP. 2010. Phenotypic plasticity's impacts on diversification and speciation. *Trends in Ecology and Evolution* **25**: 459–467. doi: 10.1016/j.tree.2010.05.006.

Qubaiova J, Ruzicka J, Sipkova H. 2015. Taxonomic revision of genus *Ablattaria* Reitter (Coleoptera, Silphidae) using geometric morphometrics. *ZooKeys* **475**: 79–142. doi: 10.3897/zookeys.477.8446.

Reginato M, Michelangeli FA. 2015. Untangling the phylogeny of *Leandra s.str*. (Melastomataceae, Miconieae). *Molecular Phylogenetics and Evolution* **96**: 17–32.

Reginato M, Michelangeli FA. 2016. Diversity and constraints in the floral morphological evolution of *Leandra s.str*. (Melastomataceae). *Annals of Botany* **118**: 445–458. doi: 10.1093/aob/mcw116.

Revell LJ. 2012. phytools: an R package for phylogenetic comparative biology (and other things). *Methods in Ecology and Evolution* **3**: 217–223. doi: 10.1111/j.2041-210X.2011.00169.x.

Rohlf FJ. 2008*a*. tpsDig2: a program for landmark development and analysis. Available at http: //life.bio.sunysb.edu/morph/.

Rohlf FJ. 2008*b*. tpsRelw1.62: Relative warps. Available at http: //life.bio.sunysb.edu/morph/.

Rohlf FJ, Slice D. 1990. Extensions of the Procrustes method for the optimal superimposition of landmarks. *Systematic Zoology* **39**: 40–59. doi: 10.2307/2992207.

Ruane S. 2015. Using geometric morphometrics for integrative taxonomy: an examination of head shapes of milksnakes (genus *Lampropeltis*). *Zoological Journal of the Linnean Society* **174**: 394–413. doi: 10.1111/zoj.12245.

Savriama Y, Gómez JM, Perfectti F, Klingenberg CP. 2012. Geometric morphometrics of corolla shape: dissecting components of symmetric and asymmetric variation in *Erysimum mediohispanicum* (Brassicaceae). *The New phytologist* **196**: 945–954. doi: 10.1111/j.1469-8137.2012.04312.x.

Schlager S. 2016. Morpho: calculations and visualisations related to geometric morphometrics. R package version 2.3.1.1. https: //CRAN.R-project.org/package=Morpho.

Shipunov AB, Bateman RM. 2005. Geometric morphometrics as a tool for understanding *Dactylorhiza* (Orchidaceae) diversity in European Russia. *Biological Journal of the Linnean Society* **85**: 1–12. doi: 10.1111/j.1095-8312.2005.00468.x.

Silva MFS, Andrade IM, Mayo SJ. 2012. Geometric morphometrics of leaf blade shape in *Montrichardia linifera* (Araceae) populations from the Rio Parnaíba Delta, North-East Brazil. *Botanical Journal of the Linnean Society* **170**: 554–572. doi: 10.1111/j.1095-8339.2012.01309.x.

Strelin MM, Benitez-Vieyra S, Fornoni J, Klingenberg CP, Cocucci AA. 2016. Exploring the ontogenetic scaling hypothesis during the diversification of pollination syndromes in *Caiophora* (Loasaceae, subfam. Loasoideae). *Annals of Botany* **117**: 937–947. doi: 10.1093/aob/mcw035.

Telhado C, Silveira FAO, Fernandes GW, Cornelissen T. In Press. Fluctuating asymmetry in leaves and flowers of sympatric species in a tropical montane environment. *Plant Species Biology*. doi: 10.1111/1442-1984.12122.

van Valen L. 1962. A study of fluctuating asymmetry. *International Journal of Organic Evolution* **16**: 125–142. http: //www.jstor.org/stable/2406192.

Viscosi V. 2015. Geometric morphometrics and leaf phenotypic plasticity: assessing fluctuating asymmetry and allometry in European white oaks (*Quercus*). *Botanical Journal of the Linnean Society* **179**: 335–348. doi: 10.1111/boj.12323.

Viscosi V, Cardini A. 2011. Leaf morphology, taxonomy and geometric morphometrics: a simplified protocol for beginners. *PLoS ONE* **6**: e25630. doi: 10.1371/journal.pone.0025630.

Viscosi V, Lepais O, Gerber S, Fortini P. 2009*a*. Leaf morphological analyses in four European oak species (*Quercus*) and their hybrids: a comparison of traditional and geometric morphometric methods. *Plant Biosystems* **143**: 564–574. doi: 10.1080/11263500902723129.

Viscosi V, Fortini P, Slice DE, Loy A, Blasi C. 2009*b*. Geometric morphometric analyses of leaf variation in four oak species of the subgenus *Quercus* (Fagaceae). *Plant Biosystems* **143**: 575–587. doi: 10.1080/11263500902775277.

Vlad D, Kierzkowski D, Rast MI, *et al*. 2014. Leaf shape evolution through duplication, regulatory diversification, and loss of a homeobox gene. *Science* **343**: 780–783. doi: 10.1126/science.1248384.

Volis S, Ormanbekova D, Yermekbayev K. 2015. Role of phenotypic plasticity and population differentiation in adaptation to novel environmental conditions. *Ecology and Evolution* **5**: 3818–3829. doi: 10.1002/ece3.1607.

Wang CN, Hsu HC, Wang CC, Lee TK, Kuo YF. 2015. Quantifying floral shape variation in 3D using microcomputed tomography: a case study of a hybrid line between actinomorphic and zygomorphic flowers. *Frontiers in Plant Science* **6**: 724. doi: 10.3389/fpls.2015.00724.

Zelditch ML, Swiderski DL, Sheets HD. 2012. *Geometric morphometrics for Biologists: a primer*, 2nd edn. London: Elsevier.

Table 1. Results of Procrustes multivariate ANOVA computed for analysis of leaf symmetry in the *T. pereirae* species complex.

	Repeat.	Factor	df	SS	MS	R^2	F	Z	Pr(>F)
All species	0.995	Ind.	538	12.83664	0.02386	0.86630	9.75086	0.90523	0.963
		Side	1	0.59989	0.59989	0.04048	245.15756	30.60226	0.001
		Ind: Side	538	1.31646	0.00245	0.08884	40.66899	1.90378	0.001
		Residuals	1078	0.06486	0.00006	0.00438	—	—	—
T. blanchetiana	0.941	Ind	59	0.21657	0.00367	0.60763	2.61096	0.69571	0.989
		Side	1	0.04343	0.04343	0.12184	30.88956	14.46684	0.001
		Ind: Side	59	0.08295	0.00141	0.23272	12.51958	1.72531	0.001
		Residuals	120	0.01348	0.00011	0.03781	—	—	—
T. carvalhoi	0.973	Ind	119	0.51202	0.00430	0.57440	2.00935	0.60037	1
		Side	1	0.11058	0.11058	0.12405	51.64035	20.37438	0.001
		Ind: Side	119	0.25482	0.00214	0.28587	36.77314	1.89802	0.001
		Residuals	240	0.01398	0.00006	0.01568	—	—	—
T. pereirae	0.996	Ind	219	2.08450	0.00952	0.70217	3.64580	0.70853	1
		Side	1	0.30345	0.30345	0.10222	116.23061	27.35763	0.001
		Ind: Side	219	0.57175	0.00261	0.19260	128.30183	1.97274	0.001
		Residuals	440	0.00895	0.00002	0.00302	—	—	—
P. rubrum	0.932	Ind	59	0.13924	0.00236	0.39654	0.81010	0.41181	1
		Side	1	0.03011	0.03011	0.08575	10.33582	6.40063	0.001
		Ind: Side	59	0.17188	0.00291	0.48949	35.27884	1.90474	0.001
		Residuals	120	0.00991	0.00008	0.02822	—	—	—
T. velutina	0.960	Ind	78	0.44517	0.00571	0.55362	2.37457	0.59872	1
		Side	1	0.15311	0.15311	0.19041	63.70445	19.20226	0.001
		Ind: Side	78	0.18747	0.00240	0.23314	20.68852	1.82641	0.001
		Residuals	158	0.01836	0.00012	0.02283	—	—	—

Repeat = Repeatability; Ind = Individuals; Ind: Side = Individuals x Side interaction; df = degrees of freedom; SS= sum of squares; MS= mean squares; R^2= proportion of variation; F= F-values; Z= Z-values; Pr(>F)= *p*-value.

Table 2. Results of the Procrustes multivariate ANOVA computed for testing the covariation of leaf shape and size in the *T. pereirae* species complex.

	df	SS	MS	R^2	F	Z	Pr(>F)
Log-centroid size	1	205.688	205.688	0.109	431.650	60.277	<0.001
Species	4	1132.861	283.215	0.598	594.346	83.930	<0.001
Log-centroid size: Species	4	47.550	11.887	0.025	24.946	20.945	<0.001
Residuals	1068	508.919	0.477	—	—	—	—

df = degrees of freedom; SS = sum of squares; MS = mean squares; R^2 = proportion of variance; F = F-values; Z= Z-values; Pr(>F) = *p*-value.

Table 3. Results of the Procrustes multivariate ANOVA computed for residuals of the regression of shape and size in the *T. pereirae* species complex.

		Df	**SS**	**MS**	**R^2**	**F**	**Z**	**Pr(>F)**
All samples	Species	4	43.798	10.950	0.137	865.182	23.559	0.001
	Populations	22	36.972	1.681	0.115	132.787	6.364	0.001
	Individuals	512	232.615	0.454	0.726	35.899	2.039	0.001
	Residuals	539	6.821	0.013	—	—	—	—
T. blanchetiana	Populations	2	2.001	1.001	0.090	43.294	4.864	0.001
	Individuals	57	18.825	0.330	0.847	14.290	1.935	0.001
	Residuals	60	1.387	0.023	—	—	—	—
T. carvalhoi	Populations	5	6.388	1.278	0.110	95.618	4.972	0.001
	Individuals	114	50.319	0.441	0.863	33.036	2.025	0.001
	Residuals	120	1.603	0.013	—	—	—	—
T. pereirae	Populations	10	16.000	1.600	0.136	369.462	5.693	0.001
	Individuals	209	100.583	0.481	0.856	111.128	2.073	0.001
	Residuals	220	0.953	0.004	—	—	—	—
P. rubrum	Populations	2	1.874	0.937	0.055	46.399	2.946	0.002
	Individuals	57	30.682	0.538	0.909	26.655	2.002	0.001
	Residuals	60	1.212	0.020	—	—	—	—
T. velutina	Populations	3	10.708	3.569	0.240	169.149	11.033	0.001
	Individuals	75	32.206	0.429	0.722	20.349	1.984	0.001
	Residuals	79	1.667	0.021	—	—	—	—

df = degrees of freedom; SS = sum of squares; MS = mean squares; R^2 = proportion of variance; F = F-values; Z= Z-values; Pr(>F) = *p*-value.

Table 4. Summary of MRPP pairwise-comparisons results from first two CVA scores of shape residuals in the *T. pereirae* species complex.

		Delta		A	*p*
T. blanchetiana	*T. carvalhoi*	1.526	1.243	0.2231	<0.001
	T. pereirae	1.655	1.29	0.202	<0.001
	P. rubrum	1.474	1.208	0.2498	<0.001
	T. velutina	1.406	1.268	0.2464	<0.001
T. carvalhoi	*T. pereirae*	1.688	1.634	0.04751	<0.001
	P. rubrum	1.163	1.26	0.3095	<0.001
	T. velutina	1.367	1.463	0.1842	<0.001
T. pereirae	*P. rubrum*	1.208	1.434	0.2657	<0.001
	T. velutina	1.519	1.744	0.09159	<0.001
P. rubrum	*T. velutina*	1.335	1.302	0.2651	<0.001

Delta = overall weighted mean of group mean distances (in order of pairwise comparisons). A = chance-corrected estimate of the proportion of distances explained by group identity. *p* = significance of test.

Table 5. *p*-values from the indices of phylogenetic signal estimated for the first two CV scores from CVA analysis of shape residuals (CV1 and CV2), log centroid size (Size), and a simulated character under Brownian motion evolution (BM) for all species within the *Tibouchina pereirae* species complex.

Character	Cmean	I	K	K*	λ
CV1	0.898	0.770	0.788	0.849	1.000
CV2	0.289	0.217	0.204	0.193	1.000
Size	0.500	0.457	0.624	0.634	1.000
BM	0.009	0.091	0.042	0.034	0.060

Cmean = Cmean Index (Abouheif, 1999); I = Moran's I index (Moran, 1948, 1950); K = Blomberg's K Index (Blomberg *et al*., 2003); K* = Blomberg's K* Index (Blomberg *et al*., 2003); λ = Pagel's lambda index (Pagel, 1999).

Table S1. Summary of sampling data for the populations of the *T. pereirae* species complex used in analyses.

Population*	Species	Latitude	Longitude	Collection number (herbarium codes)
POP01	*T. blanchetiana*	-11.544012	-41.071792	JG Freitas 791(HUEFS-224499)
POP02	*T. blanchetiana*	-11.590269	-41.207387	JG Freitas 792 (HUEFS-224500)
POP03	*T. blanchetiana*	-13.150838	-41.765007	JG Freitas 801(HUEFS-224501)
POP04	*T. velutina*	-11.500004	-41.332506	JG Freitas 793 (HUEFS-224502)
POP05	*T. velutina*	-11.169701	-40.511145	JG Freitas 842 (HUEFS-224503)
POP06	*T. velutina*	-10.665892	-40.363834	JG Freitas 843 (HUEFS-224504)
POP07	*T. pereirae*	-13.314274	-41.284381	JG Freitas 815 (HUEFS-224505)
POP08	*T. carvalhoi*	-12.723895	-41.506946	JG Freitas 822 (HUEFS-224506)
POP09	*T. carvalhoi*	-12.958375	-41.320275	JG Freitas 814 (HUEFS-224507)
POP10	*T. carvalhoi*	-12.455019	-41.482509	JG Freitas 796 (HUEFS-224508)
POP11	*T. pereirae*	-12.998419	-41.348890	JG Freitas 817 (HUEFS-224509)
POP12	*T. pereirae*	-13.000982	-41.347218	JG Freitas 818 (HUEFS-224510)
POP13	*P. rubrum*	-12.998419	-41.34889	JG Freitas 816 (HUEFS-224511)
POP14	*T. pereirae*	-13.533733	-41.877499	JG Freitas 838 (HUEFS-224512)
POP15	*P. rubrum*	-13.524427	-41.956023	JG Freitas 839 (HUEFS-224513)
POP16	*T. pereirae*	-13.522437	-41.965468	JG Freitas 841 (HUEFS-224514)
POP17	*T. pereirae*	-13.524691	-41.969567	JG Freitas 840 (HUEFS-224515)
POP18	*T. pereirae*	-12.588334	-41.391389	JG Freitas 803 (HUEFS-224516)
POP19	*T. pereirae*	-12.489776	-41.362092	JG Freitas 800 (HUEFS-224517)
POP20	*T. velutina*	-12.872387	-41.307149	JG Freitas 813 (HUEFS-224518)
POP21	*T. carvalhoi*	-12.992717	-41.348937	JG Freitas 795 (HUEFS-224519)
POP22	*T. carvalhoi*	-12.497249	-41.567415	JG Freitas 794 (HUEFS-224520)
POP23	*T. pereirae*	-13.009476	-41.379928	JG Freitas 820 (HUEFS-224521)
POP24	*T. carvalhoi*	-13.008825	-41.376033	JG Freitas 819 (HUEFS-224522)
POP25	*P. rubrum*	-13.006396	-41.375835	JG Freitas 821 (HUEFS-224523)
POP26	*T. pereirae*	-12.5697	-41.516791	JG Freitas 894 (HUEFS-224524)
POP27	*T. pereirae*	-12.571619	-41.514474	JG Freitas 802 (HUEFS-224525)

* Sampling size per population was 20 individuals except for POP06 where no more than 19 individuals were found.
HUEFS = acronym for 'Herbário da Universidade Estadual de Feira de Santana'.

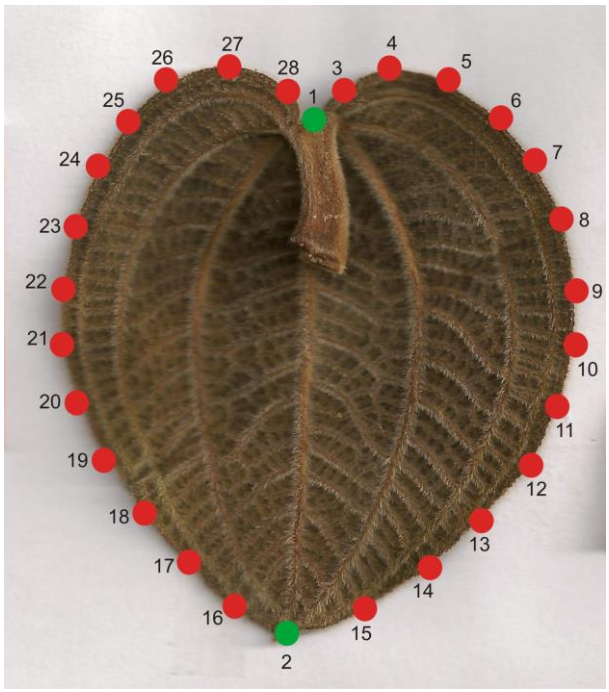

Figure 1. Leaf blade of *Tibouchina carvalhoi* as seen in abaxial view. Dots represent landmarks (1 and 2) and semilandmarks (3-28).

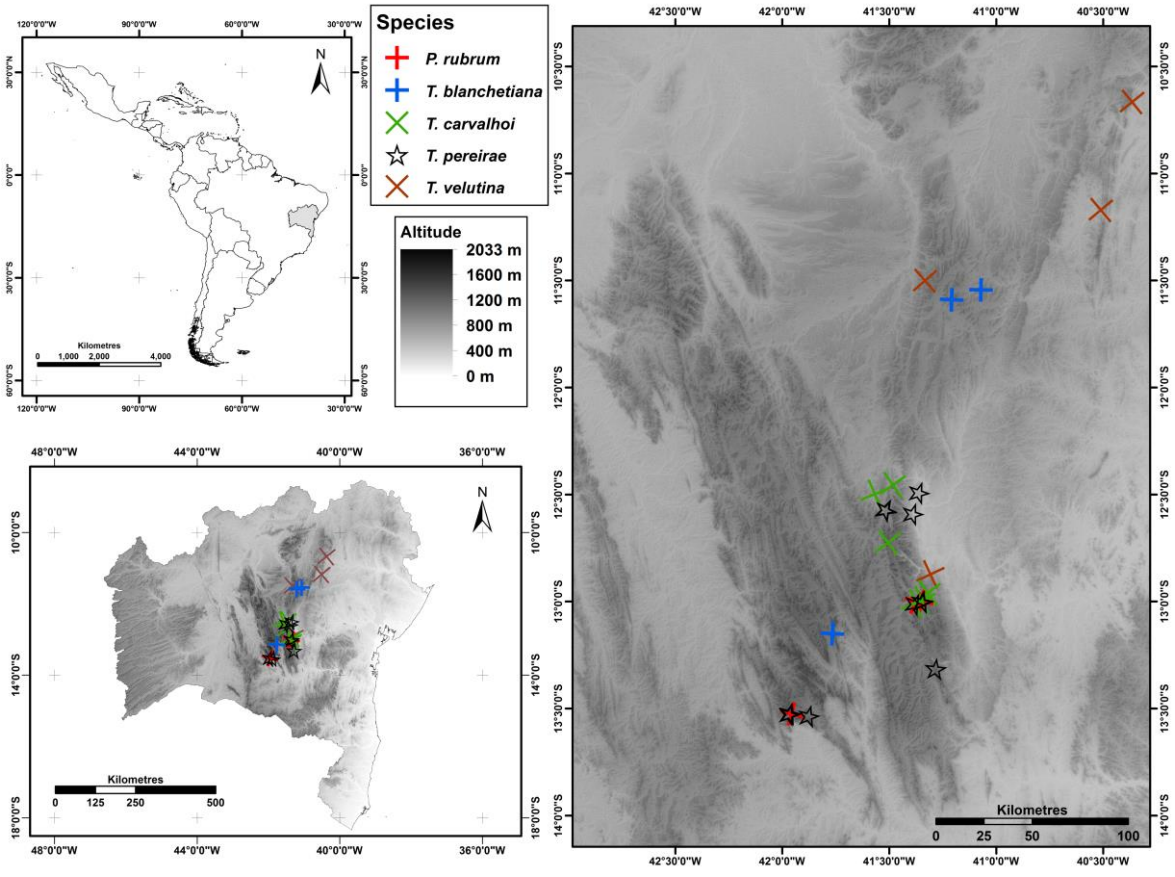

Figure 2. Distribution map of sampling localities.

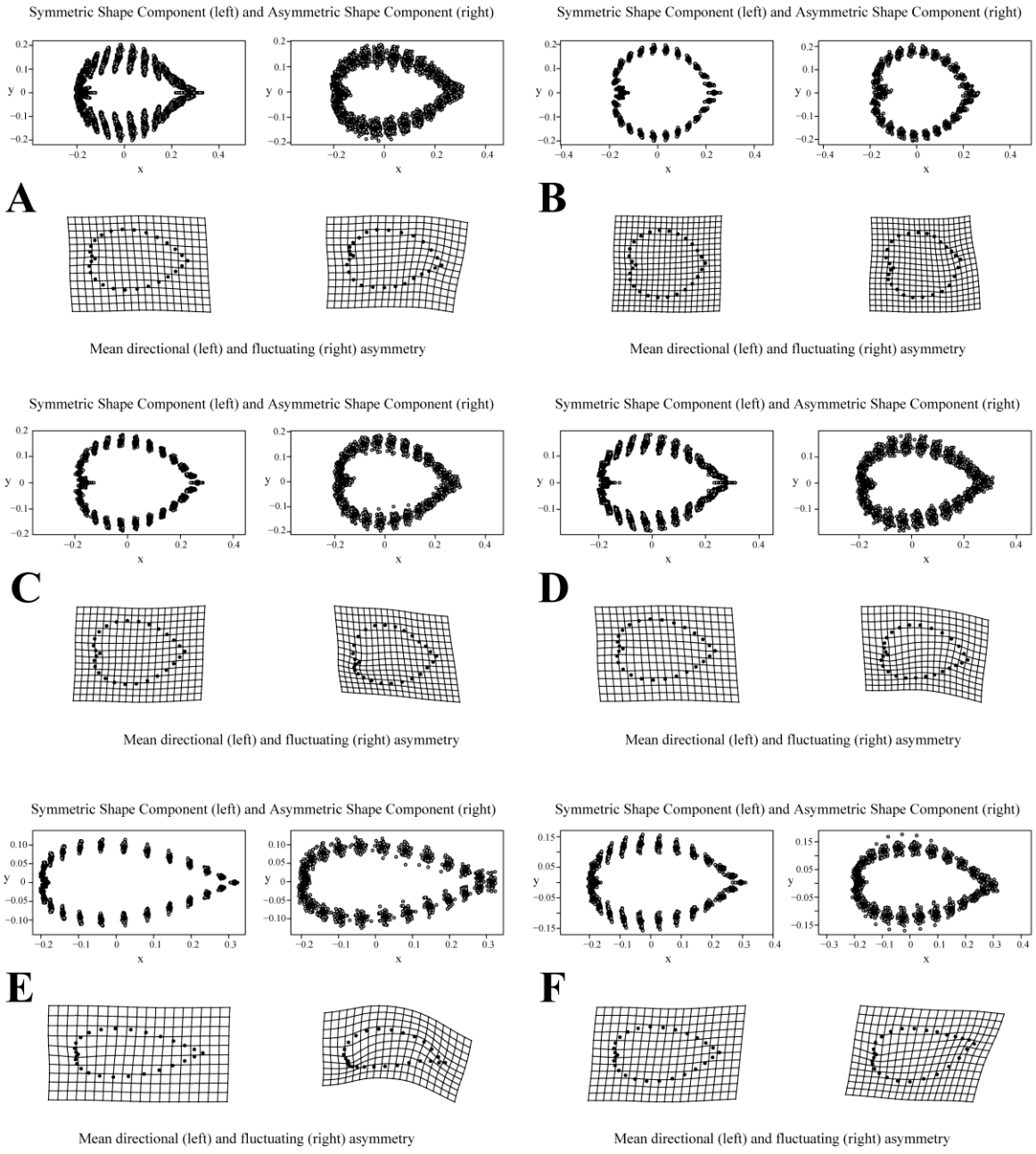

Figure 3. Plots of symmetric and asymmetric components, mean directional asymetry, and fluctuating asymmetry for all species in the *T. pereirae* species complex. A) all samples; B) *T. blanchetiana*; C) *T. carvalhoi*; D) *T. pereirae*; E) *P. rubrum*; F) *T. velutina.*

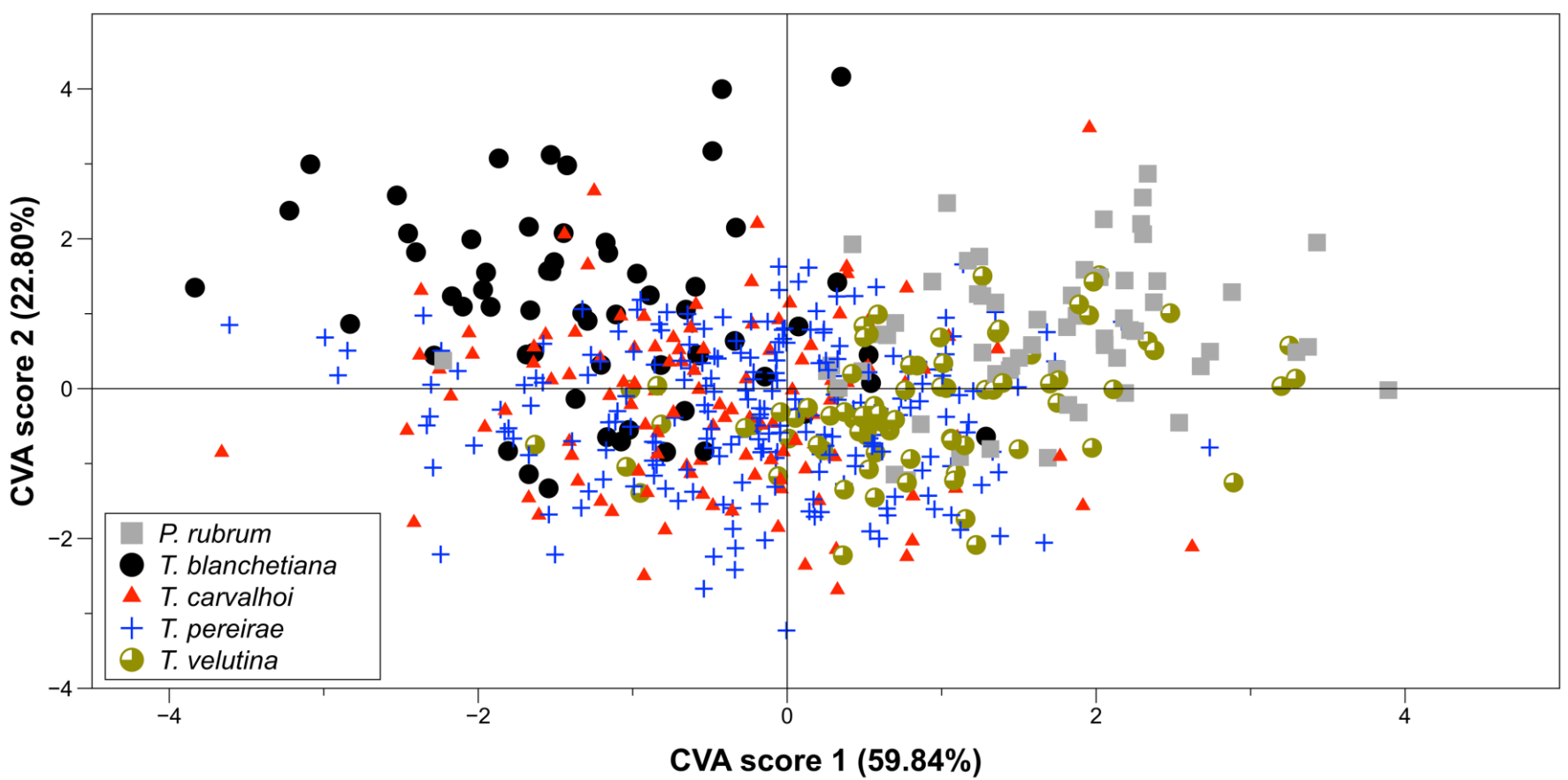

Figure 4. Scatterplot of CV scores 1 and 2 from the asymmetry component of leaves in all species of the *T. pereirae* complex

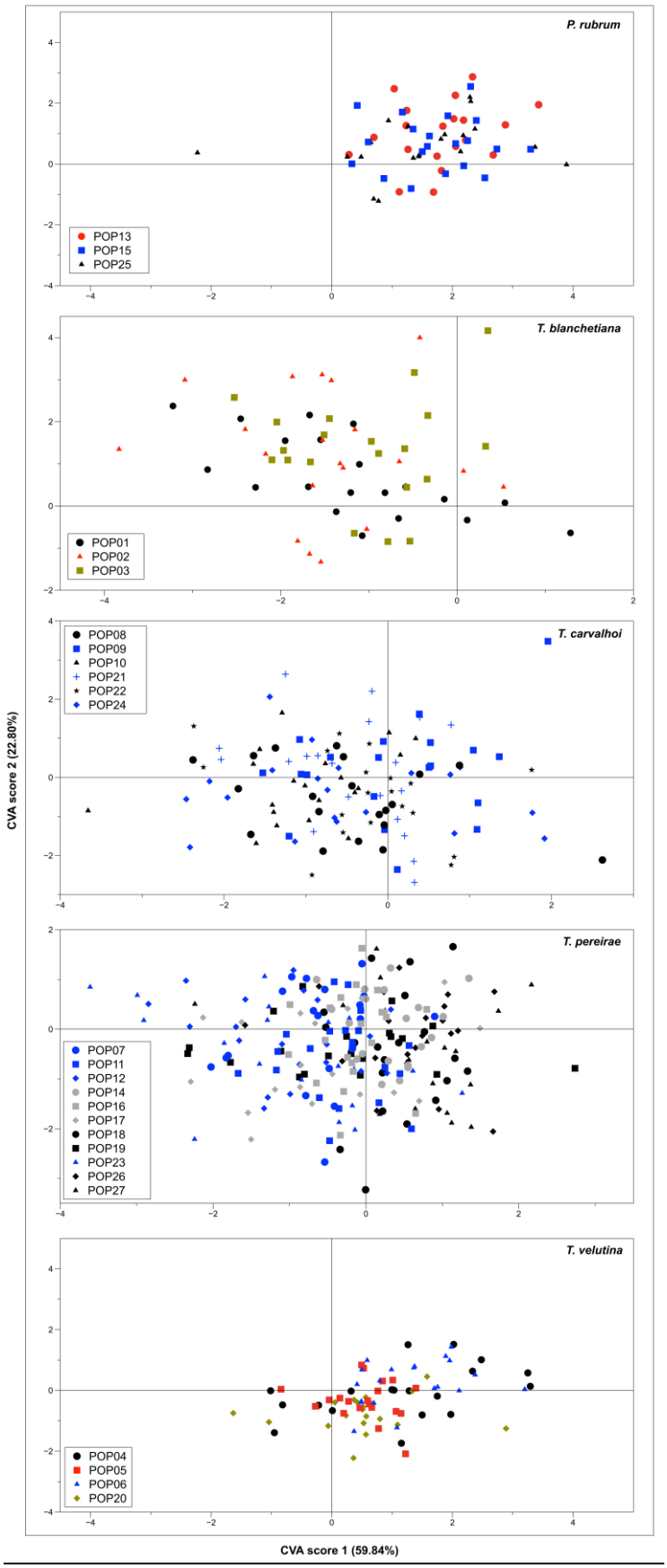

Figure 5. Scatterplots of the CVA of asymmetry components in the *T. pereirae* species complex.

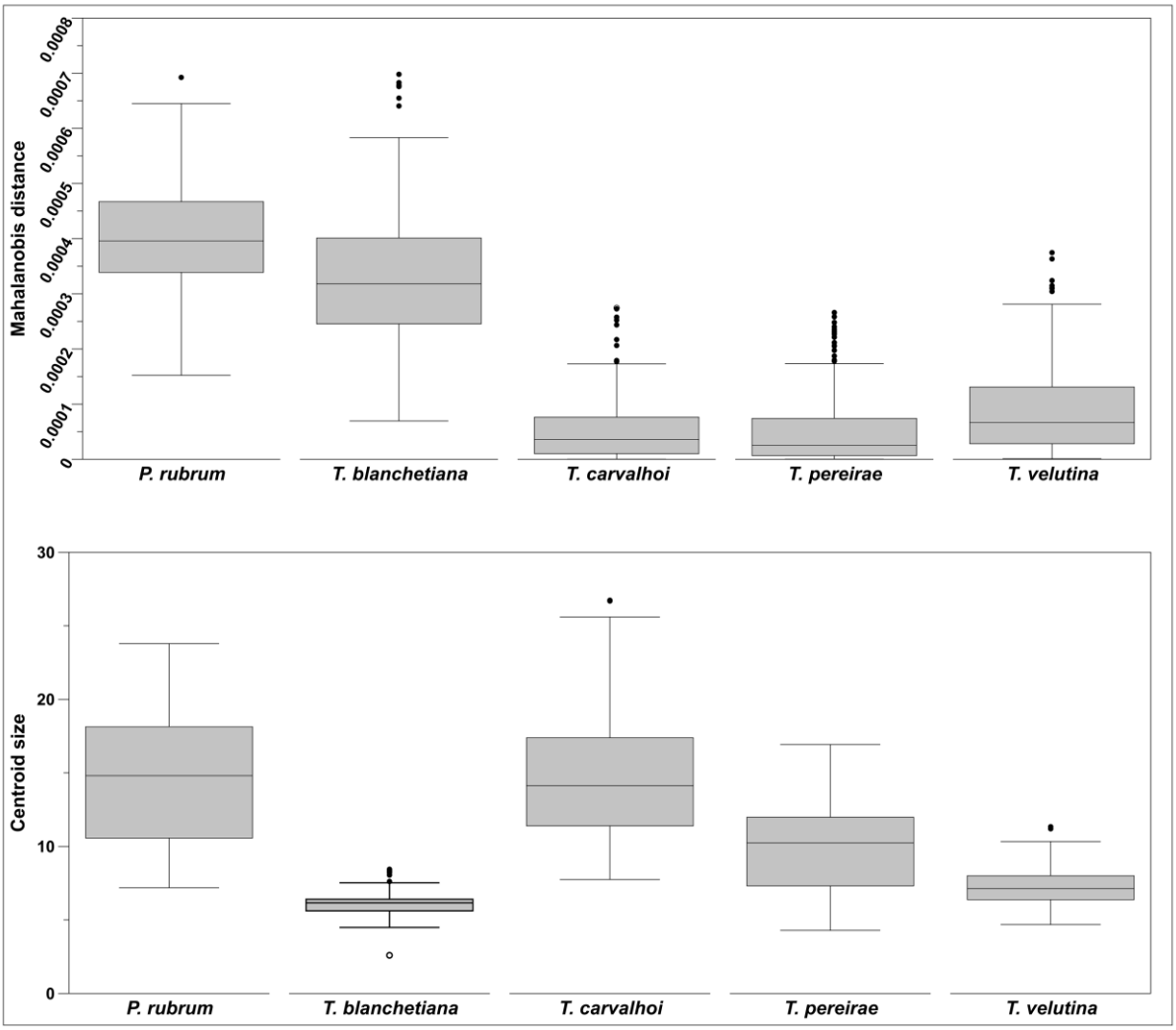

Figure 6. Boxplots of Mahalanobis distances and centroid size in the *T. pereirae* species complex. Above, Mahalanobis distances of shape coordinates within each species; Below, centroid size variation within each species.

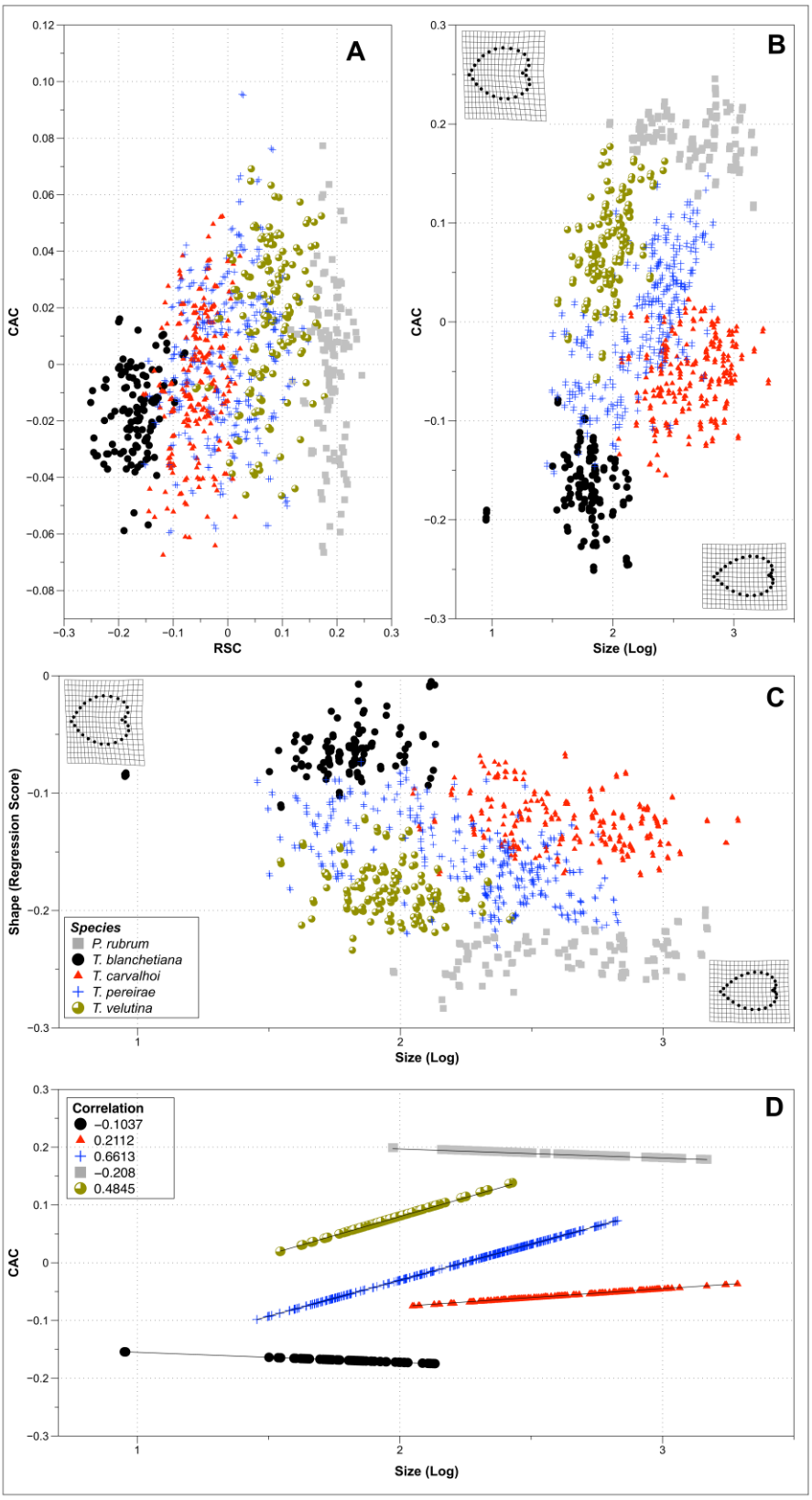

Figure 7. Scatterplots from allometry analyses of leaves in the *T. pereirae* species complex. A) Common allometric component (CAC) against size (log-transformed centroid size); B) Residual shape component 1 (RSC 1) against size (log-transformed centroid size); C) Shape regression scores against size (log-transformed centroid size); D) Correlation lines of CAC against size (log-transformed centroid size).

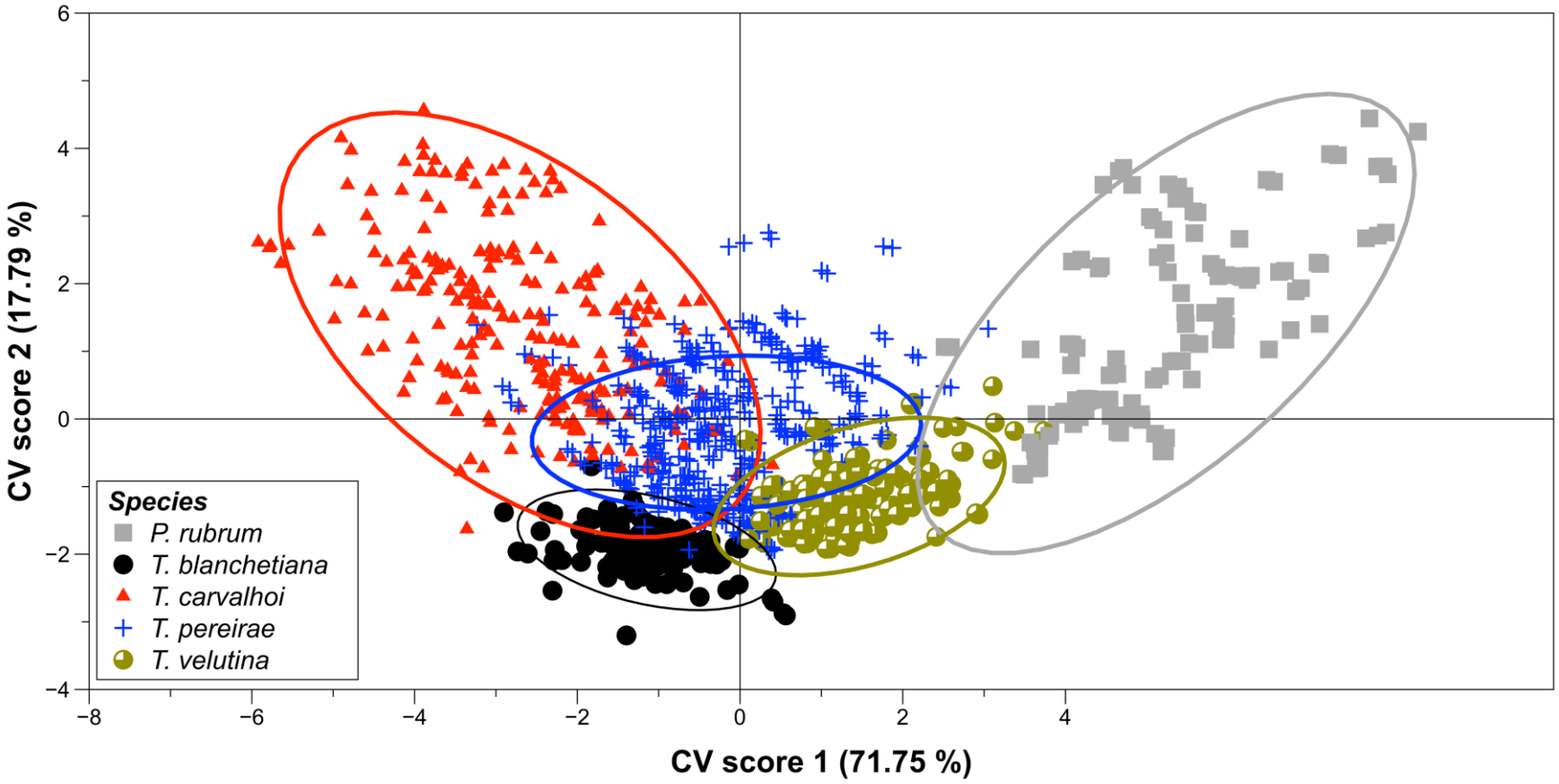

Figure 8. Scatterplots from CVA of size-corrected shape of leaves in the *T. pereirae* species complex.

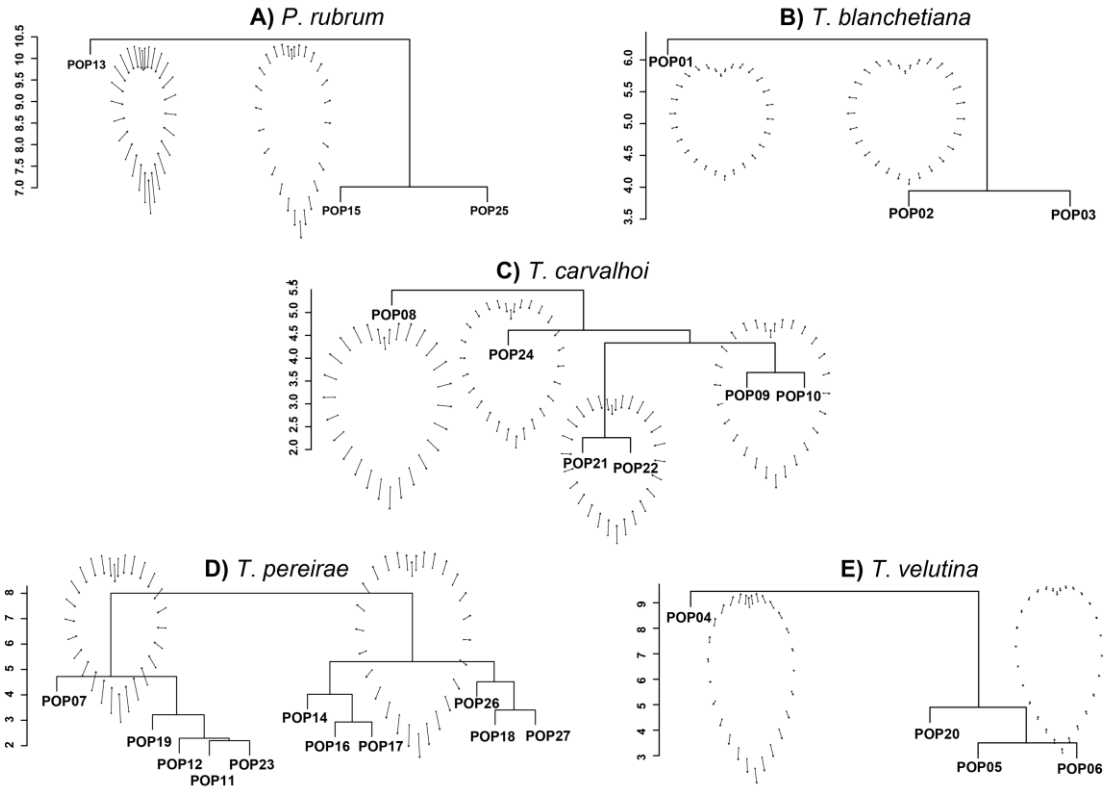

Figure 9. Dendrograms of Euclidian distances from populations of each species in the *T. pereirae* complex. A vector of deformation for each main group is depicted to represent variation from species mean. A) *P. rubrum*; B) *T. blanchetiana*; C) *T. carvalhoi*; D) *T. pereirae*; E) *T. velutina*.

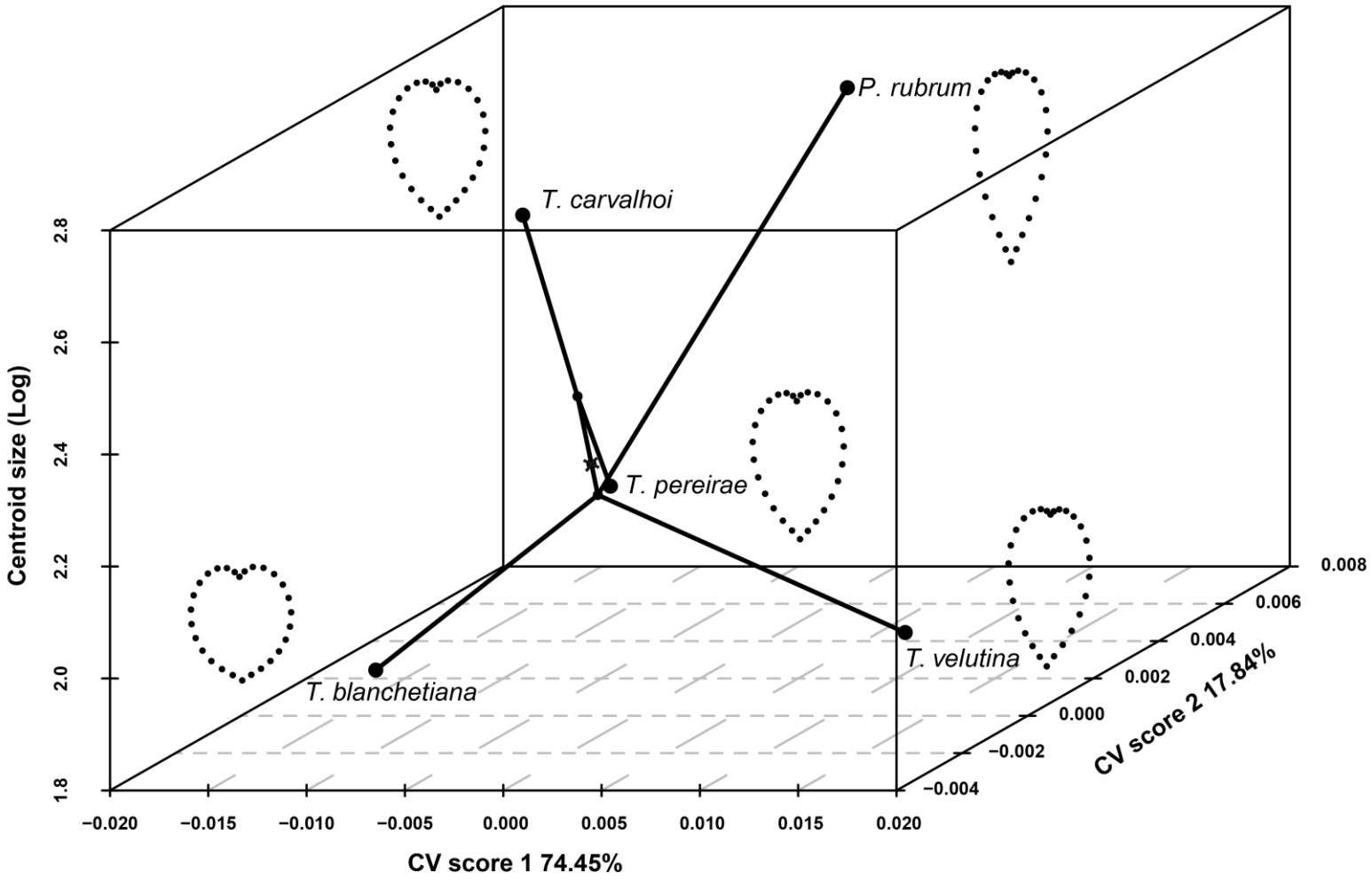

Figure 10. Phylomorphospace of the *Tibouchina pereirae* species complex. Morphospace defined by the first two CV axes of size-corrected shape and size (log centroid size). Mean shape for each species is plotted on phylomorphospace.

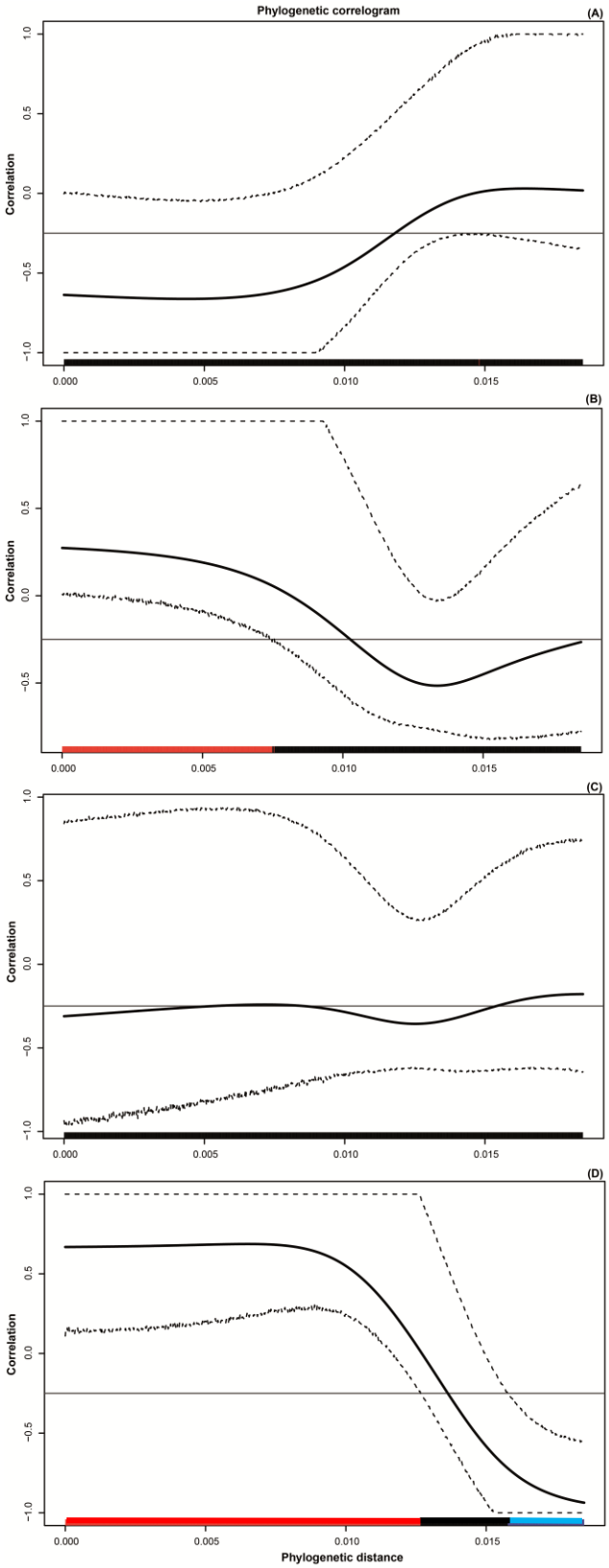

Figure 11. Phylogenetic correlograms for analysed traits. A) CV1 from CVA of size-corrected shape; B) CV2 from CVA of size-corrected shape; C) Size (log centroid size); D) BM, simulated trait under Brownian motion evolution. Solid bold black line represent Moran's I index of autocorrelation. Dotted lines represent 95% confidence intervals. Horizontal black line represent the expected value of Moran's I index under the null hypothesis of no autocorrelation. Colored bar represent significance of the autocorrelation; red, significant positive correlation; black, no significant autocorrelation; blue, significant negative correlation.

Capítulo III[3]

[3]Artigo publicado no periódico *Phytotaxa* 288(3): 249–257.

A new species of *Pleroma* (Melastomataceae) endemic to Chapada Diamantina, Bahia, Brazil

JULIANA GOMES FREITAS[1] & CÁSSIO VAN DEN BERG[2]

1 Programa de Pós-Graduação em Botânica, Universidade Estadual de Feira de Santana, Av. Transnordestina, s.n., Novo Horizonte, CEP 44036-900, Feira de Santana, Bahia, Brasil; e-mail: julebiologia@gmail.com

2 Departamento de Ciências Biológicas, Universidade Estadual de Feira de Santana, Av. Transnordestina, s.n., Novo Horizonte, CEP 44036-900, Feira de Santana, Bahia, Brasil.

Abstract – *Pleroma rubrum* (Melastomataceae, Melastomeae), a new shrubby species endemic to rocky outcrops of Chapada Diamantina, northeastern Brazil, is here described, illustrated and compared with closely related taxa. The new taxon is easily distinguished, within the *Tibouchina pereirae* species complex, by its quadrangular distal branches with a crown of long hirsute trichomes around nodes, leaves elliptic-lanceolate with reddish margins and petioles, reddish inflorescence and bracteoles, colored stipitate glands on all reproductive structures, except the pedoconnectives, involucral bracteoles, and urceolate capsules.

Keywords: Biodiversity, *Campos rupestres*, Melastomeae, Neotropical Plants, Taxonomy, *Tibouchina*

INTRODUCTION

Tibouchina Aublet (1775: 445) is one of the richest genera within Melastomataceae and the largest within Melastomeae. Its distribution is exclusively Neotropical and it ranges from México and the Caribbean to Argentina and Paraguay. There are approximately 460 species and varieties validly published, most of them occurring in the Andean region and Brazil (Todzia & Almeda 1991, Clausing & Renner 2001, Guimarães 2014). In the latter, endemism is high and 149 out of 170 reported species are considered restricted to the country (Guimarães 2016). The genus is morphologically characterized by flowers with all stamens fertile and arranged in two whorls (antesepalous and antepetalous), ovary with an apex covered with hirsute trichomes, and fruit a 4–5-locular capsule with numerous small cochleate-tuberculate seeds (Todzia & Almeda 1991, Guimarães & Martins 1997, Peralta 2002, Meyer *et al*. 2010).

The species of *Tibouchina* are an important component of several Brazilian biomes but they are common in the *Cerrado*, particularly in the *campos rupestres* ecoregion of the Serra do Espinhaço Range (Guimarães & Martins 1997, Romero 2000). Within this mountain system, the Chapada Diamantina mountains from Bahia are dominated by a highly endemic *campos rupestres* vegetation that includes many narrow endemics restricted to small areas (Alves *et al*. 2014, BFG 2015, Fernandes 2016, Silveira *et al*. 2016). Nine out of twenty-five species of *Tibouchina* distributed in these mountains are endemic to one or several mountains (Freitas 2011). Four of those endemic species, plus the new taxon here described, are morphologically and genetically similar and regarded as the *Tibouchina pereirae* species complex (Freitas 2011, Freitas *et al*. In prep.).

According to the most recent phylogenetic analysis of Neotropical Melastomeae, several genera are inserted within *Tibouchina*, as currently circumscribed, and some clades are recognized as separate genera (Michelangeli *et al*. 2013). Therefore, Eastern Brazilian species of *Tibouchina* belong to three or four genera, *Tibouchina*, *Pleroma* Don (1823: 279), *Chaetogastra* (Candolle 1828: 131), and probably *Brachyotum* (Candolle 1828: 136) Triana (1867: 729) if recognized (Michelangeli *et al*. 2013, Meyer 2016). *Itatiaia* Ule (1908: 234) and *Microlepis* (Candolle 1828: 139) Miquel (1840: 71) are now combined under *Pleroma* but generic rearrangements within the *Pleroma* clade are not yet completed (Romero & Versiane 2014, Silva *et al*. 2014, Goldenberg & Kollmann 2015). It is estimated that *Pleroma* contains 160 to 180 species mainly from the Atlantic Forest and

Cerrado biomes of Central and Eastern Brazil (Meyer & Goldenberg 2014, Oliveira *et al*. 2014).

Thus, *Pleroma* includes shrubs and trees morphologically characterized by the caducous sepals, stamens with connectives usually prolonged below the thecae and bearing ventral appendages (glandulous or glabrous), filaments usually pilose, and fruits with cochleate seeds (for further information see Michelangeli *et al*. 2013, Fraga & Guimarães 2014, Meyer & Goldenberg 2014, Oliveira *et al*. 2014, Goldenberg & Kollmann 2015, Guimarães & Silva 2015). Several new species fitting into this morphological characterization have been described within *Pleroma* the last three years to avoid future unnecessary combinations if described under *Tibouchina* (Fraga & Guimarães 2014, Meyer & Goldenberg 2014, Oliveira *et al*. 2014, Goldenberg & Kollmann 2015, Guimarães & Freitas 2015, Guimarães & Silva 2015).

Recent field collections at different localities within the Chapada Diamantina, intended for a morphometric and phylogeographic study, yield many specimens of *Pleroma* that do not fit into any of the described species in the genus. The new taxon, here proposed, is described, illustrated, and morphologically compared with closely related taxa. Distribution, ecological data and conservation status of the species are also provided.

The new taxon is included within the *Tibouchina pereirae* species complex and it is morphologically congruent with the generic limits already in use for *Pleroma* (Freitas *et al*. in prep., Meyer & Goldenberg 2014, Fraga & Guimarães 2014, Goldenberg & Kollmann 2015). Species of the complex are included within the clade now being considered as *Pleroma* but they have not yet been formally combined (Michelangeli *et al*. 2013). These new taxonomic transferences are being fulfilled by other researches and it is not within the scope of this paper. Thus, we decide to describe this new taxon under *Pleroma* rather than *Tibouchina* in advance to the formal generic rearrangements and avoid a future unnecessary combination.

MATERIALS AND METHODS

Field trips to the Chapada Diamantina for an ongoing morphometric and phylogeographic study yielded many specimens that do not correspond to any of the described species in *Tibouchina* and *Pleroma*. Analysis of additional herbarium specimens hosted at Brazilian and other international herbaria supports our hypothesis of a new taxon. These specimens are deposited at K, RB, SP, US, MBM, SPF, ALCB, CEPEC, and

HUEFS, acronyms according to Thiers (2016). Our recent collections are deposited at the herbarium of the Universidade Estadual de Feira de Santana (HUEFS). Description data and illustrations are based upon these herbarium specimens and fresh material collected.

Morphological variation of all specimens was quantified with a caliper rule. Conservation status was assessed using IUCN criteria (IUCN 2012). Estimates of Area of Occupancy (AOO) and Extension of Occurrence (EOO) were obtained through the GeoCAT online platform using geo-referenced data from known collections and the default IUCN cell width of 2 km (Bachman *et al*. 2011). Flowering and fruiting, geographic distribution, ecological data, and taxonomic relationships were discussed based upon herbarium specimens and field trips.

TAXONOMIC TREATMENT

Pleroma rubrum J.G.Freitas, *sp. nov*. (Figures 1–3)

Type: — BRAZIL. Bahia: Rio de Contas. Vertente leste do Campo do Queiroz, 13º32'S, 41º59'W, 1500 m, 24 December 1988, fl., fr., *R.M.Harley 27358* (holotype: HUEFS!; isotypes: K!, SPF!, MBM!, CEPEC!).

Diagnosis: — A species similar to *Tibouchina pereirae* Brade & Markgraf (1961: 772), *T. carvalhoi* Wurdack (1983: 134), and *T. velutina* Cogniaux (1885: 350) by its shrubby habit, leaves with dense-strigose indumentum and lilac to purple flowers. It differs from them by its quadrangular distal branches with a crown of 0.3–0.7 cm long hirsute trichomes around nodes; leaves comparatively more lanceolate; lax inflorescences; bracteoles generally involucral; hypanthium, calix, and stamens with stipitate glands; pedoconnectives with ventral bituberculate and glabrous appendages; weakly incurved style; and capsule urceolate, strigose and reddish.

Shrubs up to 2 m, distal branches greenish to reddish, quadrangular without wings, trichomes either glandular and reddish or eglandular; proximal branches brownish, cylindrical, peeling, glabrescent, nodes with a crown of hirsute trichomes 0.3–0.7 cm long. **Leaves** opposite and petiolate, 5−7-nerved, veins impressed adaxially and prominent abaxially, sometimes reddish at base, second pair emerging from first one (suprabasal); petioles (1–)2–3 cm long, generally reddish, sulcate; blade 5–14 × 1.5–4.5 cm, elliptic-lanceolate, coriaceous, apex acute to acuminate, base cuneate to subcordate, margin entire

and reddish; adaxial surface dark green, strigose, trichomes greenish or reddish, simple, free, glands sessile; abaxial surface light green, strigose, trichomes whitish, free, glands pedicellate. **Inflorescence** thyrsoid, terminal, subtended by a pair of leaf-like bracts at base; bracts lanceolate, 2–5 × 0.6–1.5 cm, green with a reddish base, revolute, caducous; rachis 15−35 cm long, greenish or reddish, stipitate glands and/or simple trichomes; bracteoles 0.5–1.5 × 0.3–0.8 cm, reddish, oval or spatulate, caducous before anthesis, involucral or not, trichomes white with reddish stipitate glands, simple. **Flowers** 5-merous, subtended by a pair of bracteoles; pedicel 0.2–0.5 cm long, reddish or greenish, trichomes either simple or with stipitate glands; hypanthium 0.5–1 × 0.3–0.5 cm, reddish, urceolate, strigose, trichomes either glandular or eglandular; sepals 0.4–0.7 × 0.2–0.3 cm, reddish, persistent on young fruits, strigose, apex apiculate, base truncate, margin ciliate, trichomes simple, reddish stipitate glands either present or absent, indumentum denser at center of lobe; petals 1.5–2 × 0.9–1.2 cm, lilac to purple, obdeltoid, apex irregular, base cuneate, margins ciliate either with or without stipitate glands; stamens 10, dimorphic, 4–6 stipitate glands, white with a reddish apex at base of filaments; antesepalous stamens with filaments 1.3–1.5 cm, base white and apex purple, pedoconnectives 0.2–0.3 cm long, extending below anthers, anthers 1.3–1.5 cm long, purple, straight, appendages glabrous; antepetalous stamens with filaments 0.8–1 cm, base white and apex purple, pedoconnectives 0.1–0.2 cm long, extending below anthers; anthers 0.8–1 cm long, rose or white, slightly curved, appendages glabrous; ovary 0.6–0.8 × 0.4–0.5 cm, free, hirsute trichomes at apex; style 1.5–3 cm long, purple or rose, weakly incurved at apex, glabrous or with stipitate glands; stigma yellowish, punctiform. **Capsule** 0.8–1.3 × 0.5–0.8 cm, reddish; seeds numerous, 0.08–0.1 cm, brownish, cochleate, tuberculate.

Phenology: — Specimens have been collected with flowers in January, February and May; fruits in February and from April to July.

Etymology: — The specific epithet alludes to the red color of the inflorescences; a character that allows easy spotting on its natural enviroment. The petioles and margins of leaves, base of bracts, and occasionally veins in the basal abaxial surface of leaves are also reddish.

Distribution and habitat: — Currently, *Pleroma rubrum* is found in the central portion of Chapada Diamantina mountain range in Bahia, Brazil. It inhabits quartzite rocky outcrops dominated by *campos rupestres* typical plant communities on altitudes ranging from 900 to

2,000 m in the municipalities of Mucugê and Rio de Contas (Figures 1, 3). Several state, federal or private conservation areas are in the zone but they are prone to different human disturbances and natural fires, exerting strong pressures to the existence of the species. Most of the specimens analyzed here shared the same enviroment with *Vellozia sincorana* Smith & Ayensu (1976: 55), colloquially known as "*canela de ema*". In Mucugê, the new species is sympatric with *Tibouchina pereirae*, sharing the same rocky outcrops (see Figure 1B).

Conservation status: — The new species is found within or close to the "Parque Nacional Chapada Diamantina" and the "Área de Proteção Ambiental Serra do Barbado" federal and state conservation areas. The Estimated Area of Occupancy (AOO) of this species is 28 km2 and its Extent of Occurrence (EOO) is 2,199.756 km2. Following the IUCN criteria, it may be considered endangered [EN B2ab (III)] due to its proximity to human communities and vulnerability. The three main areas of occurrence are included within tourist routes ("Cachoeira do Tiburtino" in Mucugê and "Pico das Almas" in Rio de Contas) or surrounding areas of strong urban development (Byzantine Cemetery in Mucugê). In addition, natural fires frequently disturb these areas. Both kinds of pressures are the main concerns for the conservation of plant communities in the *campos rupestres* ecoregion (Alves *et al*. 2014, Fernandes 2016).

Taxonomic comments: — *Pleroma rubrum* is characterized by a combination of characters from branches, leaves and inflorescences. Quadrangular distal branches with a crown of 0.3–0.7 cm long hirsute trichomes around nodes. Leaves are elliptic-lanceolate with cuneate to subcordate bases, reddish margins and petioles, and the second pair of the seven conspicuous veins is born from the first one. The inflorescence and bracteoles are reddish and all reproductive structures, except the pedoconnectives, have colored stipitate glands (see Figures 1C–D, 2); bracteoles are generally involucral; the hypanthium, calix and stamens have stipitate glands; the pedoconnectives have ventral bituberculate and glabrous appendages; the capsules are urceolate, strigose and reddish.

Populations from Mucugê have sparser and smaller stipitate glands than those from Rio de Contas. Furthermore, distal branches have a transparent and sticky 'resin' that is more conspicuous in the latter. This variation in 'resin' content could be associated to differences in humidity between localities and be an adaptation against water loss as populations from drier localities have more 'resin'.

The new species is morphologically closer to three species from the *Tibouchina pereirae* complex (*T. carvalhoi*, *T. pereirae* and *T.* v*elutina)* due to its shrubby habit and branching patterns; leaves only at apex of distal branches, slightly discolor (abaxial surface lighter green), 5–7-veined and with dense-strigose indumentum. These species are endemic to the Chapada Diamantina mountain range and inhabit the same vegetation communities but differ from each other by several morphological characters (Table 1, Figure 1I–L). Ongoing analyses of leaf morphometrics and genetic variation in the *T. pereirae* species complex confirmed that all species in the complex are morphologically and genetically different; these analyses also placed *P. rubrum* closer to *T. velutina* (Freitas *et al*. in prep.).

Tibouchina carvalhoi differs from *P. rubrum* by its sub-cylindrical distal branches (vs. quadrangular) covered by not viscous strigose indumentum with long stipitate glands (vs. viscous strigose indumentum without stipitate glands) and nodes not surrounded by a crown of hirsute trichomes (vs. surrounded by a crown of hirsute trichomes); ovate to cordate leaves (vs. elliptic-lanceolate) with prominent abaxial secondary veins (vs. not prominent) (Figure 1J) and adaxial stipitate glands in young leaves (vs. stipitate glands absent); oblong hypanthium (vs. urceolate) and costate fruits (vs. not costate).

Tibouchina pereirae differs from *P. rubrum* by its sub-cylindrical distal branches (vs. quadrangular) covered by not viscous strigose indumentum (vs. viscous strigose indumentum) and nodes lacking a crown of hirsute trichomes (vs. nodes with a crown of hirsute trichomes); elliptic-ovate leaves (vs. elliptic-lanceolate) (Figure 1K); leaf-like bracts cordate (vs. lanceolate) and bracteoles not involucral (vs. involucral); hypanthium sericeous (vs. strigose) and filaments with stipitate glands along filaments, rarely glabrous (vs. glabrous, rarely with stipitate glands at base of filaments).

Tibouchina velutina differs from *P. rubrum* by its distal branches covered with sericeous indumentum (vs. strigose), and nodes lacking a crown of hirsute trichomes (vs. nodes with a crown of hirsute trichomes); elliptic leaves up to 4 cm long (vs. elliptic-lanceolate leaves 5 to 14 cm long) (Figure 1L); inflorescence rachis greenish (vs. reddish), base of inflorescence with leaves instead of leaf-like bracts (vs. lanceolate leaf-like bracts at base of inflorescence) and bracteoles not involucral (vs. involucral); hypanthium indumentum sericeous without stipitate glands (vs. strigose with stipitate glands).

Additional specimens examined (paratypes): — BRAZIL. Bahia: Municipality of Rio de Contas, Pico das Almas, 23 January 1974 (fl), *Harley 15468* (K SPF); Fazenda Fiuza, 13º27’33”S, 41º52’24”, 4 February 1997 (fl*), Passos PCD5038* (ALCB, CEPEC); Pico das

Almas, 21 February 1987 (fl, fr), *Harley 24555* (HUEFS); Pico das Almas, 13º26'S, 41º12'W, 6 April 2005 (fr), *Santos 302* (HUEFS); Pico das Almas, 24 July 1979 (fr), *Mori et al. 12529* (US!, RB!); Municipality of Mucugê, Próximo ao cemitério bizantino, 13º00'29"S, 41º22'45"W, 27 February 2012 (fl, fr), *Freitas 821* (HUEFS); Cachoeira do Tiburtino, 12º59'53"S, 41º20'56"W, 3 May 2013 (fl, fr), *J.G. Freitas 816* (HUEFS); Gobira, 13º4'38"S, 41º22'31"W, 4 June 2004 (fr), *Borba 1840* (HUEFS).

ACKNOWLEDGEMENTS

This contribution is part of the Ph.D. thesis of JGF at the Programa de Pós-graduação em Botânica from the Universidade Estadual de Feira de Santana (UEFS). The fieldwork for the present study was financed by CNPq/FAPESB (grant PNX0014/2009). JGF is grateful to CAPES for a scholarship for doctoral studies. CvdB is grateful to CNPq for a productivity scholarship (PQ-1B). Authors are thankful to curators and staff of K, RB, SP, US, MBM, SPF, ALCB, CEPEC, and HUEFS for making the collections on their charge available to us.

REFERENCES

Alves, R.J.V., Silva, N.G., Oliveira, J.A. & Medeiros, D. (2014) Circumscribing *campo rupestre* - megadiverse Brazilian rocky montane savannas. *Brazilian Journal of Biology* 74: 355–362. https: //doi.org/10.1590/1519-6984.23212

Aublet, J.B.C.F. (1775) *Histoire des plantes de la Guiane Françoise* 1. Pierre-François Didot, London, 621 pp.

Bachman, S., Moat, J., Hill, A.W., Torre, J. & Scott, B. (2011) Supporting Red List threat assessments with GeoCAT: geospatial conservation assessment tool. *Zookeys* 150: 117–126. https: //doi.org/10.3897/zookeys.150.2109

BFG (2015) Growing knowledge: an overview of seed plant diversity in Brazil. *Rodriguésia* 66: 1–29.

Brade, A.C. & Markgraf, F. (1961) Neue Melastomataceen aus Brasilien. *Willdenowia* 2: 769–774. Available from: http: //www.jstor.org/stable/3995267 (accessed 15 December 2016)

Candolle, A.P. de. (1828) Melastomaceae. *Prodromus Systematis Naturalis Regni Vegetabilis* 3: 99–202.

Clausing, G. & Renner, S.S. (2001) Molecular phylogenetics of Melastomataceae and Memecylaceae: implications for character evolution. *American Journal of Botany* 88: 486–498. https: //doi.org/10.2307/2657114

Cogniaux, A. (1885) Melastomataceae. *In*: Martius, C.F.P., Eichler, A.W. & Urban, I. (Eds.) *Flora brasiliensis.* Vol.14. pars. 3. F. Fleischer, Lipsiae, pp. 205–510.

Don, D. (1823) An illustration of the natural family of plants called Melastomataceae. *Memoirs of the Wernerian Natural History Society* 4: 276–329.

Fernandes, G.W. (2016) The megadiverse rupestrian grassland. *In:* Fernandes, G.W. (Ed.) *Ecology and conservation of mountaintop grasslands in Brazil*. Springer, New York, pp. 3–14. https: //doi.org/10.1007/978-3-319-29808-5_1

Fraga, C.N.D. & Guimarães, P.J.F. (2014) Two new species of *Pleroma* (Melastomataceae) from Espírito Santo, Brazil. *Phytotaxa* 166: 77–84. https: //doi.org/10.11646/phytotaxa.166.1.5

Freitas, J.G. (2011) *Estudos floristicos e taxonômicos em* Tibouchina *Aubl. (Melastomataceae; Melastomeae) no estado da Bahia, Brasil*. Universidade Estadual de Feira de Santana, Feira de Santana, 183 pp.

Goldenberg, R. & Kollmann, L.J.C. (2015) Two new species of *Pleroma* (Melastomataceae) from Espírito Santo, Brazil. *Brittonia* 68: 37–45. https: //doi.org/10.1007/s12228-015-9390–4.

Guimarães, P.J.F. (2014) Two new species of *Tibouchina* (Melastomataceae) from Brazil. *Novon* 23: 42–46. https: //doi.org/10.3417/2012029

Guimarães, P.J.F. (2016) *Tibouchina*. Lista de Espécies da Flora do Brasil. Jardim Botânico do Rio de Janeiro. Available from: http: //floradobrasil.jbrj.gov.br/jabot/floradobrasil/FB19731 (accessed 29 October 2016)

Guimarães, P.J.F. & Martins, A.B. (1997) *Tibouchina* sect. *Pleroma* (D. Don) Cogn. (Melastomataceae) no estado de São Paulo. *Revista Brasileira de Botânica* 20: 11–33. https: //doi.org/10.1590/s0100-84041997000100002

Guimarães, P.J.F. & Freitas, J.G. (2015) Two new species of *Pleroma* (Melastomataceae) from Brazil. *Systematic Botany* 40: 553–560. https: //doi.org/10.1600/036364415X688736

Guimarães, P.J.F. & Silva, M.F.O. (2015) A new species of *Pleroma* (Melastomataceae, Melastomeae) from southeastern Brazil. *Phytotaxa* 205: 51–58. https: //doi.org/10.11646/phytotaxa.205.1.4

IUCN (2012) *IUCN Red List Categories and Criteria*: Version 3.1. Second edition. Gland, Switzerland and Cambridge, UK, IUCN 4: 32 pp.

Meyer, F.S. (2016) *Estudos sitemáticos no clado de* Chaetogastra *DC. e gêneros aliados (Melastomataceae: Melastomeae)*. Universidade Estadual de Campinas, Campinas, 295 pp.

Meyer, F.S. & Goldenberg, R. (2014) Two new species of *Pleroma* (Melastomataceae: Melastomeae) from Brazil. *Kew Bulletin* 69: 9527. https: //doi.org/10.1007/s12225-014-9527–8.

Meyer, F.S., Guimarães, P.J.F. & Goldenberg, R. (2010) *Tibouchina* (Melastomataceae) do estado do Paraná, Brasil. *Rodriguésia* 61: 615–638.

Michelangeli, F.A., Guimarães, P.J.F., Penneys, D.S., Almeda, F. & Kriebel, R. (2013) Phylogenetic relationships and distribution of New World Melastomeae (Melastomataceae). *Botanical Journal of the Linnean Society* 171: 38–60. https: //doi.org/10.1111/j.1095-8339.2012.01295.x

Miquel, F.A.G. (1840) Observationes de Piperaceis et Melastomaceis. *Commentarii Phytographici* 2: 31–92.

Oliveira, A.L.F., Romero, R. & Guimarães, P.J.F. (2014) A new Brazilian species and some synonyms in *Pleroma* (Melastomataceae). *Brittonia* 66: 353–357. https: //doi.org/10.1007/s12228-014-9345-1

Peralta, P. (2002) Las espécies del género *Tibouchina* (Melastomataceae) en Argentina. *Darwiniana* 40: 107–120. Available from: http: //www.jstor.org/stable/23225169 (accessed 15 December 2016)

Romero, R. (2000) *A família Melastomataceae no Parque Nacional da Serra da Canastra, Minas Gerais, Brasil*. Universidade Estadual de Campinas, Campinas, 326 pp.

Romero, R. & Versiane, A.F.A. (2014) Taxonomic novelty and typifications in *Microlepis* (Melastomataceae). *Novon* 23: 217–223. https: //doi.org/10.3417/2011077

Silva, M.F.O., Guimarães, P.J.F. & Michelangeli, F.A. (2014) Nomenclatural and taxonomic novelties in the tribe Melastomeae (Melastomataceae). *Phytotaxa* 186 (4): 222–228. https: //doi.org/10.11646/phytotaxa.186.4.6

Silveira, F.A.O., Negreiros, D., Barbosa, N.P.U., Buisson, E., Carmo, F.F., Carstensen, D.W., Conceição, A.A., Cornelissen, T.G., Echternacht, L., Fernandes, G.W., Garcia, Q.S., Guerra, T.J., Jacobi, C.M., Lemos-Filho, J.P., Le Stradic, S., Morellato, L.P.C., Neves, F.S., Oliveira, R.S., Schaefer, C.E., Viana, P.L. & Lambers, H. (2016) Ecology and evolution of plant diversity in the endangered campo rupestre: a neglected

conservation priority. *Plant and Soil* 403: 129–152. https: //doi.org/10.1007/s11104-015-2637-8

Smith, L.B. & Ayensu, E.S. (1976) A revision of American Velloziaceae. *Smithsonian Contributions to Botany* 30: 1–172. https: //doi.org/10.5479/si.0081024X.30

Thiers, B. (2016) *Index herbariorum: a global directory of public herbaria and associated staff*. New York Botanical Garden's Virtual Herbarium. Available from: http: //sweetgum.nybg.org/ih/ (accessed 11 June 2016)

Todzia, C.A. & Almeda, F. (1991) A revision of *Tibouchina* section *Lepidotae* (Melastomataceae: Tibouchineae). *Proceedings of the California Academy of Sciences* 47: 175–206.

Triana, J.J. (1867) *Brachyotum*. *In*: Bentham, G. & Hooker, J.D. (Eds.) Genera plantarum ad exemplaria imprimis in Herberiis Kewensibus servata definita. Lovell Reeve & Co., London, p. 743.

Ule, E.H.G. (1908) Melastomataceae. *Botanische Jahrbücher für Systematik, Pflanzengeschichte und Pflanzengeographie* 42: 232–236.

Wurdack, J.J. (1981) Three species of *Tibouchina* (Melastomataceae) from Bahia, Brazil. *Brittonia* 33: 304–308. https: //doi.org/10.2307/2806420

TABLE 1. Summary of the morphological characters used to separate *P. rubrum* from other related species.

Species	*P. rubrum*	*T. pereirae*	*T. carvalhoi*	*T. velutina*
Distal branches	Quadrangular	Sub-cylindrical	Sub-cylindrical	Quadrangular
Color of distal branches	Reddish	Greenish	Reddish	Greenish
Distal branches indumentum	Strigose, sparse, viscous, without stipitate glands	Strigose, sparse, not viscous, without stipitate glands	Strigose, sparse, not viscous, with long stipitate glands	Sericeous, sparse, without stipitate glands
Distal branches nodes	Surrounded by hirsute trichomes	Not surrounded by hirsute trichomes	Not surrounded by hirsute trichomes	Not surrounded by hirsute trichomes
Leaf blade form	Elliptic-lanceolate	Elliptic-ovate	Ovate to cordate	Elliptic
Leaf indumentum (when young)	Without stipitate glands	Without stipitate glands	With stipitate glands	Without stipitate glands
Leaf margins color	Reddish	Greenish	Greenish	Reddish
Inflorescence rachis color	Reddish, sometimes greenish in the populations of Rio de Contas	Greenish, rarely wine	Reddish	Greenish
Leaf-like bracts	Lanceolate, only at base of inflorescence	Cordate, at base of inflorescence, rarely along the axis of the rachis	Cordate, only at base of inflorescence	Absent, leaves at base of inflorescence
Bracteoles	Involucral	Not involucral	Not involucral	Not involucral
Hypanthium	Urceolate	Urceolate	Oblong	Urceolate
Hypanthium indumentum	Strigose, dense, with stipitate glands	Sericeous, dense, sometimes with stipitate glands	Sericeous, dense, sometimes with stipitate glands	Sericeous, dense, without stipitate glands
Filaments indumentum	Glabrous, rarely with stipitate glands at filament base	Stipitate glands along filament, rarely glabrous	Stipitate glands along filament	Glabrous
Capsule	Without costae	Without costae	Costate	Without costae

FIGURE 1. *Pleroma rubrum*: **A.** Habit at Rio de Contas, Bahia, Brazil. **B.** *Pleroma rubrum* (left) and *T. pereirae* (rigth) sharing the same rocky outcrop. **C**. Branch with inflorescence. **D**. Flower bud with involucral bracteoles. **E**. Flower, dorsal view. **F**. Inflorescence, inset highlighting leaf-like bracts. **G**. Immature capsule, lateral view. **H**. Flower, frontal view. **I**. Leaf of *P. rubrum*. **J**. Leaf of *T. carvalhoi*. **K**. Leaf of *T. pereirae*. **L**. Leaf of *T. velutina*.

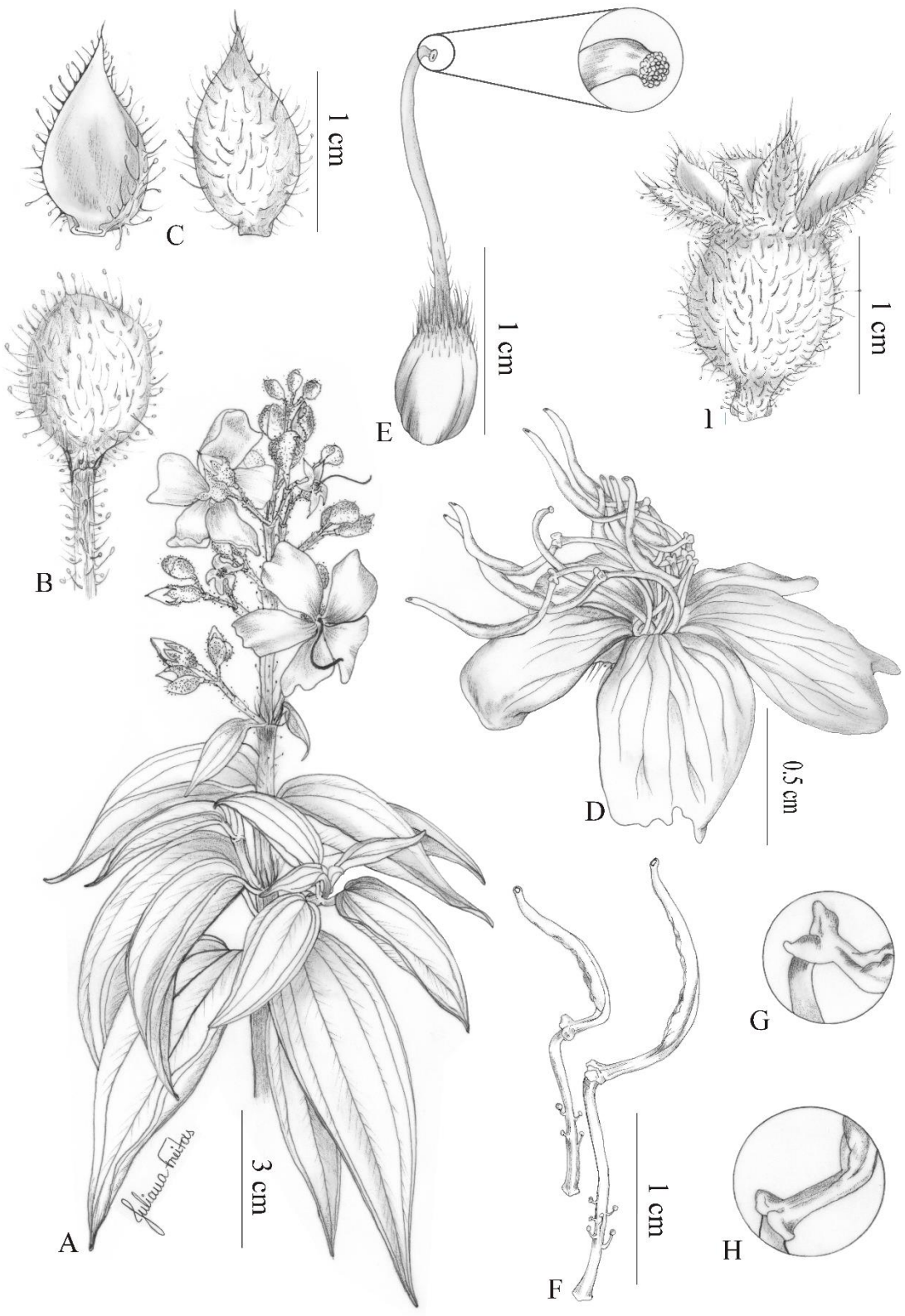

FIGURE 2. *Pleroma rubrum*: **A**. Flowering branch. **B**. Flower bud enclosed by bracteoles. **C**. Bracteoles, frontal and dorsal view. **D**. Flower. **E.** Gynoecium, details of punctiform stigma. **F**. Antesepalous and antepetalous stamens. **G**. Details of staminal antepetalous pedoconnective. **H**. Details of staminal antesepalous pedoconnective. **I**. Capsule.

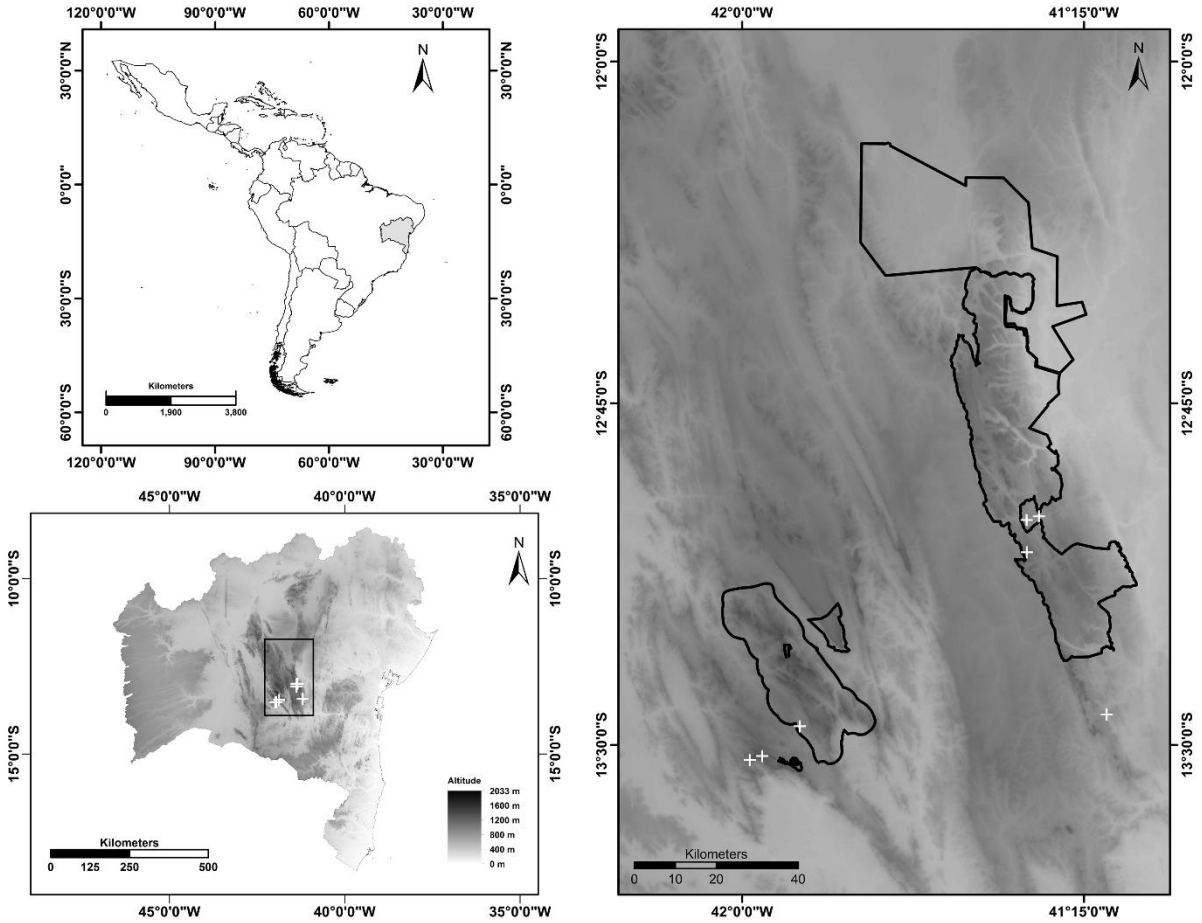

FIGURE 3. Distribution map of *Pleroma rubrum*. Natural protected areas highlighted by tick lines on the map.

CONSIDERAÇÕES GERAIS

O avanço nos estudos filogeográficos no Brasil têm revelado processos históricos e padrões espaciais e ambientais intrínsecos a diversas áreas geográficas. No entanto, análises de variação morfológica em linhagens divergentes não tem recebido a mesma atenção, apesar de que a variação morfológica dentro das linhagens é comum e muitas vezes serve como motivação inicial para estudos genéticos, como o caso do presente estudo. Buscando abordar essa lacuna, este trabalho utilizou métodos que exploram dados morfológicos e genéticos dentro do complexo de espécies *T. pereirae*, aspirando compreender as divergências dessas espécies nas diferentes formações montanhosas da Chapada Diamantina.

Nossos resultados revelam que a forma e o tamanho das folhas estão intimamente relacionados na diversidade morfológica das espécies do complexo *T. pereirae* e a sinergia de ambos os aspectos (variação da forma e do tamanho) caracteriza a variação fenotípica observada no grupo. Essa variação é sobretudo devido a diferenças dentro de cada espécie, a qual é atribuída a dois fatores biológicos que as afetam em diferentes graus: 1) Plasticidade fenotípica e 2) Adaptação local. Esses fatores exercem um papel importante para as plantas lidarem com a heterogeneidade ambiental no tempo e no espaço, uma vez que a variação morfológica das folhas influencia na adaptação das plantas em habitats desfavoráveis. Portanto, nota-se que as diferenças de forma dentro das espécies foram maiores entre as populações em duas espécies (*P. rubrum* e *T. pereirae*) e entre os indivíduos para as demais (*T. blanchetiana*, *T. carvalhoi* e *T. velutina*). Isso indica que a variação morfológica foliar está sendo mais influenciada pelas condições ambientais locais nas duas primeiras e pela plasticidade fenotípica nas três últimas.

A variação morfológica foliar (quando comparado forma e tamanho) revela isolamento geográfico apenas nas populações de *T. pereirae* entre as diferentes montanhas da Chapada Diamantina. Portanto, não podemos afirmar que existe uma estruturação geográfica da diversidade morfológica no complexo *T. pereirae*.

Um resultado a ser ressaltado nos padrões da variação morfológica do complexo *T. pereirae*, é a variação da simetria foliar, um componente aleatório e frequentemente

hereditário, que é relatado como resposta a fatores genéticos, heterogeneidade ambiental ou pressões biológicas. Contudo, diversos padrões na assimetria direcional (diferenças sistemáticas entre os lados direito-esquerdo, sem uma origem clara) e assimetria flutuante (pequenas diferenças na simetria, relacionada a instabilidades do desenvolvimento, provocadas por pressões ambientais ou biológicas) foram observados dentro das espécies. Além disso, foi observada a antissimetria que é a ocorrência de populações com indivíduos assimétricos canhotos ou destros misturados. Estes padrões revelaram importante papel na distinção das espécies. No entanto, apesar de serem resultados notáveis, são necessárias análises mais detalhadas para tirar conclusões sobre a natureza da variação assimétrica desse grupo, já que se trata de um fator pouco explorado em plantas.

Embora as espécies do complexo *T. pereirae* se distribuam em morfoespaços de forma e tamanho independentes, esses caracteres não mostram evidências de sinal filogenético claro na evolução do complexo *T. pereirae*. Portanto, não foi detectado sinal filogenético nos padões de variação morfológica observados no complexo.

Dentre as 10 regiões do DNA testadas para estudar o complexo *T. pereirae*, a região intergênica nuclear ITS e o espaçador cloroplastidial *rpl32-trnL*, mostraram-se mais propícios para o estudo da diversidade genética do grupo, por serem mais variáveis e fáceis de amplificar. Além desses, os espaçadores *trnQ-rps16*, *rps16-trnK* e o íntron *rpl16* também mostraram variação potencial para sua utilização em estudos evolutivos de *Tibouchina*. De modo contrário, o espaçador *trnD-trnT* possui variação muito elevada, devido ao alto número e tamanho das deleções (entre 10 e 130 bp de extensão) em alguns indivíduos ou populações, o que influencia na estimativa da variabilidade genética do grupo. Bem como, o espaçador *psbA-trnH* é uma região muito pequena (~220pb) e apresentou baixa variabilidade intraespecífica, não apresentando muito potencial do ponto de vista filogeográfico.

O complexo de espécies *T. pereirae* possui alta diversidade genética. Contraditoriamente, a diversidade haplotípica é semelhante entre os dois conjuntos de dados cpDNA e nrDNA. Contudo, os marcadores nucleares geralmente mostram níveis mais elevados de diversidade de haplótipos do que o cpDNA devido às suas maiores taxas de mutação quando comparados ao DNA plastidial. Além disso, a alta diversidade de haplótipos nos dados cpDNA não era esperada diante do baixo tamanho amostral e populacional, restrição de habitat e a dispersão de sementes limitada das espécies.

Esperava-se, portanto, observar um único haplótipo fixo ou baixa variação genética nos dados de cloroplastos.

Um dos desafios no desenvolvimento deste trabalho foi o baixo número de populações distribuídas nas diferentes montanhas para cada espécie do complexo, bem como a distribuição simpátrica das populações em algumas espécies, o que dificulta a aplicação de algumas metodologias espacialmente comparativas. Acredita-se que a restrição a habitats rupestres junto a baixa capacidade de dispersão via sementes são fatores que também favorecem a baixa distribuição das espécies e alta diferenciação genética das populações nas diferentes montanhas da Chapada Diamantina. No entanto, os eventos de expansão e contração das populações provocados pelas variações climáticas do passado permitiram a diferenciação das linhagens e o fluxo gênico entre as espécies.

A estimativa do número de migrantes no complexo *T. pereirae* sugere que as populações se isolaram geograficamente em um tempo suficiente para que ocorresse divergência do nrITS, mas não o suficiente para a divergência de *rpl32-trnL* entre as populações. Os padrões de migração sugeriram que as localidades mais setentrionais da Chapada Diamantina serviram como refúgio e fonte de migração para a expansão posterior das espécies nos períodos de fortes variações climáticas.

O tempo de divergência estimado para o complexo de espécies *T. pereirae* de seus parentes mais próximos, coincide com a expansão dos ambientes savânicos tropicais dominados por gramíneas C4 e a divergência de várias outras linhagens de plantas associados a estes ecossistemas (inclusive Melastomataceae e Fabaceae).

Os períodos referentes ao Plioceno e o Pleistoceno foram caracterizados por oscilações climáticas de estações glaciais secas e frias intercaladas por épocas interglaciais quentes e úmidas. Esses ciclos resultaram na diversificação do complexo de espécies *T. pereirae*, através de eventos recorrentes de contração e expansão das populações durante os períodos glaciais e interglaciais, conforme inferido nos resultados, mostrando expansão demográfica do grupo durante períodos de climas mais secos e após a última máxima glaciação (Last Maximum Glaciation - LGM).

Conforme sugerido por alguns autores, as porções altas da Cadeia do Espinhaço (e consequentemente da Chapada Diamantina) representaram, provavelmente, refúgios para a flora campestre durante os períodos interglaciais, enquanto nos períodos glaciais ocorria o

inverso e a vegetação campestre se expandia para áreas mais baixas. Dessa forma, as oscilações climáticas facilitaram tanto a diferenciação entre as populações quanto a mistura entre as espécies. Esses dados revelam a importância da história evolutiva das espécies na inferência dos padrões filogeográficos dessas áreas.

O Bioma Cerrado vem sofrendo durante as últimas décadas grandes transformações nos seus ecossistemas devido a ação humana, como mudanças na paisagem natural (agricultura, extração de madeira e plantas ornamentais, garimpo, fragmentação de habitats e/ou realização de queimadas sem o manejo adequado) ocasionando perda da biodiversidade e erosão nos solos. Essas práticas humanas causam danos irreparáveis e ameaçam a permanência de muitas espécies micro endêmicas distribuídas em mosaicos ao longo da região montanhosa. Na Chapada Diamantina, existe pouca ameaça devido à mudança de uso do solo para agricultura, que é comum às áreas mais planas do Cerrado do Centro-Oeste, exceto no planalto próximo a Mucugê, que vem sofrendo intensas mudanças. As áreas montanhosas têm baixíssimo potencial para agricultura, porém foram afetadas por garimpo durante um período bastante prolongado, e sofrem frequentes incêndios, devido ao fogo escapado de áreas agrícolas e pastagens adjacentes. As áreas de proteção ambiental da Chapada Diamantina representam uma pequena parcela deste sistema de montanhas tão diverso biologicamente, mas a maior fonte de proteção para estas espécies parece ser a declividade e altitude, junto ao difícil acesso de boa parte das áreas. Contudo, os esforços de conservação dessas áreas, favorecerão as espécies endêmicas e raras e a diversidade morfológica e genética dessa porção tão rica.